論文 / 著書情報
Article / Book Information

題目(和文)	気象観測の乏しいアジア高山域における氷河融解の気候変動影響と予測不確実性に関する研究
Title(English)	Climate change impacts on sparsely observed High Mountain Asian glaciers and their uncertainty
著者(和文)	渡邉恵
Author(English)	megumi watanabe
出典(和文)	学位:博士(工学), 学位授与機関:東京工業大学, 報告番号:甲第11266号, 授与年月日:2019年9月20日, 学位の種別:課程博士, 審査員:鼎 信次郎,鍵 直樹,中村 隆志,木内 豪,吉村 千洋
Citation(English)	Degree:Doctor (Engineering), Conferring organization: Tokyo Institute of Technology, Report number:甲第11266号, Conferred date:2019/9/20, Degree Type:Course doctor, Examiner:,,,,
学位種別(和文)	博士論文
Type(English)	Doctoral Thesis

Climate change impacts on sparsely observed High Mountain Asian glaciers and their uncertainty

気象観測の乏しいアジア高山域における氷河融解の気候変動影響と予測不確実性に関する研究

Megumi Watanabe

渡辺　恵

July, 2019

Abstract

It is unclear glacier melt response (e.g., the magnitude and timing of changes in glacier melt) and the extent of contribution of glacier melts towards river flow in the context of climate change for major river basins originating in High Mountain Asia. Here I evaluate glacier melt response to climate change at a major river basin scale for 11 basins using glacier melts estimated by a glacier model. Furthermore, I attempt to add the runoff outputs of climate models with the glacier melts into a "total runoff" to reveal the hydrological impact of the glacier melts. Our simulation implied that the glacier melt response to climate change is regionally different. However, the annual total runoff would increase caused by primarily an increase in non-glacier melt components across 11 basins until the end of the 21st century. The relative contribution of glacier melts to the total runoff would significantly decrease towards the end of the 21st century in some basins and it might have implications on seasonal water supplies.

Climate forging is one of the most significant sources of uncertainties to project glacier melt by using glacier models. I applied a calibration method for a glacier model "HYOGA2" to evaluate uncertainty from climate forcing. Two additional meteorological parameters have been applied to calibrate HYOGA2. Three precipitation products were used for calibration of the glacier model and bias correction for GCM outputs (daily temperature and precipitation).

Observed past climate data used as input in glacier models are expected to differ among datasets, particularly those for precipitation at high elevations. Differences among observed past climate datasets have not yet been described as a cause of uncertainty in projections of future changes in glacier mass, although uncertainty caused by varying future climate projections among general circulation models (GCMs) has often been discussed. Differences among observed past climate datasets are expected to propagate as uncertainty in future changes in glacier mass due to bias correction of GCMs and calibration of glacier models. I project ensemble future changes in the mass of glaciers in Asia through the year 2100 using a glacier model. A set of 18 combinations of inputs, including two observed past air temperature datasets, three observed past precipitation datasets, and future air temperature and precipitation projections from three GCMs were

used. The uncertainty in projected changes in glacier mass was partitioned into three distinct sources: GCM uncertainty observed past air temperature uncertainty, and observed past precipitation uncertainty. Our findings indicate that, in addition to the differences in climate projections among GCMs, differences among observed past climate datasets propagate fractional uncertainties of about 15% into projected changes in glacier mass. The fractional uncertainty associated with observed past precipitation was 33 – 50% that of the observed air temperature. Differences in observed past air temperatures and precipitation did not propagate equally into the ultimate uncertainty of glacier mass projection when ablation was dominant.

Additionally, I also projected glacier melt forced by GCM shuffling forcing data. One GCM showed almost the same spread of glacier melt projections among precipitation products as a difference between some GCMs. Some simulations showed a larger difference in projected glacier melt caused by GCM temperature output than a difference caused by GCM precipitation output.

I showed that the difference among observed past climate datasets had a serious impact on the assessment of future glacier melts. Therefore, the development of a new past climate dataset at high elevations is required to reduce the uncertainty arising from the difference among the observed past climate datasets. Notably, the exploitation of improved data sets of precipitation is receiving widespread attention. I developed a precipitation dataset by combining gauge, satellite, reanalysis precipitation datasets to decrease uncertainties in projecting future changes in glacier mass balance arising from the spread among observed datasets. The satellite radar-derived precipitation improved the spatial distribution at high elevations. The developed precipitation dataset was validated using local rain gauge observation.

和文要旨

本論文は「Climate change impacts on sparsely observed High Mountain Asian glaciers and their uncertainty（気象観測の乏しいアジア高山域における氷河融解の気候変動影響と予測不確実性に関する研究)」というタイトルであり、以下の 6 章により構成される。

第一章「Introduction（序論)」では、本研究の背景、目的が述べられるとともに、論文の構成が示されている。

第二章「Temporal dynamics of glacier melts and hydrological impact（氷河融解の時間変化と水資源への影響)」では、これまで限られた氷河についてしか気候変動への応答は予測されていなかったのに対し、アジア高山域全域を対象として氷河の応答を予測した。河川へ流れ込む氷河融解水の時系列変化に着目して、地域による氷河融解の進行度合いの違いを分類した。その結果、違いをもたらす要因は氷河の存在する地理条件であることを示した。また、これまで氷河融解の大河川流域における水資源への影響を評価した研究は、いくつかの上流域に限られていた。本研究ではアジア高山域の 11 大河川全てを下流域も含めて対象とし、氷河融解の水資源への予測を行った。しかしながら、氷河融解および水資源変動の予測結果が、予測に用いる気象外力に著しく依存する可能性が示唆された。そこで、予測結果の違いをさらに議論し、ひいては予測の精度をより高める必要があるため、気象外力に関連した予測不確実性を要因別に定量化し、予測不確実性を低減することを目的とした次章以降の課題について取り組むべきことが提案された。

第三章「Updated calibration of the glacier model for the uncertainty assessment（不確実性評価に向けた氷河モデルのキャリブレーション改良)」では、気象外力に起因する氷河融解の予測不確実性を定量化するために、従来の氷河モデルの改良を行った。アジア高山域のように、氷河モデルへの気象外力である気温や降水量などの気象観測が不足している地域の場合、従来の氷河モデルでは、将来シミュレーション開始時の氷河質量収支に大きな差異が生じることが予備実験から分かった。そこで、気象外力に起因した氷河融解予測の不確実性を定量化するために、気温と降水量に関する数値シミュレーション上のパラメータを追加することでキャリブレーション方法を改良し、過去期間の氷河質量収支の差異を解消した。これにより、気象観測の不足した場所において、複数のインプットデータを用いた場合にも、将来シミュレーション開始時の質量収支の差異に依存せずに気象外力データの違いが予測へ与える影響を定量化することができるようになった。

第四章「Uncertainty assessment（不確実性評価）」では、第三章でキャリブレーション方法も含め改良した氷河モデルを用いて、将来と過去の気象外力データに起因する不確実性の定量化を行った。気象外力データとしては、気候モデル出力の将来気温と降水量データ、観測を基にした過去気温データ、観測を基にした過去降水量データを用い、各データ間のばらつきによってもたらされる氷河融解の将来予測の違いを定量化した。これまで既往の氷河モデル研究では、氷河融解予測の不確実性の要因として、将来の気温と降水量を計算する気候モデル出力の違いについてのみ議論されることが多かった。しかしながら、本研究では、初めて過去の観測気象データの選択に起因する将来予測の不確実性を定量化した。全ての種類の気象外力データのばらつきによってもたらされる氷河融解予測の不確実性全体に対して、これまで議論されてこなかった過去の観測気象データの違いに起因する不確実性は、21世紀末時点で約 15 %の寄与であることが明らかとなった。既往の氷河モデル研究では、それぞれ単一の過去の観測気象データを用いることが一般的であったが、予測の不確実性を考慮するために、複数の過去観測気象データを用いることが推薦されるとの結論が得られたといえる。

第五章「Development of precipitation dataset（降水量データ開発）」では、第四章で定量化した観測の気象データによる不確実性を低減するための提案を行う。過去の気象外力のうち、特に山地での観測降水量データの不確実性は周知されており、国際的な研究枠組みにおいても喫緊の課題であると広く認識されている。山岳域ではアクセスの困難さから現地観測が極めて不足しているため、地形によらず一様に観測することのできる衛星観測などを活用し、様々な手法を組み合わせて、観測に基づいた分布型降水量データを作成する手法を提案した。数ある衛星の中でも最も降水の検出能力の高い衛星レーダ観測を利用することにより、データを作成した。また、このデータの利用に伴う氷河融解の将来予測の不確実性の低減を推計した。改良した過去降水量データの検証として、限られた地点数のものではあるが雨量計観測を用いた検証も行った。この検証結果では、既存の他の分布型降水量データよりも本研究で作成したデータが現地雨量に近いことが確認された。

第六章「Conclusions（結論）」ではこれまでの章を総括すると共に、今後取り組むべき課題などを提示する。

以上を要するに、本研究は、氷河融解が下流の水資源へ甚大な影響をもたらすことを背景とし、気象観測の極めて不足したアジア高山域を対象にして、気候変動による氷河融解への影響およびそれに伴う不確実性について明らかにした。

Publication list

0.1 Chapter 2

- Watanabe, M., Nakano, K., Kawagoe, S., Asaoka, Y. and Kanae, S.: Estimation of the tropical glacier in Bolivia using satellite imagery, *Journal of Japan Society of Civil Engineers (JSCE)*, Ser.B1, Vol.68, Issue 4, pp.313-318, 2012.

- Watanabe, M., Koirala, S., Hirabayashi, Y. and Kanae, S.: Glacier melt response and annual hydrological impact throughout 21st century for major river basins originating in High Mountain Asia, *Journal of Japan Society of Civil Engineers (JSCE)*, Ser.B1, Vol.71, Issue 4, pp.445-450, 2015.

0.2 Chapter 3

- Watanabe, M., Yanagawa, A., Hirabayashi, Y., Watanabe, S., Sakai, A. and Kanae, S.: Uncertainty from climate forcing of projections in glacier melt for High Mountain Asia,*Journal of Japan Society of Civil Engineers (JSCE)*, Ser.B1, Vol.74, Issue 4, pp.211-216, 2018.

0.3 Chapter 4

- Watanabe, M., Yanagawa, A., Watanabe, S., Hirabayashi, Y. and Kanae, S., Quantifying the range of future glacier mass change projections caused by differences among observed past-climate datasets. *Climate Dynamics*, Vol.53, Issue 3 – 4, pp.2425 – 2435, 2019.

0.4 Other

- Orimo, N., Seto, R., Yoshida, N., Watanabe, M. and Kanae, S.: Analysis of long-lived typhoons over the Indochinese peninsula, *Journal of Japan Society of Civil Engineers (JSCE)*, Ser.B1, Vol.74, Issue 5, pp.213-218, 2018.

- Watanabe, M., Yoshikawa, S., Yamazaki, D. and Kanae, S.: Intensification of rainfall extremes in a warmer climate derived from observations and d4PDF over Japan,

Journal of Japan Society of Civil Engineers (JSCE), (under revision).

Acknowledgements

First and foremost I am extremely grateful to my supervisor, Prof. Shinjiro Kanae for his invaluable advice, continuous guidance, endless supply, and patience during my Ph.D. study. I' m proud of, and grateful for, my time working with him.

I would also like to thank and acknowledge Prof. Tsuyoshi Kinouchi, Prof. Naoki Kagi, Assoc. Prof. Chihiro Yoshimura, Assoc. Prof. Takashi Nakamura who supports my research as sub-chief examiners of my doctoral dissertation.

I cannot express enough thanks to Kanae Lab. researchers and staff for their continued and dedicated support and encouragement: Dr. Aki Yanagawa, Dr. Sayaka Yoshikawa, Dr. Yoshihiko Iseri, Dr. Kaoru Kakinuma, Dr. Sujan Koirala, Dr. Jaeil Cho, Dr. Wee Ho Lim, Dr. Yukiko Imada, Dr. Chihiro Miyazaki, Dr. Rie Seto, Dr. Natsuki Yoshida, and Ms. Yoko Umibe. I offer my sincere appreciation for the learning opportunities provided by them.

My completion of this study could not have been accomplished without the extensive professional guidance by Prof. Yukiko Hirabayashi, Dr. Satoshi Watanabe, Assoc. Prof. Shinta Seto, Prof. Shin Sugiyama, Prof. Koji Fujita, Assoc. Prof. Akiko Sakai, Prof. Seiki Kawagoe, and Assoc. Prof. Dai Yamazaki, members in Hirabayashi Lab., members in Global Hydrology Group in the University of Tokyo. They were instrumental in defining the path of my research. For this, I am extremely grateful.

I would also like to thank the Japan Society for the Promotion of Science for providing me with the necessary funding to accomplish this research.

I extend my gratitude to all of my lab members and many researchers whose support enabled me to keep my research moving forward.

My appreciation also goes out to my family especially Ken and friends for their encouragement and support all through my studies.

Immense gratitude as always to Go for his patience and support.

Contents

List of Figures

List of Tables

Chapter 1

Introduction

1.1 Glaciers under climate change

Glaciers are perennial masses of land ice that originates from compressed snow. They flow downwards to elevations under the force of gravity. Glaciers occur where climate conditions and topographic characteristics allow snow to accumulate over several years and to transform gradually into firn (snow that persists for at least one year) and finally to ice. Under the force of gravity, this ice flows downwards to elevations with higher temperatures where various processes of ablation (loss of snow and ice) dominate over accumulation (gain of snow and ice). The sum of all accumulation and ablation processes determines the mass balance of a glacier. Accumulation is in most regions due mainly to solid precipitation. Ablation is, in most regions, mainly due to surface melting with subsequent runoff. Redistribution of snow by wind and avalanches can contribute to both accumulation and ablation.

Climate warming enhances melting in the cryosphere. That is already having and will continue to have profound global consequences [*Energy and Exchanges*, 2013; *Stocker*, 2014]. Glaciers are one of the components of the cryosphere. Almost all glaciers worldwide have continued to shrink as revealed by the time series of measured changes in glacier length, area, volume, and mass [*Stocker*, 2014]. Current glacier extents are out of balance with current climatic conditions, indicating that glaciers will continue to shrink in the future even without further temperature increase [*Stocker*, 2014]. Future global-scale mass change in glaciers is predicted by glacier models. Several modeling studies have attempted to provide future changes in glacier mass worldwide [*Marzeion et al.*, 2012; *Hirabayashi et al.*, 2013; *Radić et al.*, 2014; *Huss and Hock*, 2015].

The High Mountain Asia (HMA) region includes central, southwestern, and southeastern Asia, as well as the Altay and Sayan regions of northern Asia. In the HMA there is the largest glacier concentration outside the polar regions. Observed mass changes in glaciers are necessary to calibrate and validate glacier models, but those are quite limited especially for Asian glaciers at high mountains [*Zemp et al.*, 2015].

1.2 Impact of glacier melting

The retreat of glaciers raises major concerns about not only sea-level rise, but also the sustainability of global and local water resources [*Immerzeel et al.*, 2010; *Kaser et al.*, 2010; *Huss and Hock*, 2018]. Glaciers are natural buffers of hydrological seasonality by releasing meltwater during dry seasons in particular. Downstream impacts of changes in glaciers might be considered in terms of irrigation for agriculture or hydropower production.

1.3 Uncertainty of glacier modeling

The HMA contains the largest mass of land glacier ice except for the poles. The HMA glaciers are retreating and losing mass at rates comparable to glaciers in other regions of the world [*Fujita and Nuimura*, 2011; *Bolch et al.*, 2012; *Kääb et al.*, 2012; *Brun et al.*, 2017][*Fujita and Nuimura*, 2011]. Meltwaters from HMA glaciers flow into downstream rivers; large human populations depend on glacier-fed water supplies. The impact of climate change on the extent of glacier melt is of major interest. The HMA includes the Tibetan Plateau, for which observed climatic datasets and GCM climate projections are among the sparsest worldwide [*Stocker*, 2014]. This region is characterized by high-level orography and a large proportion of solid precipitation, both of which would be expected to greatly bias observations.

1.4 Objective and outline of this study

This study aims to assess climate change impacts on sparsely observed High Mountain Asian glaciers and their uncertainty.

To achieve it, the objective of this research can be listed as:

- Assessment of temporal dynamics of glacier melts under climate change and hydrological impacts on major Asian rivers

- Update of calibration of the current glacier model to apply sparsely observed regions for uncertainty assessment of glacier melt projection
- Uncertainty assessment to quantify the range of future glacier mass change projections caused by differences among observed past-climate datasets
- Development of a precipitation dataset at high elevations to decrease the uncertainties in projecting glacier melts

Chapter 2 describes the temporal dynamics of glacier melts under climate change over a wide range of glaciers using a glacier model and climate models with climate scenarios. Chapter 2 also assessed hydrological impact based on those temporal dynamics of glacier melts and runoff for all Asian major rivers. Method, details of the data, validation results, and other analyses including regional differences will be also documented. This chapter indicates that the projected glacier temporal dynamics could be affected by climate forcing when we used current glacier models.

Chapter 3 describes the updated calibration of the glacier model for the uncertainty assessment. To assess related uncertainties to the projection of glacier temporal dynamics and hydrological impacts, updating calibration of current glacier models especially for High Mountain Asia due to the lack of observed climate data is required. The details of the method used data and validation of the updated calibration will be explained.

Chapter4 assessed uncertainties in the projection of glacier melt arising from the spread of climate forcing. I project ensemble future changes in the mass of glaciers in Asia through the year 2100 using a glacier model. A set of 18 combinations of inputs, including two observed past air temperature datasets, three observed past precipitation datasets, and future air temperature and precipitation projections from three GCMs were used. The uncertainty in projected changes in glacier mass was partitioned into three distinct sources: GCM uncertainty observed past air temperature uncertainty, and observed past precipitation uncertainty.

Chapter 5 shows an attempt to development of precipitation datasets to decrease uncertainties in projections of glacier melts, which were quantified in Chapter4. Satellite radar-derived precipitation data were used to improve the spatial distribution of precipitation at high elevations. The validation of the developed precipitation data will also be described.

Chapter6 provides the summary of the entire dissertation, conclusions of the study,

and directions for future research.

Chapter 2

Temporal dynamics of glacier melts and hydrological impact

2.1 Backgroud

Rivers originating in High Mountain Asia most heavily depend on its meltwater in the world. Downstream areas of the rivers have large human populations depending on their resources [*Immerzeel et al.*, 2010; *Immerzeel and Bierkens*, 2012]. Observed mass losses revealed by observations [*Cogley*, 2009; *Gardner et al.*, 2013; *Kääb et al.*, 2015] and projected accelerated future mass losses [*Marzeion et al.*, 2012; *Radić et al.*, 2014] of most Asian glaciers raise concerns about the sustainability of water supplies and resulting socioeconomic implications. There is a prevailing hypothesis that due to accelerated melting under a warming climate, glacier runoff will increase initially but will decrease as the stored glacier reduces [*Jansson et al.*, 2003](Figure 2.1). A few notable results were demonstrated by *Rees and Collins* [2006]; *Immerzeel et al.* [2013] that glacial meltwater was projected to be on a rising limb around the middle of the 21st century to the latter half of the century in selected upstream basins in the Indus and Ganges. However, spatial variation of glacial meltwater evolutions within HMA (at a smaller scale than regional scale) in response to climate change has not been addressed by previous studies. To assess the sustainability of water supplies in major rivers we need to investigate glacial meltwater evolutions for all glaciers located at HMA. We also need to reveal the impact of climate change on the whole HMA or regional (e.g., basin-scale) difference of the impact in HMA.

Although changes in runoffs from mountain glaciers in HMA raise major concerns about the sustainability of local water resources, projections of future changes in runoffs

taking into account glacial meltwater by glacier modeling are limited in terms of assessment for the entire basins of major rivers. There is a remarkable study [*Lutz et al.*, 2014] that future runoff was projected for upstream basins of five major rivers: Indus; Ganges; Brahmaputra; Salween and Mekong originating in HMA, but their study did not project future change in the runoff for entire basins including downstream areas. It thus cannot be said that the sustainability of water resources for entire basins originating in HMA was assessed, and further research should be needed. Five major rivers, which *Lutz et al.* [2014] assesses their runoffs could not represent other rivers because the feature of each river should differ. Further research about the assessment for other major rivers such as Yellow or Amudarya also remains to be conducted in terms of the entire water resource originating in HMA. *Lutz et al.* [2014] presented the result using a single glacio-hydrological model, but the difference among models could cause uncertainty to assess the rivers. Therefore, using other glacier models and hydrological models for the assessment is also required.

In such circumstances, here, we project future changes in glacier melts using a glacier model at 11 major river basins originating in HMA. We discuss the regional difference of climate change impact glacier melting by classifying the projected future changes in glacier melts at each basin. We also present future changes in runoffs taking into account glacier melts at 11 basins and quantify the contribution of glacier melts for the entire basins originating the mountain glaciers.

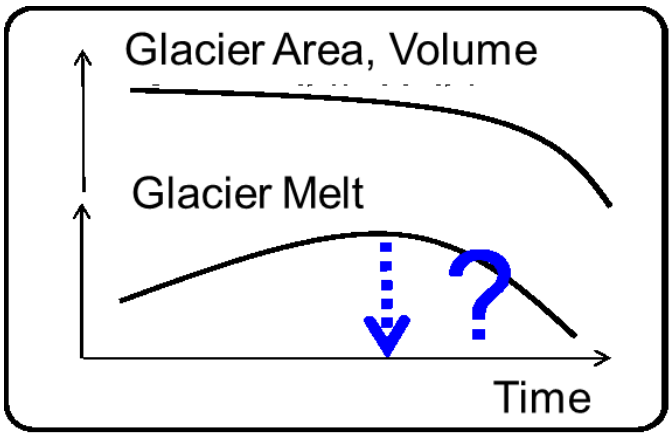

Figure 2.1: Schematic diagram of the temporal dynamics of glacier melts

2.2 Method

2.2.1 Overall

Our study region covers high-mountain Asia (26.5 – 55.5N, 66.5 – 104.5E), which corresponds to the regions of central Asia, southwestern Asia, southeastern Asia, and Altay and Sayan of northern Asia in the Randolph Glacier Inventory [*Pfeffer et al.*, 2014]. The impact of glacier melt was analyzed in 11 major basins (Tarim, Syr Darya, Amu Darya, Indus, Ganges, Brahmaputra, Irrawaddy, Salween, Mekong, Yangtze, and Yellow) originated in the glaciers of high-mountain Asia (Figure 2.2).

Glacier meltwater calculated by a glacier model was used to assess future changes in glacier melt. This glacier meltwater by the glacier model and runoff calculated by GCMs were used to assess the hydrological impact of glacier melting on each downstream basin. The glacier meltwater by the glacier model was added into the runoff by GCMs to show total runoff including the glacier melt component in downstream basins.

This study did not calculate the temporal storage of glacier melts inside glaciers and the process of transport of glacier meltwater and runoff into river mouths. Therefore, the temporal storage of glacier melt inside glaciers can be ignored for a period of more than one year [*Cuffey and Paterson*]. This study analyzed annual runoff because the water

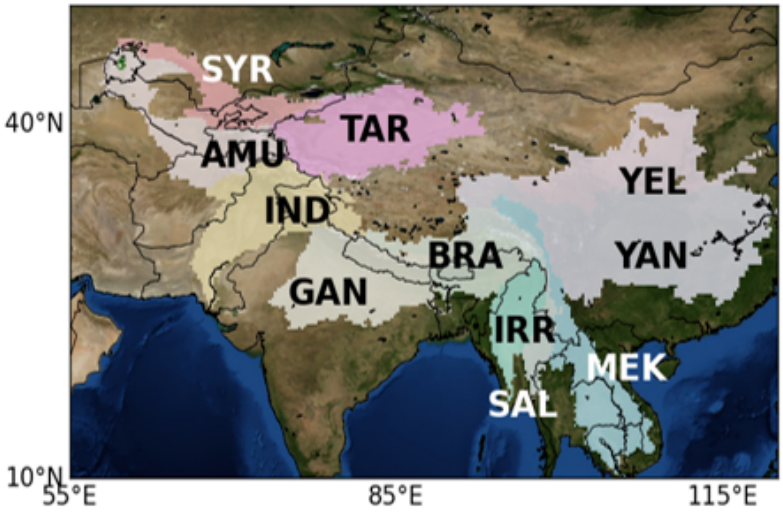

Figure 2.2: Study area, TAR: Tarim, SYR: Syr Darya, AMU: Amu Darya, IND: Indus, GAN: Ganges, BRA: Brahmaputra, IRR: Irrawaddy, SAL: Salween, MEK: Mekong, YAN: Yangtze, YEL: Yellow

budget should be almost balanced for more than a one-year period.

2.2.2 Glacier melt (Glacier model)

We used the model HYOGA2, which was developed for global-scale mass-balance calculations and applied to project the volume evolution of all glaciers outside the Antarctic and Greenland ice sheets through 2100 [*Hirabayashi et al.*, 2013]. Glacier mass balance was calculated using the glacier model forced by daily precipitation and surface air temperature. The melt rates of the surfaces of snow and ice at each elevation band were calculated using a simple degree-day approach and then aggregated to estimate the mass balance for each glacier. Subgrid-scale variation in changes in glacier and snow mass was considered by dividing a model grid cell into 50 m elevation bands. The surface air temperature was assumed to decrease at a constant lapse rate of -0.65 ° C $(100m)^{-1}$. The glacier model assumes that only precipitation that falls as snow affects the mass balance. Precipitation is assumed to fall as snow if the air temperature of the elevation band is less than or equal to 2° C.

The glacier volume was obtained using the equation:

$$A = (\frac{V}{c_a})^{\frac{1}{\gamma}} \tag{2.1}$$

where A km^2 and V km^3 are, respectively, the total glacier area and volume in each glacier, and c_a and γ are model parameters. For all valley glaciers, the model assumed fixed parameter values: $\gamma = 1.375$ from *Bahr et al.* [1997] and $c_a = 0.2055\ m^{3-2\gamma}$ from *Chen and Ohmura* [1990]. For all ice cap glaciers, the model assumed fixed parameter values: $\gamma = 1.25$ from *Bahr et al.* [1997] and $c_a = 1.7026\ m^{3-2\gamma}$ from *Chen and Ohmura* [1990].

The retrospective simulation of HYOGA2 was forced by the observation-based global 0.5° gridded dataset of daily precipitation and near-surface temperature (H08; [*Hirabayashi et al.*, 2008]) The future simulation was forced by six GCMs, which the bias was corrected by using the observation data H08.

The root-mean-square error between the results of the retrospective simulation with HYOGA2 and the available observed mass balance was close to the range of the error estimation for a global glacier model reported by *Marzeion et al.* [2012].

2.2.3 Runoff (GCM)

Runoff calculated by GCMs was used. The runoff was corrected to fit the calculated runoff by multi-land surface models participated in Global Soil Wetness Project 2 （GSWP2） [*Dirmeyer et al.*, 2006]). The correction was done for the climatology of monthly runoff. This correction was validated using observed river discharge at 67 gauge stations by Global Runoff Data Center (GRDC). To validate the calculated runoff by the GCMs which was corrected by GSWP2, the runoff by the GCMs was converted into river discharge using river rooting model the Catchment-based Macro-scale Floodplain Model （CaMa-Flood） [*Yamazaki et al.*, 2011]). The validation result showed that the correction of the calculated GCM runoff using GSWP2 worked successfully. The correlation coefficient between the calculated and the observed river discharge improved from 0.89 to 0.95 through the correction.

2.2.4 Simulation setting

Simulations of future glacier mass balance were forced by six GCMs involved in the fifth phase of the Coupled Model Inter-comparison Project (CMIP5) using the highest emissions scenario (representative concentration pathway [RCP] 8.5). PRC8.5 was used to detect an extreme signal of the glaciers to climate change. The six GCMs were selected in conditions: (1) GCMs, which were developed from individual institutions; (2) GCMs, which calculate daily runoff and daily surface air temperature, and daily precipitation. Under these conditions, CCCma-CanESM2, CNRM-CM5, INM-CM4, MPI-ESM-LR, MRI-CGCM3, NCC-NorESM1-M were selected. We used all available GCMs to show the uncertainty range caused by GCM selection.

2.2.5 Analyses

We examined how glaciers would fare (glacier evolution stages) under continuous rising temperature by a trend test of changes in glacier melts until 2100 projected by the glacier model. We analyzed the trend of glacier melts following *Jansson et al.* [2003]' s concept, which under a warming climate, glacier runoff will increase at the initial stage of receding but will decrease at the last stage. We analyzed the long-term trend of projected changes in glacier melts from 2006 to 2099 using the Mann-Kendall test [*Gilbert*, 1987]. Mann-Kendall test is a method to test trends the magnitude relation or order of data. We tested the trends at 5% of the level of significance.

2.2.5.1 Hydrological impacts

Total runoff, which is the sum of the projected glacier melts by the glacier model and the projected runoff by the GCMs and the contribution rate of glaciers, which is the rate of the glacier melts to the total runoff were calculated in each basin. The glacier melts projected by the glacier model and the runoff projected by the GCMs were validated individually as described above (in (2) glacier model and (3) runoff (GCM)). The total runoff and the contribution rate of glaciers were analyzed to assess the hydrological impacts of glaciers melting at a basin scale. Runoff from seasonal snowfall and rainfall on the glacierized areas were derived from the projected runoff by the GCMs.

2.3 Results

In the 10 basins except for the Ganges, the glacier areas were projected to decrease continuously until the end of the 21st century, but the glacier melts in 10 basins were projected to respond differently among the basins (Figure 2.3). The 10 basins except the Ganges were classified into three types (Figure 2.5, Figure 2.6) according to a definition of glacier melt progress based on the projected glacier melts from each basin. To define the glacier melt progress trends of the projected glacier melts (averaged glacier melt in each of the basins) from 2006 to 2100 by the glacier model were analyzed. Indus, Brahmaputra, and Irrawaddy, which showed a downward trend of the projected glacier melts were classified into “ADVANCED”. Tarim, Yangtze, Yellow, and Mekong, which showed an upward trend of the glacier melts were classified into “EARTY”. The Syr Darya, Amu Darya, and the Salween did not show significant trends in the glacier melts. Those basins were classified into “UNKNOWN”.

The future changes in total runoff were projected by adding the glacier meltwater calculated by the glacier into the runoff calculated by GCMs. The total runoffs were projected to continue to increase until the end of the 21st century in all 11 basins (Figure 2.4). The total runoffs were projected to increase with increasing the projected runoff by the GCMs.

2.4 Discussion

2.4.1 Temporal dynamics of glacier melts

2.4.1.1 Classification

"ADVANCED" type basins showed downward trends of glacier melts (Figure 2.3) and they seem to correspond to the downward trend of schematic diagram for the temporal dynamics of glacier melt presented by *Jansson et al.* [2003] (Figure 2.1; Figure 2.5). On the other hand, "EARLY" type basins showed upward trends of the glacier melts (Figure 2.3). It implies that the melting stage corresponds to the upward trend of the schematic diagram (Figure 2.1) and the glacier melts haven't reached their peak during the 21st century. Other basins classified as "UNKNOWN" are unknown where they reach the stage because they don't have any significant trends.

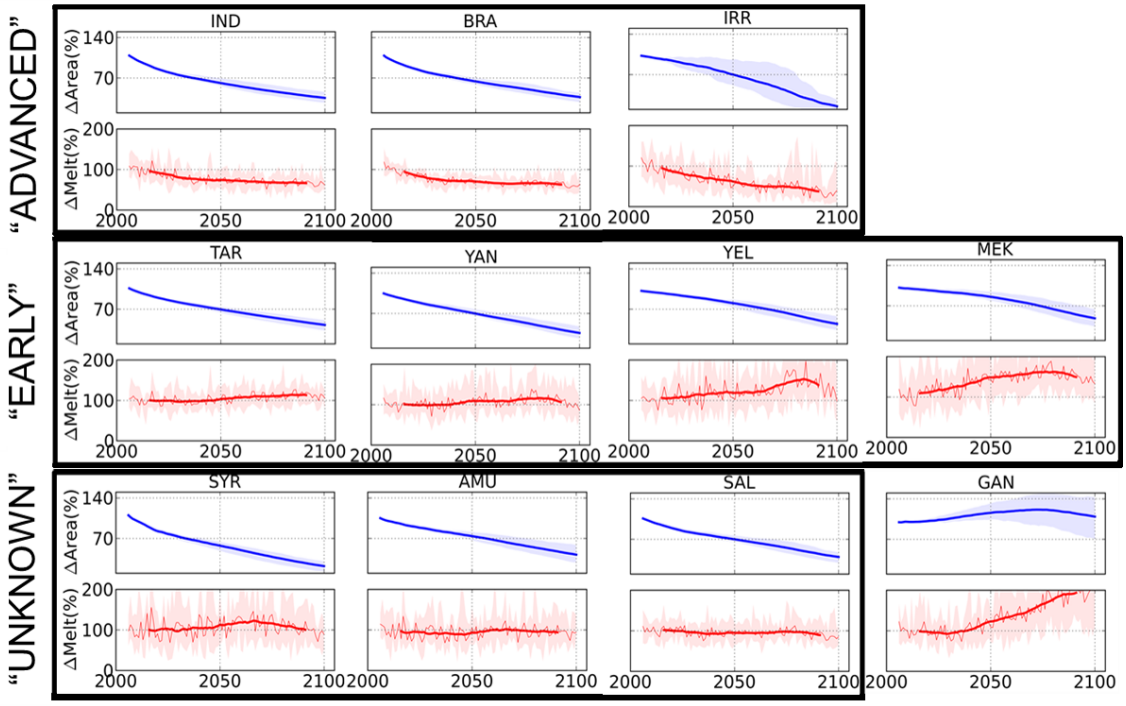

Figure 2.3: Projected change in glacier area and glacier melt. Blue: rate of change in total glacier area (%) in each of the basins relative to 2006-2015 average; Red: rate of change in averaged glacier melt in each of the basins relative to 2006-2015 average; thin lines represent average of the 6 GCMs; shade represents the range of the 6 GCMs; thick lines represent 20-yr moving average.

2.4.1.2 Geographical conditions

Indus basin which was classified as "EARLY" type was implied that it had a melting peak before the 21st century. On the other hand, previous studies (*Rees and Collins* [2006]; *Immerzeel et al.* [2013]) showed a specific basin within Indus experienced the melting peak around 2050. This difference between our study and the previous studies implies that a specific basin doesn't represent the whole basin's behavior.

Air temperatures at the glacierized areas might be a potential cause of the classified melting types. Air temperatures at the glacierized areas in "ADVANCED" basins showed relatively higher values, while those in "EARLY" basins showed lower values (Figure 2.7). "UNKNOWN" basins showed the middle temperatures between "ADVANCED" and "EARLY". Although we also examined snowfalls in the glacierized areas, trends of snowfall didn't become a defining element in the three melting types (Figure 2.8).

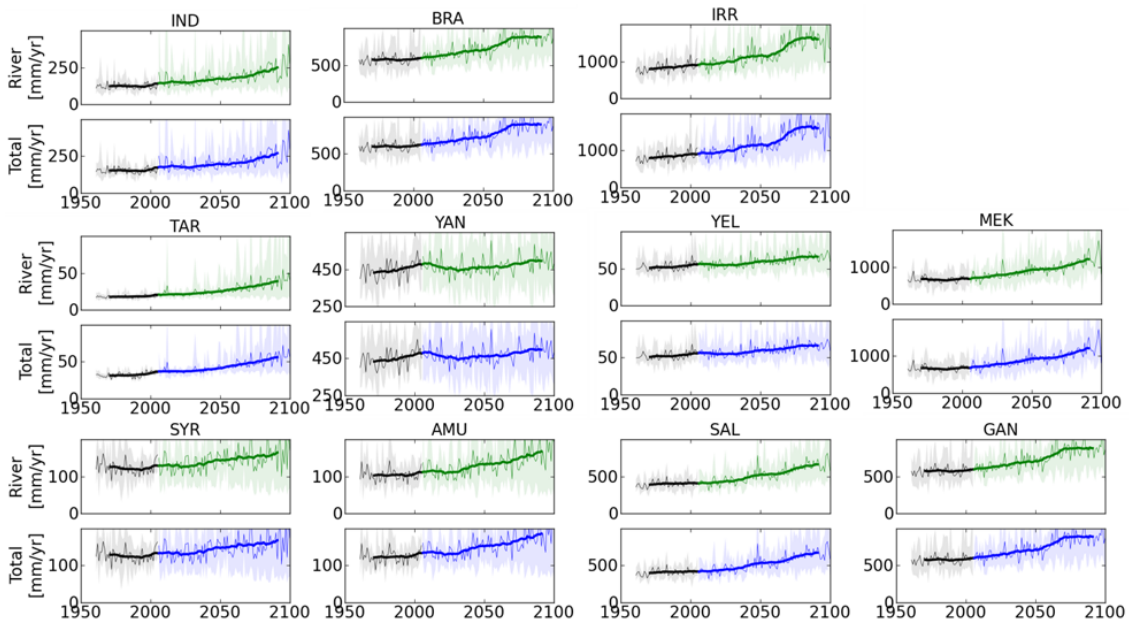

Figure 2.4: Projected runoff without and with glacier melt. The results are based on the average of the different downscaled GCM runs. Green represents: projected river runoff by the GCMs. Blue represents: projected total runoff (runoff + glacier melt). The river runoff and total runoff values are expressed as a catchment average in $mmyr^{-1}$.

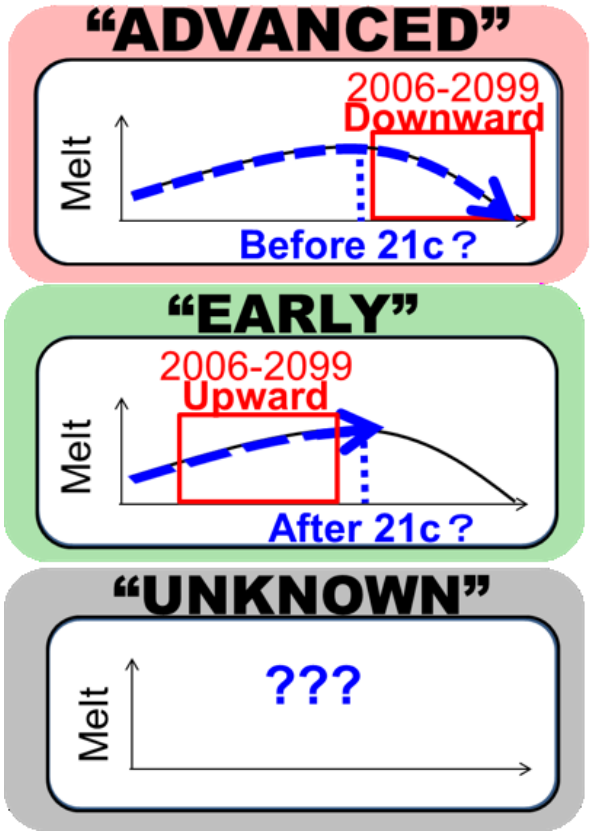

Figure 2.5: Classification of glacier melt type. Black lines are schematic diagrams of long-term dynamical change in glacier melts; Blue dashed arrowed lines represent the calculated change in glacier melts for 2006-2099.

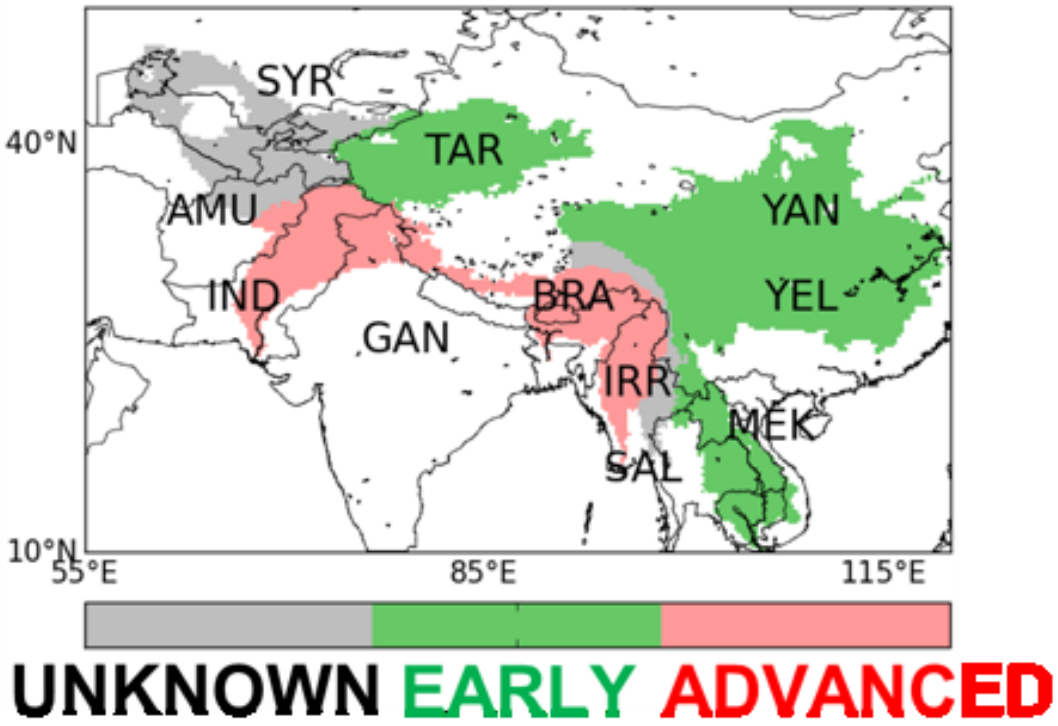

Figure 2.6: Map of melt type classification. Red represents "ADVANCED" type; Green represents "EARLY" ; Black represents "UNKNOWN" in Figure 2.5.

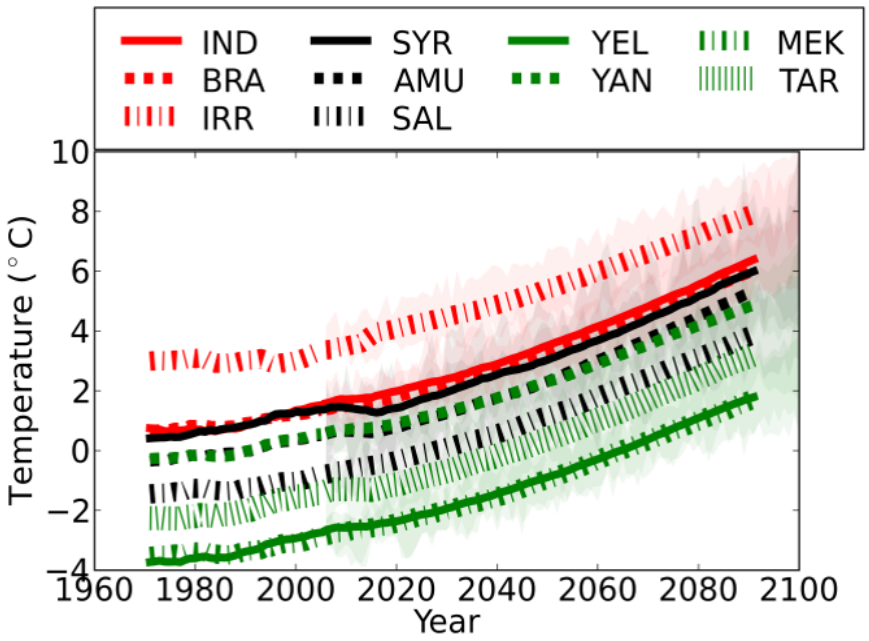

Figure 2.7: Surface annual air temperature in the glacierized area 20-yr moving average. Lines represent the average of the GCMs; shade represents the range from the GCMs; Red represents "ADVANCED" type; Black represents "UNKNOWN" type; Green represents "EARLY" type.

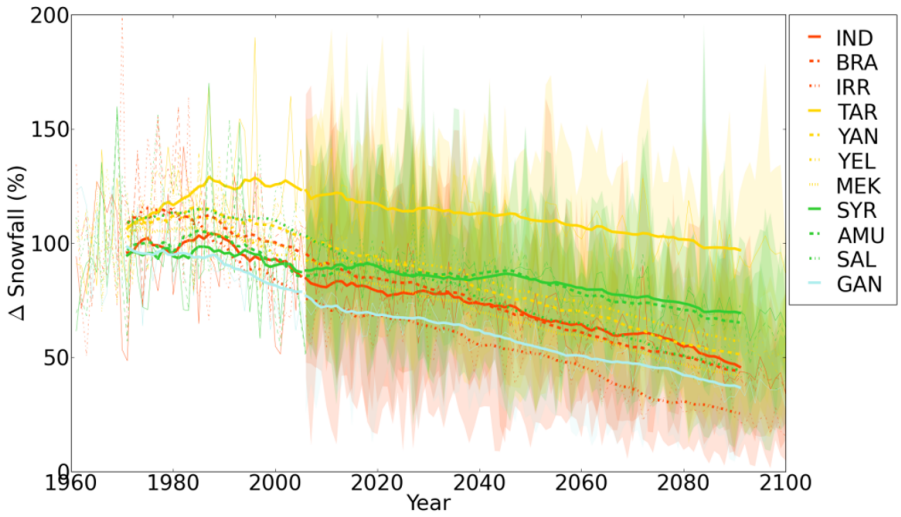

Figure 2.8: Change in snowfall in the glacierised area

Table 2.1: Change in the contribution of glacier melt for runoff (%), change in annual average from 1961-1970 to 2091-2100; The numbers in the brackets are absolute value of annual average glacier melt (mm).TAR: Tarim, SYR: Syr Darya, AMU: Amu Darya, IND: Indus, GAN: Ganges, BRA: Brahmaputra, IRR: Irrawaddy, SAL: Salween, MEK: Mekong, YAN: Yangtze, YEL: Yellow.

Basin	TAR	YAN	YEL	MEK	IND	BRA	IRR	SYR	AMU	SAL	GAN
1961-1970av.	43(13)	0.2(1)	0.2(0)	0.04(0)	20(30)	4(25)	0.02(0)	2(3)	14(18)	2(9)	1(4)
2091-2100av.	30(17)	0.2(1)	0.3(0)	0.04(1)	8(20)	2(17)	0.00(0)	2(3)	10(18)	1(9)	1(8)

2.5 Conclusion

This study showed that the future response of glaciers to climate change using the future changes of glacier melts projected by the glacier model. This study also quantified the future hydrological impact of glacier melts for the 11 downstream basins using the glacier melts projected by the glacier model and the runoff projected by the GCMs.

2.5.1 Temporal dynamics of glacier melts

The responses of glaciers to climate change differed depending on geographical features where glaciers are located at. The responses of glaciers to climate change differed depending on the annual mean air temperature where the glacier was located at. The 11 basins were classified into three types ("EARLY", "UNKNOWN", "ADVANCED") depending on the response of glaciers to climate changes except for the Ganges basin. The peak of glacier meltwater was projected to be before the early 21st century in the case of "EARLY Type". The peak of "ADVANCED Type" was projected to be after the 22nd century.

2.5.2 Hydrological impacts of glacier melting

Annual runoff was projected to increase in all 11 basins in the future. The main reason for these increases was not the increase in glacier melt. Future changes in glacier melt were not the most dominant factor to change annual runoff quantity at major river basin scale (Table 2.1). However, at Indus and Brahmaputra, dependency on glacier melt was projected to decrease dramatically. It implied that these basins could have a problem with water resources in dry seasons.

2.5.3 Possible future direction

The impact of seasonal runoff should be assessed as further work. In this study, the period for the assessment and the choice of glacier model and climate scenario could be uncertain of the result. Therefore, extending the assessment into the 22nd century or using a multi-glacier model and multi-climate scenario need to be achieved in future work.

Chapter 3

Updated calibration of the glacier model for the uncertainty assessment

3.1 Backgroud

Observed past climate data which are used as input data in glacier models are expected to be different among datasets especially for precipitation at high elevations. The difference in the observed past climate datasets has not been pointed out as one of the causes of the uncertainties in projecting future glacier mass changes yet although the uncertainty caused by the spread of future climate projections among GCMs has been often discussed. The differences in the observed past climate datasets are expected to propagate the uncertainty in future glacier mass changes due to bias correction of GCMs and calibration of glacier model.

The spread of future climate projections among GCMs is not the only cause of uncertainty in projecting future glacier mass change. Even observed past air temperature and precipitation which are used as input data in glacier models are expected to be different among climate datasets. These differences among observed air temperature and precipitation datasets also could cause uncertainty in projecting future glacier mass change in addition to the spread of climate projections by GCMs. The difference among observed climate datasets for the past lies in the Spatio-temporal interpolation of a naturally discontinuous and intermittent field and/or the assumptions needed to convert a physical

measurement from remote sensing [*Energy and Exchanges*, 2013].

HYOGA2 is a glacier model and it computes glacier mass balances forced by daily precipitation and surface air temperature. HYOGA2 computes the mass of melted glaciers using a degree-day approach. HYOGA2 calibrates only melt factors as parameters for the degree-day approach. Therefore, it was pointed out that the glacier model simulation might not be accurate because of the limitations of the global climate input data sets, at glaciers located in poorly gauged regions such as High Mountain Asia [*Hirabayashi et al.*, 2013].

The initial error of the glacier model because of the limitations of the global climate input data sets would affect the assessment of the uncertainty of future change in glacier mass. Therefore, HYOGA2 needs to be reduced the initial error by calibrating air temperature and precipitation. Other global glacier models often calibrate air temperature and precipitation in addition to the melt factors [*Hirabayashi et al.*, 2013; *Huss and Hock*, 2015]. We try to apply a similar method.

In this chapter, we try to update the calibration method for the glacier model to quantify each source of uncertainty in the mass change projections of Asian glaciers.

3.2 Method

3.2.1 Target

Our study region covers high-mountain Asia (26.5 – 55.5N, 66.5 – 104.5E), which corresponds to the regions of central Asia, southwestern Asia, southeastern Asia, and Altay and Sayan of northern Asia in the Randolph Glacier Inventory [*Pfeffer et al.*, 2014]. In the study region, long-term in-situ observed mass balance data is available for ten glaciers. Those observed mass balance data at the 10 glaciers were used to calibrate a glacier model. Around the 10 glaciers, there are 1,442 glaciers. From the 1,442 glaciers, 304 glaciers were randomly selected (reliability: 95%; Request error: 5%) to show an overall trend for High Mountain Asia. We projected total glacier melts for the 304 glaciers and analyzed them.

3.2.2 Glacier model

We used the model HYOGA2, which was developed for global-scale mass-balance calculations and applied to project the volume evolution of all glaciers outside the Antarctic and Greenland ice sheets through 2100 [*Hirabayashi et al.*, 2013]. Glacier mass balance was

calculated using the glacier model forced by daily precipitation and surface air temperature. The melt rates of the surfaces of snow and ice at each elevation band were calculated using a simple degree-day approach as follows:

$$\begin{aligned} Mg_i &= (T_i - T_0)DDF_{ice} \quad if T_i > T_0, \quad and \quad S_i(t) = 0 \\ &= 0 \quad otherwise \end{aligned} \tag{3.1}$$

and then aggregated to estimate the mass balance for each glacier. Subgrid-scale variation in changes in glacier and snow mass was considered by dividing a model grid cell into 50 m elevation bands. The surface air temperature was assumed to decrease at a constant lapse rate of -0.65 °C $(100m)^{-1}$. The glacier model assumes that only precipitation that falls as snow affects the mass balance. Precipitation is assumed to fall as snow if the air temperature of the elevation band is less than or equal to 2°C.

A is updated after each time step based on the new total glacier volume using the following equation:

$$A = (\frac{V}{c_a})^{\frac{1}{\gamma}} \tag{3.2}$$

where A km^2 and V km^3 are, respectively, the total glacier area and volume in each glacier, and c_a and γ are model parameters. For all valley glaciers, the model assumed fixed parameter values: $\gamma = 1.375$ from *Bahr et al.* [1997] and $c_a = 0.2055$ $m^{3-2\gamma}$ from *Chen and Ohmura* [1990]. For all ice cap glaciers, the model assumed fixed parameter values: $\gamma = 1.25$ from *Bahr et al.* [1997] and $c_a = 1.7026$ $m^{3-2\gamma}$ from *Chen and Ohmura* [1990].

3.2.3 Climate forcing data for past period

Observed past air temperature and precipitation datasets were used as references for bias correction of GCMs and calibration of the glacier model to determine parameters. To evaluate the uncertainty in projections of changes in glacier mass arising from the observed past climate datasets, a set of three combinations of one observed past air temperature

dataset and three observed past precipitation datasets were defined. We used CRU air temperature, APHRODITE precipitation, Sakai precipitation, and MSWEP precipitation.

3.2.3.1 Observed past air temperature dataset 1: CRU-based

CRU provides gridded surface air temperature and precipitation data such as CRU TS 3.10, which interpolates in situ observations and has often been used in global glacier modeling studies [*Marzeion et al.*, 2012, 2018; *Giesen and Oerlemans*, 2013; *Hirabayashi et al.*, 2013; *Slangen et al.*, 2017]. Therefore, we used a CRU-based temperature [*Hirabayashi et al.*, 2008].

3.2.3.2 Observed past air temperature dataset 2: EAR-Interim

Daily ERA-Interim reanalysis data [*Dee et al.*, 2011] including surface air temperature, geopotential height were used to calculate glacier mass balance. Several previous studies which have projected glacier melt at a large scale used air temperature data in ERA-Interim. Air temperature in ERA-Interim is represented better than in another reanalysis product on glaciers in High Mountain Asia [*Sakai et al.*, 2015].

3.2.3.3 Observed past precipitation dataset 1: APHRODITE

For gridded precipitation data based on in situ observations in Asia, the precipitation product suite "Asian Precipitation – Highly Resolved Observational Data Integration Towards Evaluation of Water Resources" (APHRODITE; *Yatagai et al.* [2012]), which has the most extensive rain gauge network, was used to project changes in the mass of glaciers in Asia, rather than global precipitation datasets such as that provided by CRU [*Lutz et al.*, 2014]. Therefore, we used APHRODITE precipitation.

3.2.3.4 Observed past precipitation dataset 2: Sakai

Sakai et al. [2015] estimated precipitation contributing to glacier mass at the median elevation of glaciers, which is presumed to be at equilibrium line altitude (ELA) such that mass balance is zero at that elevation, by tuning adjustment parameters of precipitation. They decided on correction factors for APHRODITE precipitation for the glacierized area in High Mountain Asia.

3.2.3.5 Observed past precipitation dataset 3: MSWEP

Beck et al. [2017] corrected precipitation observations using gauged discharge data when developing Multi-Source Weighted-Ensemble Precipitation (MSWEP), the latest global gridded precipitation product. In this study, we also used MSWEP to calculate changes in the mass of glaciers.

3.2.4 Calibaratoin

The individual glaciers obtained from the RGI (Randolph Glacier Inventory) inventory were firstly aggregated into one large glacier in 0.5° grid cells. Then, parameters for each cell were calibrated until yielding the maximum agreement with the cell-specific long-term (1981 – 2004) average of total glacier mass balance. Two approaches were tested to calibrate glacier mass balance. Gridded mass balance observed data developed in *Hirabayashi et al.* [2013] were used for our calibration. It is based on *Dyurgerov and Meier* [2005, 1997]; *Serreze et al.* [2000].

The first approach calibrated two parameters: the degree-day factors (DDFs) for ice and snow respectively. This method was applied to the previous study using HYOGA2 [*Hirabayashi et al.*, 2013]. The second approach calibrated four parameters: the DDFs for ice and snow, adjustment factors for precipitation (Cp), and temperature data (dT) (Figure 3.1). The method of calibrating adjustment factors related to precipitation and temperature data is a commonly used method in previous global glacier studies [*Marzeion et al.*, 2012; *Radić et al.*, 2014]. The latest global glacier model also applied a similar calibration method [*Huss and Hock*, 2015]. We also calibrated adjustment factors for precipitation and temperature data additionally following the previous studies. The order of calibration of each parameter (Figure 3.1) was decided by following *Huss and Hock* [2015]. First, adjustment for precipitation data was calibrated. If no agreement is found within the tested range, Cp is set to the value that resulted in the smallest deviation from modeled mass balance and observations. Secondly, the DDFs were calibrated. If the target mass balance cannot be reproduced within the DDFs parameter range we assume that there is a systematic error in the temperature data. Thus, in a final third step, we systematically shift the air temperature series by dT. The range of each parameter was described in Table 5.1. The spatial distributions of parameters were shown in Figure 3.2, Figure 3.3, Figure 3.4 and Figure 3.5.

We calibrated each parameter of two methods for a combination of two temperature

data and four precipitation data. However, the precipitation data in *Sakai et al.* [2015] already corrected the precipitation data using glacier elevation information. Therefore, we calibrated only the DDFs and adjustment factor of temperature data for the second method in two combinations of *Sakai et al.* [2015] precipitation data, temperature data, and ERA-interim temperature data.

3.3 Results

3.3.1 calibration

In the case of the first approach of calibration method (only the DDFs were calibrated), modeled glacier mass balance did not have a good agreement with observed glacier mass balance using any combination of observed past air temperature and precipitation datasets (Figure 3.6, black). The modeled glacier mass balance using the first approach of calibration (only the DDFs were calibrated) underestimated compared with observed mass balance. In the case of the second approach of calibration method (Cp, the DDFs and the dT were calibrated), mostly modeled glacier mass balance had a good agreement with observed mass balance (Figure 3.6, Red).

The two calibration methods have been applied to the glacier model. Figure 3.6 compares modeled and observed long-term average glacier mass changes aggregated into one large glacier in 0.5° grid cells for the calibration period. As expected, for the average mass balance of each glacierized grid by the former approach which calibrated the degree day factors (DDFice and DDFsnow) there are discrepancies between modeled and observed mass balance. There is a tendency for the model to overestimate mass loss compared with the observations in most combinations of precipitation and temperature data. In contrast, for the latter approach which calibrated the adjustment factors for precipitation and temperature data (Cp and dT) additionally the model results more fitted to the observations than the former calibration approach in any combinations of climate data even though there is still discrepancy. Using temperature data of ERA-Interim with calibrating only the DDFs reduced the error by approximately 200% (with APHRODITE precipitation) compared with that using temperature data of CRU (Table 3.2). However, it still overestimated glacier mass loss compared with the observed mass balance at some glacierized grids (the average error was around 50% in Table 3.2). Calibrating Cp and dT with Sakai or MSWEP precipitation and ERA-Interim temperature reduced the average error from

65% to 49% or from 67% to 39%, respectively (Table 3.2). The model forced by Sakai precipitation overestimated glacier mass loss at some glacierized grids before calibrating Cp and dT whereas it underestimated glacier mass loss using MSWEP.

The adjustment factor for precipitation were determined as upper limit (2.0) in many grids in most of combinations of climate forcing datasets (Figure 3.2). The adjustment factor for air temperature dT were determined as nearly lower limit when using the combinations with CRU-based air temperature dataset around Karakoram regions (Figure 3.5).

3.4 Discussion

It is well known that observed past precipitation datasets such as APHRODITE often underestimate precipitation at high elevations. The glacier model used in this study could have underestimated glacier accumulation because of underestimated precipitation. Therefore, the glacier model overestimated glacier mass loss compared with observed glacier mass loss when the adjustment factor of precipitation was not calibrated (the second approach of calibration method). When the adjustment factors for precipitation and air temperature were calibrated the bias of observed past precipitation and air temperature datasets were adjusted and the difference of glacier mass balance between modeled and observed decreased.

The both of underestimation of APHRODITE precipitation and the warm bias of CRU temperature caused underestimating snowfall and overestimating glacier melts without adjusting the bias of climate forcing data. The modeled mass balance forced by the precipitation data which inversely corrected orographic bias such as Sakai or MSWEP and ERA-interim reanalysis temperature is close to the observed mass balance without adjusting climate forcing data compared with the modeled mass balance forced by simply interpolated observation based products (APHRODITE and CRU). There is still discrepancy in some glacierzed areas although Sakai or MSWEP precipitation and ERA-Interim temperature area used for the glacier model. The overestimating snowfall in the glacier model resulted from overestimation of precipitation in MSWEP caused by the interpolation method. The underestimation of modeled glacier mass loss forced by Sakai precipitation might be a consequence of underestimation of precipitation or limitation of using the point glacier mass balance observation for the calibration. Although Sakai or MSWEP precipi-

tation and ERA-Interim temperature data are preferable to simulate glacier mass balance in most glacierized areas, the error of modeled mass balance could be reduced more by calibrating the bias of each climate forcing data.

3.5 Conclusion

In sparsely observed High Mountain Asian, to assess propagation of uncertainty in projection of future glacier mass balance arising from difference among observed past climate datasets I updated the calibration method of the glacier model. I updated the calibration method to exclude initial errors of the glacier mass balance simulation; otherwise, the initial error could affect the assessment of uncertainty arising from difference among observed past climate datasets. After we additionally calibrated the adjustment factors for precipitation and air temperature, the modeled glacier mass had the good agreement with the observed mass balance and the initial errors of modeled glacier mass balance were excluded.

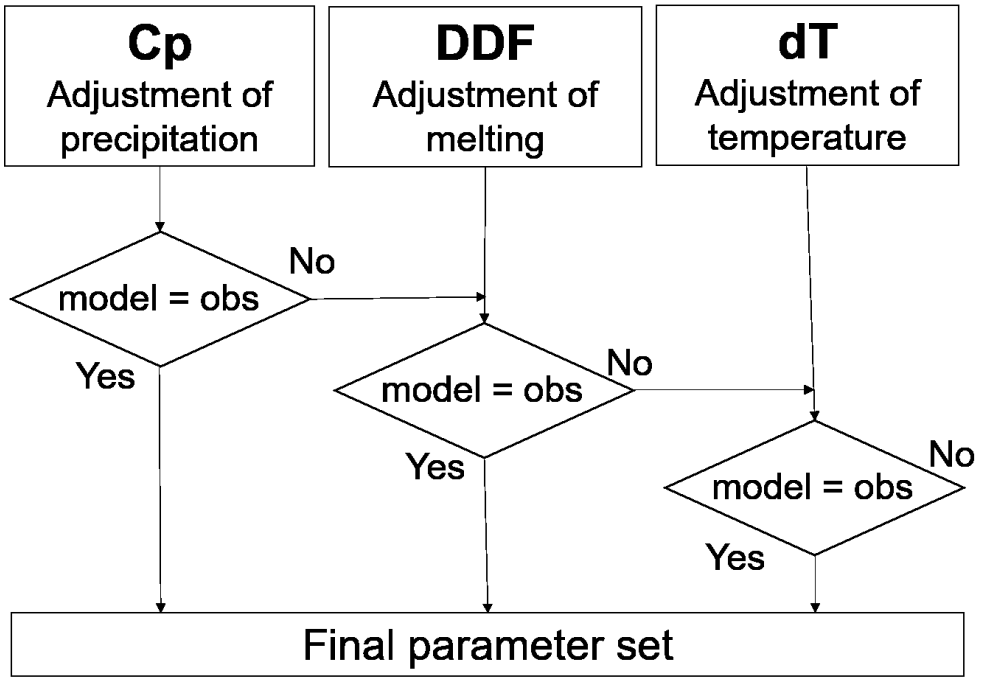

Figure 3.1: Visualization of the calibration scheme

Table 3.1: The ranges of parameters

Parameter	Range
Cp (Adjustment factor for precipitation) [-]	0.8 to 2.0
DDFice (The degree-day factor) [mm $^{\circ}C^{-1}$ day^{-1}]	4 to 20
DDFsnow (The degree-day factor) [mm $^{\circ}C^{-1}$ day^{-1}]	1 to 4
dT (Adjustment factor for air temperature) [℃]	-5.0 to 5.0

Table 3.2: Comparisons of averaged calibration errors. The calibration errors were calculated as the relative errors of modeled annual glacier mass balances compared to the observed mass balances for 1980 – 2004. The relative errors (%) were averaged for glacierized grids for which observed glacier mass balances were available. The DDFs were calibrated using Method 1 and the Cp, DDFs, and dT calibrated employing Method 2.

Climate forcing	Method1 (%) T	Method2 (%)
APHRODITE P - CRU T	260	52
Sakai P – CRU T	163	37
MSWEP P – CRU T	132	47
APHRODITE P – ERA-Interim T	54	50
Sakai P – ERA-Interim T	65	49
MSWEP P – ERA-Interim T	67	39

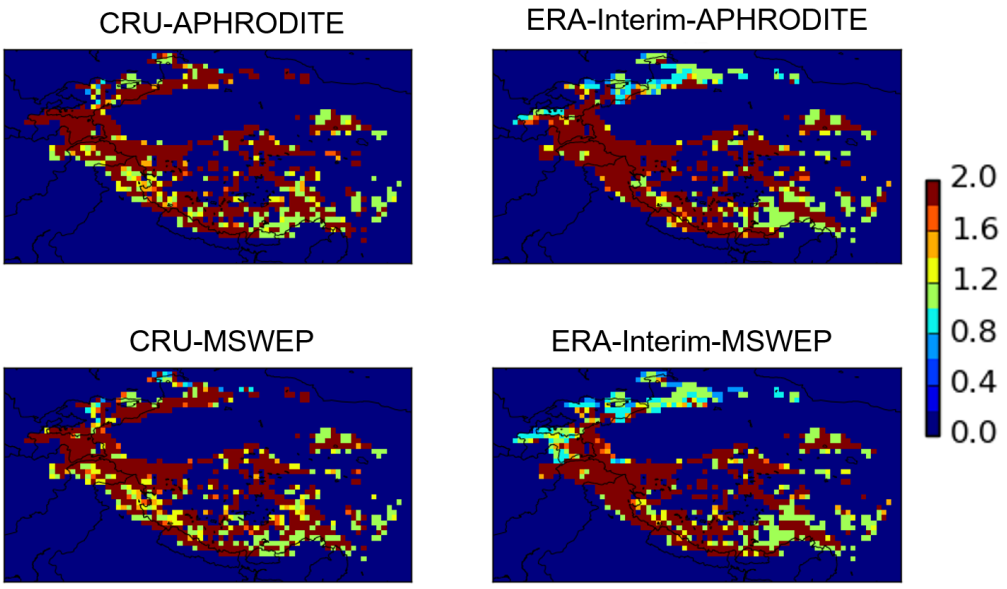

Figure 3.2: Determined Adjustment factors for precipitation

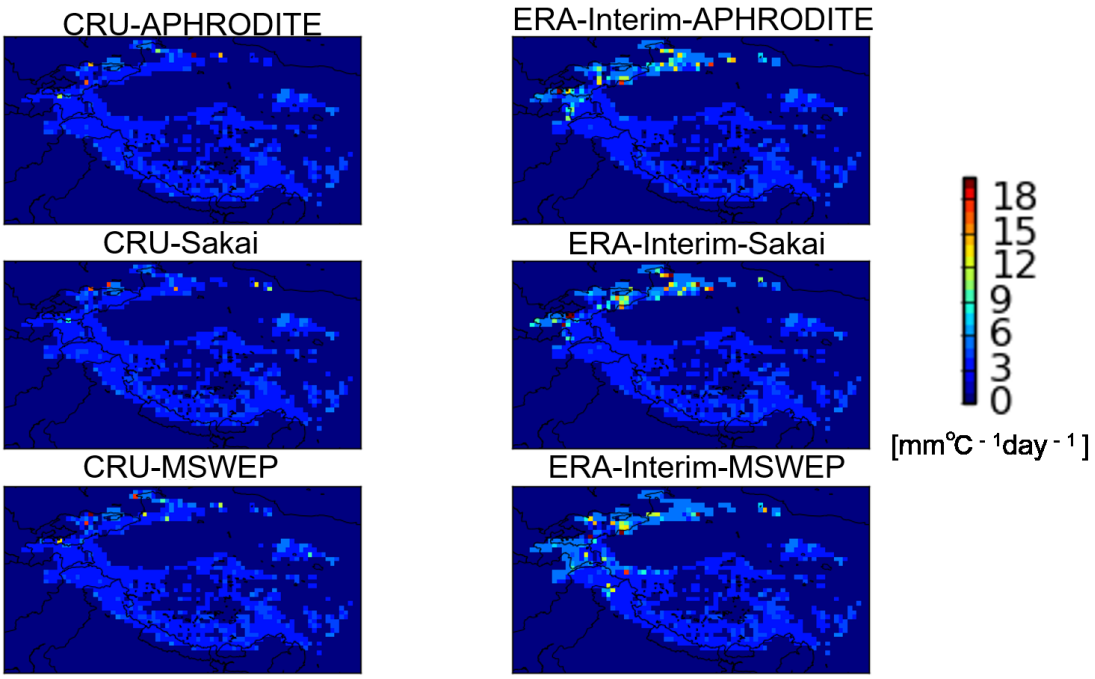

Figure 3.3: Determined degree-day factor for ice

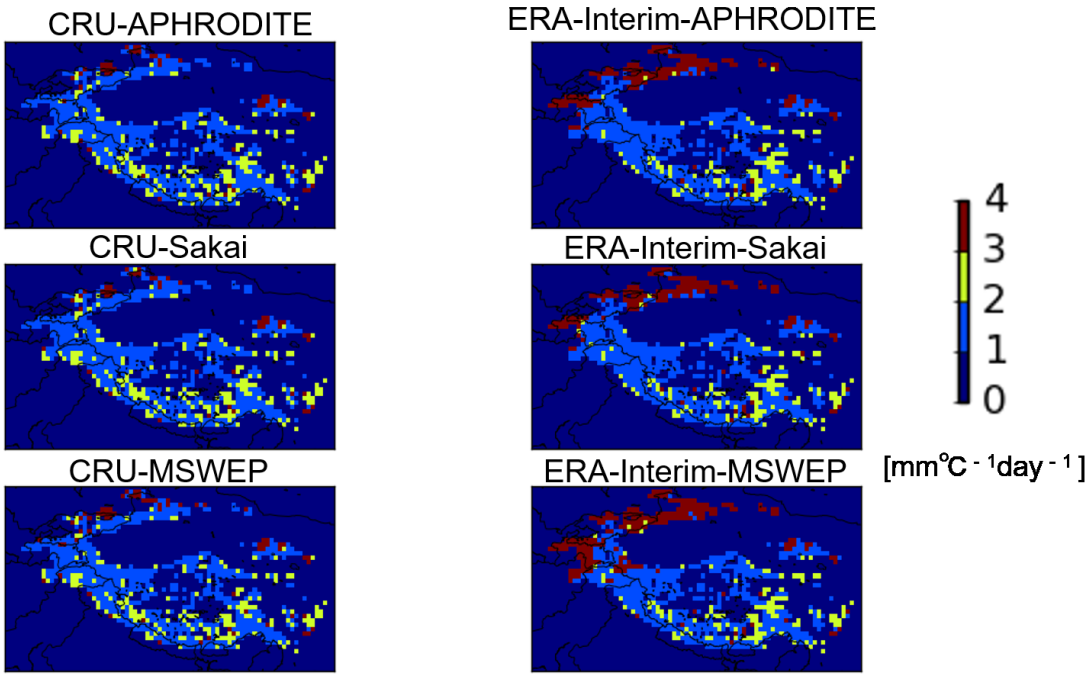

Figure 3.4: Determined degree-day factor for snow

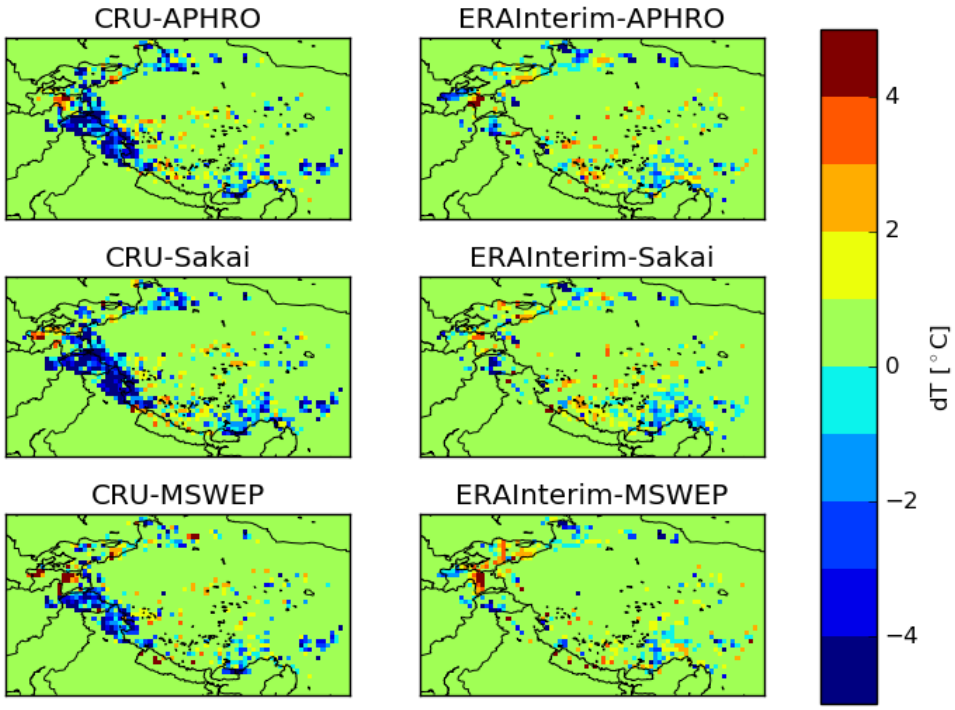

Figure 3.5: Determined Adjustment factors for air temperature

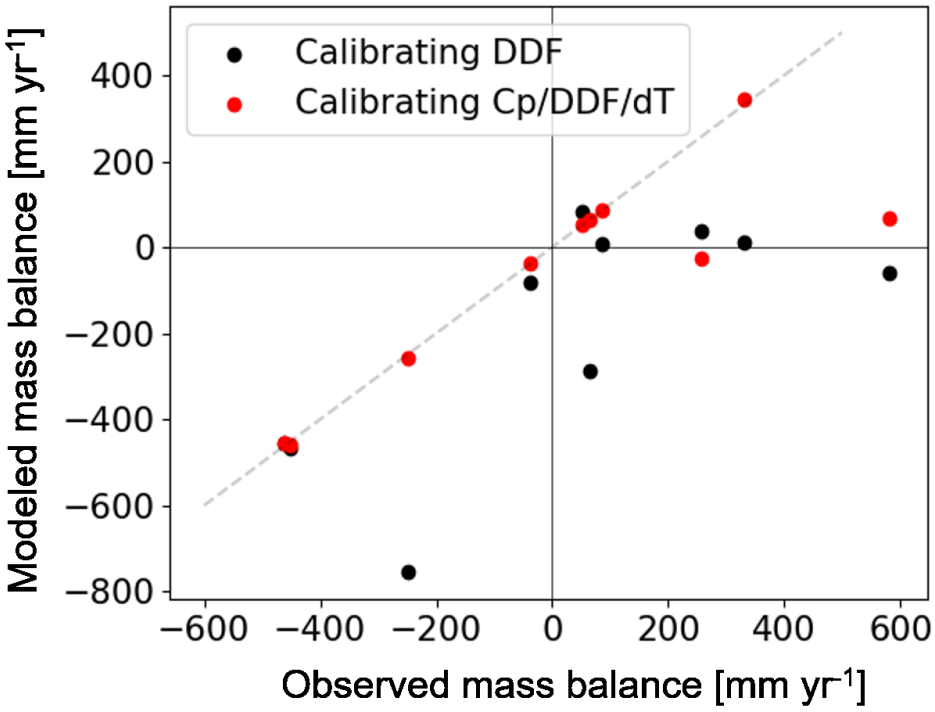

Figure 3.6: Validation of the calibrated glacier mass balance. Comparison of modeled and observed average annual glacier mass balance for 1980-2004 using CRU based air temperature - APHRODITE precipitation)

Chapter 4

Uncertainty assessment

4.1 Background

Worldwide, glaciers have reacted sensitively to recent changes in climate forcing and are expected to experience continued mass loss throughout the twenty-first century [*Stocker*, 2014]. Glacial retreat raises major concerns about the sustainability of global and local water resources, sea level rise, and natural hazards [*Immerzeel et al.*, 2010; *Kaser et al.*, 2010; *Fujita et al.*, 2013; *Stocker*, 2014]. Future global mass changes in glaciers are predicted by various glacier models. Several studies have attempted to predict future changes worldwide [*Marzeion et al.*, 2012; *Hirabayashi et al.*, 2013; *Radić et al.*, 2014; *Huss and Hock*, 2015]. To simulate such changes, glacier models use climate projections as input such as future air temperature and precipitation from general circulation models (GCMs). The climate projections of the various GCMs differ markedly, even among those using the same emissions scenarios [*Stocker*, 2014]. Such ranges are defined as "uncertainties" in the present study. Uncertainty in terms of climate prediction has several distinct sources. Model uncertainty reflects limitations in model structure and the parameterization used to represent geophysical processes. The internal variability of a climate system reflects the natural fluctuations that arise in the absence of any radiative forcing of the planet. These model uncertainties and internal variabilities will here be termed "GCM uncertainties." We used a single climate scenario (RCP8.5), we did not explore scenario uncertainty. Uncertainties among climate projections propagate to projections of mass changes along the modeling chain, thus from GCMs to glacier models. The latter models address these uncertainties when projecting future changes in glacier mass [*Marzeion et al.*, 2012; *Hirabayashi et al.*, 2013; *Radić et al.*, 2014; *Huss and Hock*, 2015].

The range of future climate projections among GCMs is not the only source of uncertainty in projections of future changes in glacier mass. Even observed past air temperatures and precipitation, which are used as input data in glacier models, are expected to differ among climate datasets. These differences could also cause uncertainty in projections. The differences among climate datasets arise from spatiotemporal interpolation of naturally discontinuous and intermittent field data and the assumptions needed to obtain physical measurements from remote sensing [*Energy and Exchanges*, 2013]. As is well known, the significant differences among observed past precipitation datasets derived from mountainous areas reflect under-representation of gauge locations at high elevations and wind-induced undercatch of solid precipitation [*Adam et al.*, 2006; *Hirabayashi et al.*, 2008; *Biemans et al.*, 2009]. Some authors have expressed concern that these differences might affect simulations of glacio-hydrological budgets [*Bookhagen and Strecker*, 2008; *Andermann et al.*, 2011; *Palazzi et al.*, 2012; *Dahri et al.*, 2016]. The differences may markedly influence projections of future changes in glacier mass.

Differences among past air temperature and precipitation datasets propagate uncertainties into simulations featuring bias correction of GCMs, and calibration (Figure 4.1), both of these steps are required when projecting changes in glacier mass using glacier models [*Marzeion et al.*, 2012; *Giesen and Oerlemans*, 2013; *Hirabayashi et al.*, 2013; *Bliss et al.*, 2014; *Huss and Hock*, 2015]. The data serve as references for bias correction and forcing factors when calibrating glacier models that seek to determine parameters such as melting factors and adjustment parameters for climatic data. Thus, uncertainties in climatic datasets propagate into projections of future changes in glacier mass.

Most previous glacier model studies have used a single air temperature dataset and a single precipitation dataset to project changes in glacier mass, and did not assess the uncertainty arising from differences among climate datasets [*Marzeion et al.*, 2012; *Giesen and Oerlemans*, 2013; *Hirabayashi et al.*, 2013; *Bliss et al.*, 2014; *Huss and Hock*, 2015]. Why this is so is unknown but studies using other impact models such as hydrological models have also tended to do this. One reason could be that it is difficult to handle heterogeneous climate datasets with different spatiotemporal resolutions, domains, and data formats, and this hampers assessment of the impacts of uncertainty derived from those datasets.

Koppes et al. [2015] assessed the temperature-sensitivity of glacier meltwater to 2100 in terms of observed past air temperature data, past climate forcing in the Indus River

basin was evaluated. The glacier model parameters were constant among all simulations, even when different observed past air temperatures were employed, GCMs were not used to project future changes in glacier mass. Thus, a further study assessing the impacts of differences among observed past air temperatures and precipitation is necessary. In addition, the uncertainties propagated by bias correction of GCMs and determination of glacier model parameters require evaluation because most prior glacier models used such methods.

The HMA contains the largest mass of land glacier ice with the exception of the poles. The HMA glaciers are retreating and losing mass at rates comparable to glaciers in other regions of the world [*Fujita and Nuimura*, 2011; *Bolch et al.*, 2012; *Kääb et al.*, 2012; *Brun et al.*, 2017]. Meltwaters from HMA glaciers flow into downstream rivers, large human populations depend on glacier-fed water supplies. The impact of climate change on the extent of glacier melt is of major interest. The HMA includes the Tibetan Plateau, for which observed climatic datasets and GCM climate projections are among the sparsest worldwide [*Stocker*, 2014]. This region is characterized by high-level orography and a large proportion of solid precipitation, both of which would be expected to greatly bias observations.

Therefore, we assessed the uncertainty caused by differences in observed past air temperature and precipitation datasets, and also uncertainty arising from differences among GCMs. The uncertainties in future glacier mass change projections caused by the differences in observed past climate data used to correct GCM biases and calibrate glacier models were assessed. We focused on particularly the HMA, for which past air temperature and precipitation data are scant and GCM future climate projections are uncertain.

4.2 Methods

4.2.0.1 Overview

We projected changes in the mass of Asian glaciers through 2100 using a glacier model based on two observed past air temperature datasets, three observed past precipitation datasets, and three GCMs to quantify the potential uncertainties, as described above (Figure 4.1). The uncertainty was partitioned into three distinct sources: GCM uncertainty, observed past air temperature uncertainty, and observed past precipitation uncertainty.

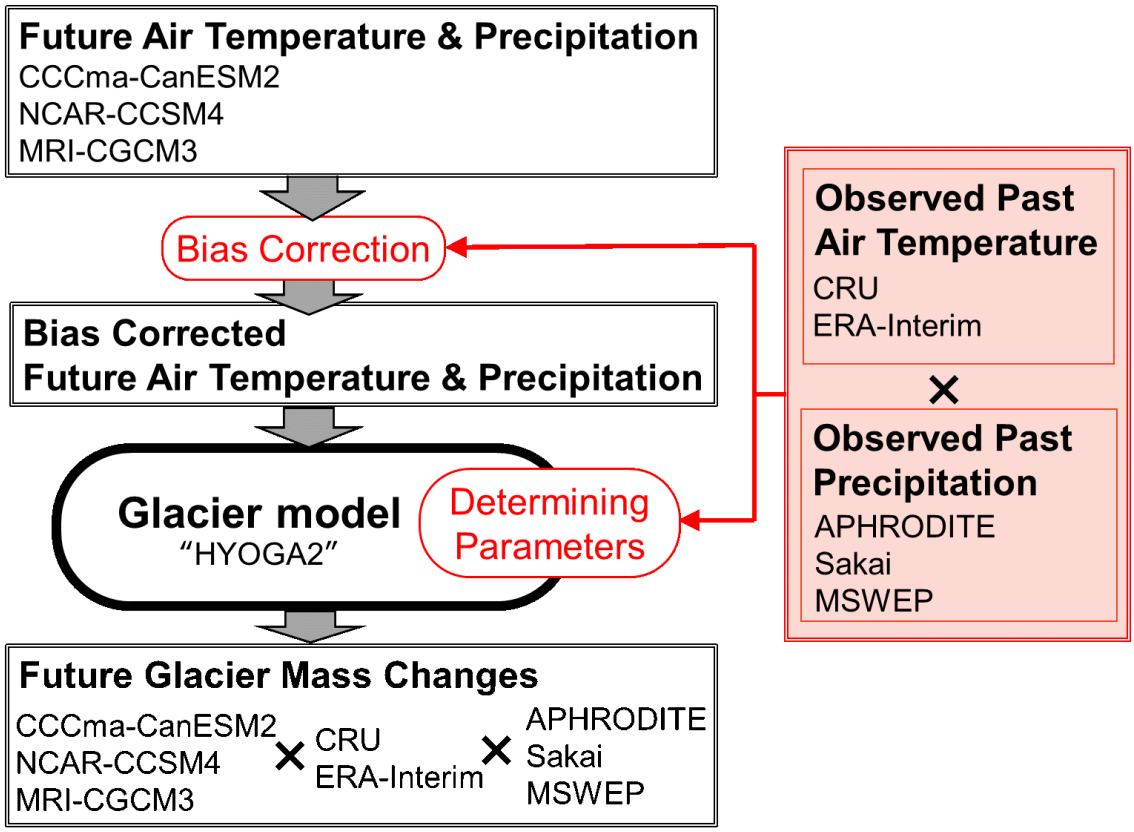

Figure 4.1: Overview of projection of changes in glacier mass. "Future Air Temperature & Precipitation" data from the climate projections of GCMs (CCCma-CanESM2, NCAR-CCSM4, and MRI-CGCM3) served as climate forcing factors when making predictions. The "Future Air Temperature & Precipitation" data were corrected by the "Bias Correction" procedure using "Observed Past Air Temperature" (CRU, ERA-Interim) and "Observed Past Precipitation" (APHRODITE, Sakai, MSWEP) as references. The "Observed Past Air Temperature" and the "Observed Past Precipitation" also served as forcing factors in the "Glacier model HYOGA2" during calibration of "Determining Parameters." Finally, using "Bias Corrected Future Air Temperature & Precipitation" as a future climate forcing parameter, the "Glacier model HYOGA2" calculated "Future Glacier Mass Changes" for each combination of input data (18 combinations of three "Future Air Temperature & Precipitation" datasets of the GCMs, two "Observed Past Air Temperature" datasets, and three "Observed Past Precipitation" datasets). Here, "X" indicates combinations.

4.2.1 Targeted glaciers

Our study region was the high mountains of Asia (26.5 – 55.5N, 66.5 – 104.5 E), corresponding to central, southwestern, and southeastern Asia, as well as the Altay and Sayan regions of northern Asia in the Randolph Glacier Inventory (RGI6.0). In this area, 19 observations of glacier mass balance are available for use in calibrating glacier models for experiments. Eight of these data points were well calibrated (i.e., calibration errors were within $\pm$ 50%). Some points were not well calibrated: warm bias was evident in observed air temperature datasets, the observed precipitation datasets exhibited large spreads, and the quality of mass balance observations was suspect. From 1,084 glaciers located near the eight points in the RGI6.0, 28 glaciers where the range of mass balance for the calibration period was small in all simulation runs were chosen randomly (reliability: 95%, request error: 5%). The area-weighted means of the mass balances of these 28 glaciers shown in Figure 4.2 were used to assess uncertainty in the experiments.

4.2.2 Glacier model

We used the model HYOGA2, which was developed for global-scale mass-balance calculations and applied to project the volume evolution of all glaciers outside the Antarctic and Greenland ice sheets through 2100 [*Hirabayashi et al.*, 2013]. We updated the calibration method for the glacier model to quantify each source of uncertainty in the mass change projections of Asian glaciers (see 2.5.2. for details, [*Watanabe et al.*, 2018]). The distributed glacier input data for the model was also updated to the latest RGI.

Glacier mass balance was calculated using the glacier model forced by daily precipitation and surface air temperature. The melt rates of the surfaces of snow and ice at each elevation band were calculated using a simple degree-day approach and then aggregated to estimate the mass balance for each glacier. Subgrid-scale variation in changes in glacier and snow mass was considered by dividing a model grid cell into 50 m elevation bands. The surface air temperature was assumed to decrease at a constant lapse rate of -0.65 $^\circ$ C $(100m)^{-1}$. We did not incorporate precipitation lapse rates because each precipitation dataset considered the orography. We calculated the differences between the grid cell altitudes of each observed air temperature dataset and the median glacier altitude. We used this difference to derive the temperature lapse rate for each glacier. The model assumes that only snow affects the mass balance. Precipitation was assumed to be snow if the air temperature of the elevation band was less than or equal to 2° C. The basic

model structure is similar to that of other global glacier models such as the Global Glacier Evolution Model (GloGEM, [*Huss and Hock*, 2015]), the Radic and Hock model [*Radić et al.*, 2014], and the Marzeion model [*Marzeion et al.*, 2012].

In our study area, the average annual mass balance of the 28 HMA glaciers (Section 2.2 and Figure 4.2) was simulated as – 0.21 ± 0.14 m w.e. $year^{-1}$ from 2003 to 2009. The observed annual mass balance of all HMA glaciers was – 0.22 ± 0.10 m w.e. $year^{-1}$ from 2003 to 2009 *Gardner et al.* [2013]. The modeled and observed values are similar, although a direct comparison is inappropriate. The root mean-square error between the modeled and observed mass balances *Gardner et al.* [2013] was 0.14 m w.e. $year^{-1}$, thus less than the error range of other global glacier models [*Marzeion et al.*, 2012; *Radić et al.*, 2014], although, again, direct comparisons are inappropriate. *Marzeion et al.* [2012] reported that the root mean error between the modeled and observed mass balance of HMA (North) was 0.33 ± 0.11 m w.e. $year^{-1}$, for HMA (West) 0.42 ± 0.20 m w.e. $year^{-1}$, and for HMA (South) 0.37 ± 0.16 m w.e. $year^{-1}$. *Radić et al.* [2014] reported that the root mean error between the modeled and observed HMA mass balance was 1.05 m w.e. $year^{-1}$. The latest model study [*Huss and Hock*, 2015] estimates were – 0.05 m w.e. $year^{-1}$ for 2001 – 2005 and – 0.3 m w.e. $year^{-1}$ for 2006 – 2010 for the HMA. Our results are similar (– 0.02 m w.e. $year^{-1}$ for 2001 – 2005, – 0.36 m w.e. $year^{-1}$ for 2006 – 2010).

4.2.3 Observed past air temperature and precipitation data

Observed past air temperature and precipitation datasets were used as references for bias correction of GCMs and calibration of the glacier model to determine parameters. To evaluate the uncertainty in projections of changes in glacier mass arising from the observed past climate datasets, a set of six combinations of two observed past air temperature datasets and three observed past precipitation datasets was defined. We used CRU air temperature, ERA-Interim air temperature, APHRODITE precipitation, Sakai precipitation, and MSWEP precipitation. These six combinations met the following conditions: temporal resolution: daily; spatial resolution: $\leqq 0.5^{\circ}$ and period: from 1980. We were also influenced by earlier glacier model studies. The differences among the selected observed past air temperature and precipitation datasets were described in Table 4.1, Table 4.2 and Table 4.3.

CRU provides gridded surface air temperature and precipitation data, CRU TS 3.10 interpolates in situ observations and has often been used in global glacier modeling studies

[*Marzeion et al.*, 2012, 2018; *Giesen and Oerlemans*, 2013; *Hirabayashi et al.*, 2013; *Slangen et al.*, 2017]. In terms of gridded precipitation data based on in situ observations in Asia, the precipitation product suite "Asian Precipitation – Highly Resolved Observational Data Integration Towards Evaluation of Water Resources" (APHRODITE, *Yatagai et al.* [2012]) features the most extensive rain gauge network and has be:en used to project mass changes in Asian glaciers in preference to global precipitation datasets such as that of the CRU [*Lutz et al.*, 2014]. Hence, we used a combination of CRU-based temperature [*Hirabayashi et al.*, 2008] and APHRODITE-based precipitation data.

Some glacier models use re-analyses of climate data, such as the air temperature and precipitation data from ERA-40, ERA-Interim, or WDEFI that were originally provided by the European Centre for Medium-Range Weather Forecasts (ECMWF), to project changes in glacier mass. Such models typically produce less accurate estimates of precipitation than of air temperature [*Parker*, 2016]. Precipitation re-analyses often require further downscaling, particularly for high-elevation sites [*Radić et al.*, 2014]. *Radić et al.* [2014] used ECMWF reanalysis data for air temperature and another gridded precipitation product based on interpolated in situ observations [*Beck et al.*, 2005].

Moreover, gridded precipitation products that interpolate in situ observations, including APHRODITE, often underestimate precipitation at high elevations [*Adam et al.*, 2006; *Sakai et al.*, 2015]. To overcome this issue, *Sakai and Fujita* [2017] used a combination of ECMWF reanalysis air temperature and APHRODITE data corrected based on regional-scale analyses of glacier morphometry (*Sakai et al.* [2015], 'Sakai precipitation') to calculate changes in the mass of glaciers in Asia. [*Beck et al.*, 2017] corrected precipitation observations using gauged discharge data when developing Multi-Source Weighted-Ensemble Precipitation (MSWEP), the latest global gridded precipitation product. In this study, we combined ECMWF reanalyses of air temperature and MSWEP gridded precipitation to project future changes in glacier mass.

Furthermore, we used three other combinations of air temperature and precipitation datasets (CRU temperature – Sakai precipitation, CRU temperature – MSWEP precipitation, ERA-Interim temperature – APHRODITE precipitation) to assess the uncertainty in projections of future changes in glacier mass arising from the observed past air temperature and precipitation datasets.

4.2.4 Climate forcing for future predictions

Simulations of future glacier mass balance were forced by three GCMs (CCCma-CanESM2, NCAR-CCSM4, MRI-CGCM3) involved in the fifth phase of the Coupled Model Intercomparison Project (CMIP5) using the highest emissions scenario (representative concentration pathway [RCP] 8.5). Three GCMs were selected to cover the range of future changes in glacier mass based on a preliminary experiment for glaciers in the HMA (Supplement 1). Glacier melt in the 21st century was projected from the preliminary experiment using nine GCMs, which were selected based on the availability of variables for input to the glacier model (HYOGA2) and to avoid duplication of GCM developers. Among the nine GCMs, CCCma-CanESM2, NCAR-CCSM4, and MRI-CGCM3 projected the greatest, median, and smallest changes in glacier mass, respectively. The differences of future air temperature and precipitation among the selected three GCMs were described in Table 4.4, Table 4.5 and Table 4.6.

4.2.5 Bias correction

Despite continuous efforts to improve the capability of GCMs to simulate historical climates, the use of downscaling methods is essential for impact assessment studies of climate change. In this study, a statistical downscaling method called "bias correction" was applied to GCM-simulated data because it has a lower computational cost than dynamical downscaling approaches. We used a trend-preserving bias-correction method [*Watanabe et al.*, 2012] to preserve GCM-simulated signals in future projections. This rendered it possible to assess uncertainties in glacier projection induced by variation among GCMs. We used two observed past air temperature and three observed past precipitation datasets as reference data when bias-correcting three GCMs. The GCM simulation data were compared to observation-based daily climatic data to estimate biases over the 30 years from 1981 to 2010 (1981 to 2007 for the APHRODITE and Sakai precipitations). During bias correction, we adjusted means, temperature standard deviations, and precipitation coefficients of variance. Finally, the GCM-simulated daily air temperature and precipitation data for 2006 – 2100 were corrected.

4.2.6 Glacier model parameters

We derived model parameters via calibration. *Hirabayashi et al.* [2013] calibrated the degree-day factors (DDFs) for ice and snow with HYOGA2. We calibrated the adjustment

factors for precipitation (Cp) and temperature (dT) data in addition to the DDFs with HYOGA2, as have previous studies [*Marzeion et al.*, 2012; *Radić et al.*, 2014; *Huss and Hock*, 2015]. The calibration order was that of *Huss and Hock* [2015]. Individual glacier data obtained from the RGI were first aggregated into a large glacier per 0.5° grid cell. Then the parameters for each cell were calibrated until we obtained the maximum extent of agreement with the cell-specific long-term (1981 – 2004) average of the total glacier mass balance. The gridded mass balance data of *Hirabayashi et al.* [2013], which are based on those of others[*Dyurgerov*, 2010; *Dyurgerov and Meier*, 2005, 1997; *Serreze et al.*, 2000], were used for calibration. Each parameter was determined for each of six combinations of observed past air temperature and precipitation data (Table 4.1 and Table 4.2). We did not calibrate the Sakai precipitation because the data are already calibrated [*Sakai et al.*, 2015].

4.2.7 Sources of uncertainty

As mentioned above, we partitioned uncertainty into GCM, observed past air temperature, and observed past precipitation uncertainties following *Hawkins and Sutton* [2011]; *Wada et al.* [2013]. We calculated the variance of each uncertainty, assuming that they were independent. The total variance (Vt) was the sum of the variance of climate projections from the GCMs (Vg), the variance among different observed past air temperature datasets (Va), and the variance among different observed past precipitation datasets (Vp). Vg was approximated by calculating the variance across the GCMs for a given observed past air temperature and precipitation dataset pair, repeating this exercise for each dataset combination, and then calculating an average variance. Va and Vp were calculated in the same manner. We preferred this method because the works of both [*Hawkins and Sutton*, 2011; *Wada et al.*, 2013] were similar to ours, in that three or four climate scenarios and 5 to 14 GCMs were used to assess fractional uncertainties.

4.3 Results

4.3.1 Projected annual mass balance of glaciers

The model projected a total of 18 mass change patterns in Asian glaciers through 2100 using two observed past air temperature datasets, three observed past precipitation datasets, and three GCMs (Table A.3, Figure 4.3). All simulations projected continuous mass loss

throughout the 21st century (Figure 4.3). The magnitude of loss varied substantially depending on the extent of the temperature increase and associated precipitation changes, which were determined by the choice of air temperature and precipitation products as well as the GCM. The average annual mass loss was projected to be around -3 m w.e. $year^{-1}$ by the end of the 21st century. The projection range was from around -2 m w.e. $year^{-1}$ to a maximum of almost -5 m w.e. $year^{-1}$.

4.3.2 Attribution of uncertainties in projected changes in glacier mass

Figure 4.4 shows the fraction of the total variance in changes in glacier mass explained by the GCMs and the observed past air temperature and precipitation datasets (details in 2.8). The variances explained by the GCMs and the observed past air temperature and precipitation datasets were derived for six (two observed past air temperature and three observed past precipitation datasets), nine (three GCMs and three observed past precipitation datasets), and six (three GCMs and two observed past air temperature datasets) patterns.

Figure 4.4 indicates the fractional (relative) uncertainty in future glacier mass change caused by each input component (GCM, observed past air temperature, and observed past precipitation). The fractional uncertainty arising from the GCMs was around 60% at the beginning of the 21st century, and then increased slightly to become about 85% at the end of the century. The fractional uncertainty arising from observed past air temperature was about 35% at the beginning of the century but decreased to around 10% at the end of the century. This contributed the second largest proportion of the total uncertainty. The fractional uncertainty arising from observed past precipitation accounted for around 5 – 10% of all uncertainty throughout the century.

4.3.3 Resolving the components of future changes in glacier mass

We found that differences in observed past climatic datasets (air temperature and precipitation) propagated about 5 – 35% fractional uncertainty throughout the 21st century (Section 3.2). To understand how observed past air temperature and precipitation data propagate uncertainties into future changes in glacier mass, three further analyses were conducted.

4.3.3.1 Observed past air temperature and precipitation for bias correction and glacier model calibration

The mean annual average air temperature and total precipitation, which were used for bias correction and model calibration, differed among the observed past climatic datasets (Table 4.1 and Table 4.2). In particular, the differences among observed past precipitation datasets were quite large, with the values from MSWEP being nearly double those of other datasets. The coefficient of variation for the observed past precipitation datasets was larger than that for the observed past air temperature datasets (Table 4.3).

4.3.3.2 Attribution of uncertainties in projected air temperature and precipitation

Projected future air temperature and precipitation were the only climatic factors driving future changes in modeled glacier mass. We partitioned the uncertainty components of projected future air temperature and precipitation after bias correction; we derived adjustment factors for precipitation (Cp) and air temperature (dT). Figure 4.5 shows the fractional (relative) uncertainties attributed to the GCM, observed past air temperature dataset, and observed past precipitation dataset for projected future air temperature (Figure 4.5a) and precipitation (Figure 4.5b). The uncertainties for both propagated from not only the different GCMs but also the differences in observed past climatic data used for bias correction and calibration. We confirmed that the past observed past precipitation varied significantly among datasets (Table 4.1, Table 4.2 and Table 4.3) and that differences in observed past precipitation were the dominant component of the uncertainty in projections of future precipitation (Figure 4.5b).

4.3.3.3 Components of glacier mass budget

After determining future air temperature and precipitation employing bias correction and calibration, we used the model to calculate glacier ablation (mass loss) and glacier accumulation (mass gain), and derived a mass budget. Finally, the components of changes in glacier mass were resolved into ablation and accumulation (Figure 4.6). Ablation was the mass loss yielding positive temperature sums in the model (details in Section 2.3). Accumulation was calculated as mass transferred from the snowpack above glaciers to glacier ice. The snowpack was calculated based on precipitated snow. We confirmed that the difference in observed past precipitation was the dominant fractional uncertainty in pro-

jections of future precipitation (Figure 4.5b), but the accumulation, which was calculated based on future precipitation, was much smaller than the amount of ablation (Figure 4.6). The impact of accumulation was very small compared to that of ablation; accumulation did not counter ablation.

4.3.4 Discussion

The uncertainty in projected changes in glacier mass was partitioned into three distinct sources: GCM uncertainty, observed past air temperature uncertainty, and observed past precipitation uncertainty. The fractions of uncertainty arising from the choice of past air temperature and precipitation datasets were about 15%, whereas that due to climate projections by the various GCMs was about 85% by the end of the century (Figure 4.4). We confirmed that this result did not depend on the time period used to derive moving averages of uncertainty fractions (Supplement 3). Observed past precipitation differed significantly among datasets, and these differences propagated to become the dominant fraction of uncertainty in future precipitation projections (Table 4.1 and Figure 4.5b). However, the range of future precipitation was not the major uncertainty in projections of future changes in glacier mass (Figure 4.4).

Previous global glacier model studies have often discussed the uncertainty in projecting future changes in glacier mass caused by the range of future air temperature and precipitation projections among GCMs [*Giesen and Oerlemans*, 2013; *Hirabayashi et al.*, 2013; *Huss and Hock*, 2015; *Radić et al.*, 2014], but none have considered the uncertainty caused by differences in climate datasets used for bias correction of GCMs and calibration of glacier models. *Koppes et al.* [2015] quantified the sensitivity of projections of glacier runoff to observed past air temperature datasets (past climatic forcings). The model parameters were held constant when using various observed past air temperature datasets; GCMs were not employed. We evaluated the uncertainties in projected mass changes caused by both observed past air temperatures and precipitation. Uncertainties arising from observed past climatic data are propagated not only by past climatic forcing but also by parameters of the glacier model and the GCM bias corrections. We are the first to identify the sources of uncertainty [*Marzeion et al.*, 2012; *Hirabayashi et al.*, 2013; *Radić et al.*, 2014; *Huss and Hock*, 2015; *Koppes et al.*, 2015].

Ideally, there should be no differences in observed past climatic data. However, such differences propagated about 15% of the fractional uncertainty into projected future change

in glacier mass by the end of the century. The remaining fractional uncertainty caused by GCM spread includes variabilities caused by each model' s underlying theory and they would remain, although part of it can be reduced by the continuous efforts to improve GCMs. However, the fractional uncertainties arising from differences in observed past air temperatures and precipitation must be reduced. We found that use of some combinations of observed past climate datasets was relatively less biased when simulating past glacier mass balance using the HYOGA2 (Supplement 2). The combination may differ by the glacier model chosen. Further studies are necessary to evaluate observed past climate datasets when using them to compute changes in glacier mass using a method similar to that described in *Massonnet et al.* [2016]. Additional studies to develop enhanced observed past climate datasets are also needed. State-of-the-art remote sensing satellites such as the Global Precipitation Measurement (GPM) Dual-Frequency Precipitation Radar (DPR) will reduce the differences among observed past climate datasets in regions with glaciers region. The GPM GPR seeks to measure both light and solid precipitation accurately and comprehensively. Modern rain gauges with windshields (e.g., the Geonor system) will be used to correct satellite observations, which may be unreliable if the topography is complex.

The impact of the differences among observed past precipitation datasets on projected changes in glacier mass was expected to be large due to the significant differences among the datasets. Although these differences caused a major fraction of the uncertainty in projected future precipitation, which was the dominant factor in calculating glacier accumulation, they did not trigger significant variation in the ultimate glacier mass change projection. This is because accumulation was not the dominant component of the glacier mass budget in this simulation. The use of a high-emissions scenario, the characteristics of the sampled glaciers, and the sensitivity of the temperature index glacier model to changing temperature may have resulted in less accumulation.

The results presented here refer to glaciers in the high mountains of Asia, and the uncertainties are not directly transferable to other study sites. Here, we assessed uncertainties in several past climatic datasets; we treated the gridded datasets as observational datasets. If local observation uncertainty could be directly assessed, it might be larger than we found; very few local data are available for glaciers. Additional uncertainties might arise from the choice of bias correction method or simplifications to the glacier model. The effects of model simplification are difficult to assess, as in most cases no al-

ternative model exists. Therefore, future work should include multiple glacier models and should assess different glaciated regions, which could eventually lead to a comprehensive uncertainty assessment.

4.4 Conclusion

We projected mass changes in Asian glaciers through 2100 using a glacier model. We used a set of 18 combinations of two observed past air temperature datasets, three observed past precipitation datasets, and projected air temperatures and precipitations from three GCMs as inputs to assess the uncertainties arising from each component. The uncertainty was partitioned into three distinct sources: GCM uncertainty, observed past air temperature uncertainty, and observed past precipitation uncertainty. We found that the fractional uncertainties arising from the choice of observed past air temperature and precipitation datasets were about 15% by the end of the 21st century because of bias correction and parameter choice, although that due to climate projections by the various GCMs was dominant. The fractional uncertainties of observed past climatic datasets must be reduced. Differences in observed past climatic data affected estimates of future temperature and precipitation data input into the glacier model. However, these did not propagate equally into the major uncertainty in projection of glacier mass based on the mass budget. Differences among observed past precipitations were more significant than those among observed past air temperatures, but the fractional precipitation uncertainty was about 33 – 50% that of temperature when glacier ablation was dominant. This study suggests that glacier models should use multiple observed past climate datasets for bias correction and glacier model calibration for projection of future changes in glacier mass.

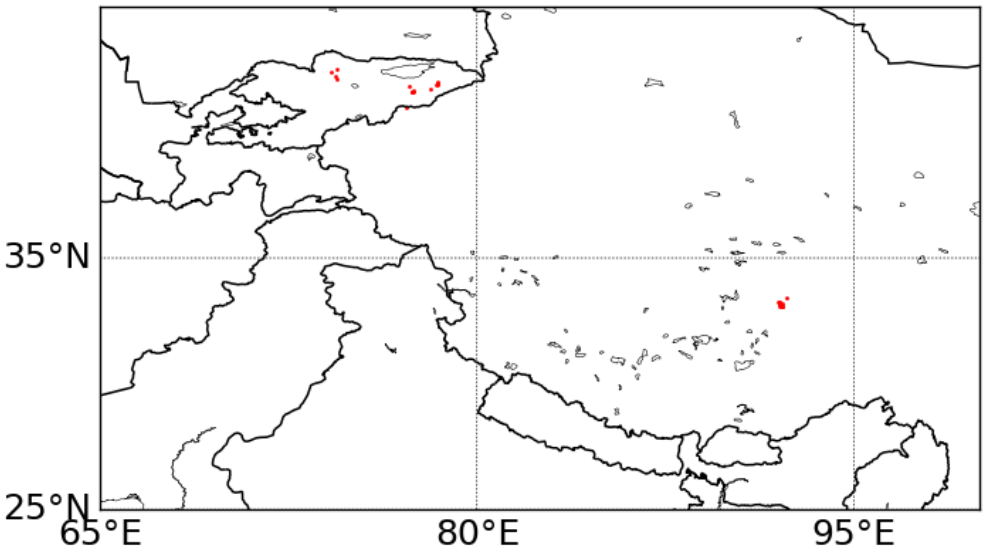

Figure 4.2: Location of targeted glaciers (26.5 – 55.5N, 66.5 – 104.5E). Red dots show the centers of each targeted glacier. Black lines: Geopolitical borders

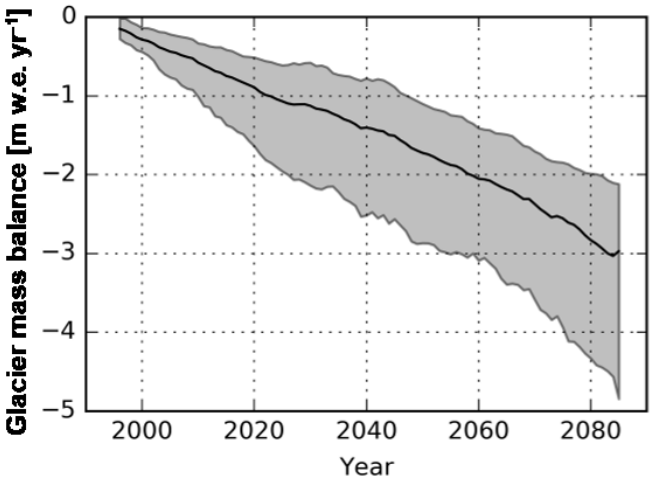

Figure 4.3: Ensemble projections of future changes in glacier mass through 2100 using a set of 18 combinations of observed air temperature datasets, observed precipitation datasets, and GCMs; the 30 yr moving average of annual glacier changes through 2100 is shown for each simulation. Shading indicates the maximum and minimum range of the 18 simulations in each year. Thick lines indicate the mean of 18 simulations in each year

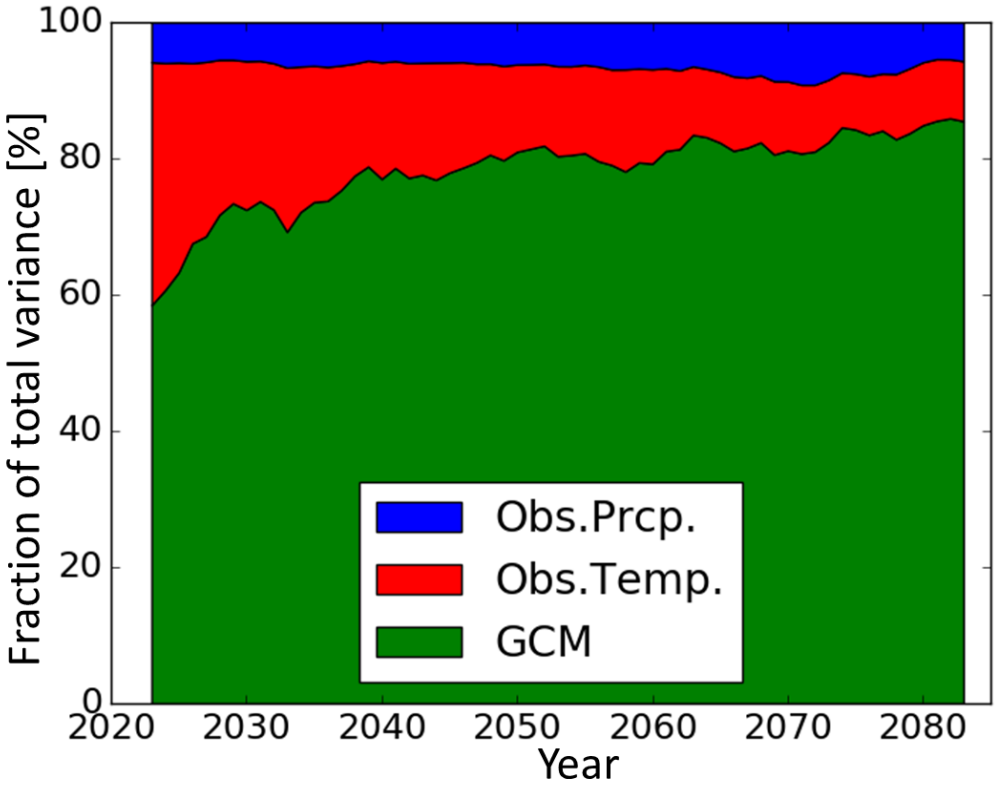

Figure 4.4: Fraction of total variance in projections of changes in glacier mass explained by GCM, observed air temperature, and observed precipitation, 30 year moving average

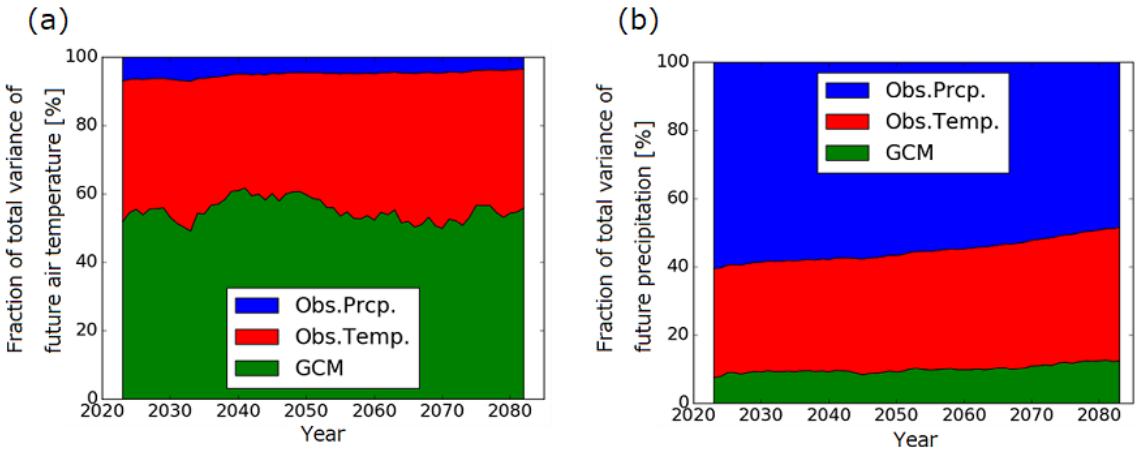

Figure 4.5: Fraction of total variance in projections of air temperature (a) and precipitation (b) explained by the GCM, observed air temperature, and observed precipitation, 30 year moving average

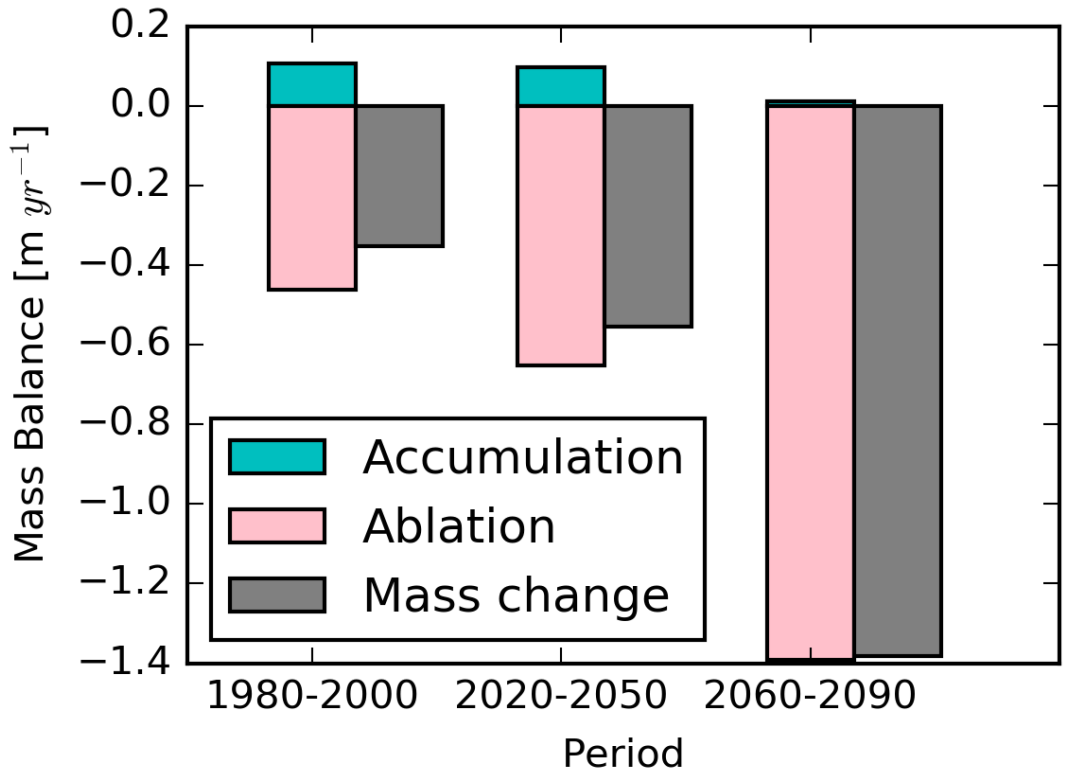

Figure 4.6: Modeled components of the glacier mass budget. Bars show 20 – 30 year averages of accumulation (light blue), melt (pink), and mass change rates (gray) based on ERA-Interim observed past air temperatures, MSWEP observed past precipitation data, and future climate projections by MRI-CGCM3 (20-year average for 1980 – 2000, 30-year averages for 2020 – 2050 and 2060 – 2090)

Table 4.1: Climate forcing used for GCM calibration and bias correction. Annual average air temperatures for 1980 – 2004 in the targeted glacierized areas.

Used data	Temeprature (° C)
CRU	-7.8
ERA-Interim	-8.8

Table 4.2: Climate forcing used for GCM calibration and bias correction. Annual total precipitation for 1980 – 2004 in the targeted glacierized areas.

Used data	Precipitation ($mm \quad year^{-1}$)
APHRODITE	378
Sakai	566
MSWEP	714

Table 4.3: Coefficients of variation in annual average air temperatures and annual total precipitation among datasets used for GCM calibration and bias correction, 1980 – 2004 in the targeted glacierized areas

Variable	CV
Air temperature	-0.06
Precipitation	0.25

Table 4.4: Climate forcing for future projections. Annual average air temperatures from the GCMs (bias corrected using ERA-Interim, before the application of the adjustment factor dT) for 2060 – 2080 in the targeted glacierized areas.

Used data	Temeprature ($^\circ$ C)
CCCma-CanESM2	-2.9
NCAR-CCSM4	-4.0
MRI-CGCM3	-4.5

Table 4.5: Climate forcing for future projections. Annual total precipitation from the GCMs (bias corrected using MSWEP, before the application of the adjustment factor Cp) for 2060 – 2080 in the targeted glacierized areas.

Used data	Precipitation ($mm \quad year^{-1}$)
CCCma-CanESM2	796
NCAR-CCSM4	699
MRI-CGCM3	896

Table 4.6: Coefficients of variation in annual average air temperatures and annual total precipitation among the bias corrected GCMs, 2060 – 2080 in the targeted glacierized areas

Variable	CV
Future air temperature	-0.17
Future precipitation	0.10

Table 4.7: Simulation settings used to project future changes in glacier mass using two observed past air temperature datasets, three observed past precipitation datasets and future air temperature and precipitation data yielded by three GCMs

	Obs.past T	Obs.past P	GCM (future T and P)
1	CRU	APHRODITE	CCCma-CanESM2
2	CRU	APHRODITE	NCAR-CCSM4
3	CRU	APHRODITE	MRI-CGCM3
4	ERA-Interim	APHRODITE	CCCma-CanESM2
5	ERA-Interim	APHRODITE	NCAR-CCSM4
6	ERA-Interim	APHRODITE	MRI-CGCM3
7	CRU	Sakai	CCCma-CanESM2
8	CRU	Sakai	NCAR-CCSM4
9	CRU	Sakai	MRI-CGCM3
10	ERA-Interim	Sakai	CCCma-CanESM2
11	ERA-Interim	Sakai	NCAR-CCSM4
12	ERA-Interim	Sakai	MRI-CGCM3
13	CRU	MSWEP	CCCma-CanESM2
14	CRU	MSWEP	NCAR-CCSM4
15	CRU	MSWEP	MRI-CGCM3
16	ERA-Interim	MSWEP	CCCma-CanESM2
17	ERA-Interim	MSWEP	NCAR-CCSM4
18	ERA-Interim	MSWEP	MRI-CGCM3

Table 4.8: The parameters of the glacier "HYOGA2" model. The degree-day factors (DDFs) for ice and snow, and adjustment factors for precipitation (Cp) and temperature (dT) data, are shown.

	Input observed past climate data	Median	Standard deviation
DDFsnow (mm °C day^{-1})	CRU-APHRODITE	1.0	0.700
	ERA-Interim-APHRODITE	3.0	0.997
	CRU-Sakai	1.0	0.700
	ERA-Interim-Sakai	3.0	0.997
	CRU-MSWEP	1.0	0.700
	ERA-Interim-MSWEP	3.0	0.997
DDFice (mm °C day^{-1})	CRU-APHRODITE	3.0	0.700
	ERA-Interim-APHRODITE	5.0	1.56
	CRU-Sakai	3.0	0.700
	ERA-Interim-Sakai	4.5	2.428
	CRU-MSWEP	3.0	0.700
	ERA-Interim-MSWEP	5.0	3.239
Cp (-)	CRU-APHRODITE	2.0	0.437
	ERA-Interim-APHRODITE	1.0	0.537
	CRU-MSWEP	2.0	0.412
	ERA-Interim-MSWEP	0.8	0.598
dT (°C)	CRU-APHRODITE	1.0	2.146
	ERA-Interim-APHRODITE	1.5	0.840
	CRU-Sakai	-0.375	0.951
	ERA-Interim-Sakai	1.0	0.367
	CRU-MSWEP	2.0	1.653
	ERA-Interim-MSWEP	1.875	0.466

Chapter 5

Development of precipitation dataset

5.1 Background

In chapter 4, we showed that the difference among observed past climate datasets had a serious impact on the assessment of future glacier melts. Therefore, the development of a new past climate dataset at high elevations is required to reduce the uncertainty arising from the difference among the observed past climate datasets. Notably, the exploitation of improved data sets of precipitation is receiving widespread attention from one of the important international research projects for the global water and energy cycles, Global Energy and Water Exchanges (GEWEX). The significant difference among observed past precipitation datasets in mountainous areas due to the under-representation of gauge locations at high elevations and wind-induced under-catch of solid precipitation is well known [*Adam et al.*, 2006; *Hirabayashi et al.*, 2008; *Biemans et al.*, 2009].

Gridded climate data (air temperature and precipitation) such as in-situ observation-based data or reanalyses data forces glacier models for the past period. The climate data for the past period is also used to calibrate glacier models and to correct the bias of climate projections calculated by climate models. However, available in-situ observations are generally scattered and mostly cover the valleys (Figure 5.3). Therefore, the scarcity of in-situ observations coupled with high orographic influences has prevented a comprehensive assessment of air temperature and precipitation distribution at high elevations. Meanwhile,

reanalyses are frequently used to drive hydrological models or glacier models for the

same purposes as traditional observations because they provide comprehensive snapshots of conditions at regular intervals over long timer periods. Reanalyses have the potential to estimate conditions well at high mountainous areas with scarce in-situ observations even though reanalyses rely on both observations and model-based forecasts. It is known that models used in reanalysis tend to give a typically more accurate estimation for temperature than precipitation. Therefore, we have selected and developed inversely corrected or satellite-derived data sets additionally for precipitation. To overcome underestimates of orographic precipitation, inversely estimation methods using gauged discharge data or satellite-derived glacier elevation have been developed for hydrological or glacier models [*Beck et al.*, 2017; *Sakai et al.*, 2015]. Remotely sensed precipitation data also can be available for scares for ungauged or sparsely gauged regions because satellites can observe consistently at broad areas. The Precipitation Radar (PR) is the spaceborne rain radar and that can achieve quantitative rainfall estimation to represent local precipitation patterns concerning landscape morphology. We have developed another precipitation data set by combing a climatology from the PR because that rain detection ability was found to be significantly more sensitive than that of infrared or microwave sensors.

5.2 Method

We developed a precipitation dataset by combining gauge, satellite, reanalysis precipitation datasets. We developed the precipitation dataset for the southern area and the northern area separately due to limitations of satellite coverage. The satellite used in this study only covers the southern area. Therefore, we developed the precipitation dataset for the southern area by mainly using satellite data. For the northern area, we developed the precipitation dataset by combining gauge and reanalysis data and introducing a correction for gauge under-catch and orographic effects by referring to streamflow observations.

5.2.1 The Southern area

For the southern area, we developed a precipitation data set by combing time-series variation from MSWEP [*Beck et al.*, 2017] with a high-resolution climatology from the Precipitation Radar (PR) observations onboard the Tropical Rainfall Measuring Mission (TRMM) satellite ranging from 35° N to 20° N, from 60° E to 105° E. Remotely sensed precipitation data can be relatively available for high resolution at broad areas to represent local

precipitation patterns concerning landscape morphology. The PR is the first spaceborne rain radar and the only instrument on TRMM that can achieve quantitative rainfall estimation over land as well as the ocean. The PR rain detection ability was found to be significantly more sensitive than that of infrared or microwave sensors. MSWEP combined a few satellite-based precipitation products derived from microwave sensors, precipitation radar, and so on. Here, we used only the PR observations because it is more sensitive to precipitation.

We used the TRMM product 2A25 which provides estimated surface rainfall rate from the TRMM Precipitation Radar (PR) data to develop a precipitation climatology. The PR sensor makes one or two snapshots of the Earth's surface per day (depending on the latitude). Therefore, measurements are infrequent and have to be averaged over a long time span. We processed these data for 10 consecutive years from 1998 to 2007 and interpolated the orbital data onto equally spaced approximately 5×5 km grid boxes. The instantaneous rainfall amounts (mm/hr) were converted to mean annual rainfall (mm/yr). Mean rainfall intensity was derived by accumulating 10 years of data divided by total observation numbers.

The PR observation underestimates snowfall because of its design. The PR-derived precipitation was corrected for rainfall and snowfall separately by rain gauge observations (APHRODITE). Correction factors were decided by each linear regression for rainfall sampling and snowfall sampling. Conditions for choosing sampling grids to decide the correction factors are (1) Choose grid boxes in areas with snowfall (Tibetan Plateau and the Himalayas, Meddle East and Japan) shown in Figure 5.1 and Figure 5.2 ; (2) Choose grid boxes including at least one gauge station at 0.25° grid box in APHRODITE (Figure 5.3 and Figure 5.4); (3) Choose grid boxes with small spatial variation of precipitation in one grid. Precipitation form (snow and rain) was judged based on air temperature.

There are 49 observation angle bins within the scanning angle of $\pm\, 17^\circ$ in the PR. The incidence-angle dependency of estimated surface rainfall obtained from the PR was investigated [*Hirose et al.*, 2012]. We compared incidence-angle differences to derive precipitation climatology at the target area. We used all angle bins observations to collect as many as possible samples because there were no significant incident-angle differences. Time series variation was created from the daily precipitation data based on MSWEP. Time series variation of TRMM data was added by the ratio of mean daily precipitation from 1998 to 2007 between TRMM derived data and the data based on MSWEP.

5.2.2 The Northern area

For the northern area, firstly, we merged a gauge-based dataset APHRODITE and a reanalysis dataset JRA55 [*Kobayashi et al.*, 2015; *Harada et al.*, 2016] to take advantage of both datasets (Figure 5.5) . Here we did not combine satellite datasets because satellite datasets did not show good correlations with gauged observations in this area [*Beck et al.*, 2017]. APHRODITE was combined by being weighted based on gauge density. JRA55 was combined by weighted based on correlations with station observations

Secondly, the merged dataset has introduced the correction for gauge under-catch and orographic effects following *Beck et al.* [2017]. The correction was introduced by referring to streamflow observations catchment-average precipitation from streamflow observations. The "true" precipitation (P) was inferred by using Long-term streamflow observations (Q) and potential evaporation (Ep) assuming that P=E+Q. To correct the merged datasets, correction ratios for the merged datasets were calculated by comparing the catchment-average precipitation between the merged dataset and the inferred dataset (Figure 5.6). The calculated correction ratios were interpolated by linear weighting scheme based on topography such as elevation and wind direction shown in Figure 5.7 and Figure 5.8 (Figure 5.9). Finally, the interpolated correction ratios were applied to the merged precipitation dataset from APHRODITE and JRA55.

5.3 Results and Discussion

5.3.1 Precipitation

Our product showed highly resolved precipitation for the mountain range in the southern area. The spatial resolution of our product for the southern area was 10 times higher than the previously used precipitation product in the glacier model (Figure 5.10). We compared our precipitation dataset and APHRODITE for the southern area with another local precipitation dataset based on gauged observation in Nepal (Figure 5.11). Our dataset had much annual mean precipitation by 2% than APHRODITE for 1998 to 2007 for the southern area. Our dataset also had much annual mean snowfall by 30% than APHRODITE for the Southern area. We also compared our dataset and station observations. We found that our dataset was closer to the station observations compared with APHRODITE for the southern area.

We also validated our precipitation dataset for the northern area using station obser-

vations (Figure 5.13) from Pakistan Water and Power Development Authority (WAPDA). We compared the correlation coefficient with the station observations among our dataset and three previous precipitation datasets (APHRODITE, MSWEP, and JRA55). We found that our dataset had a better correlation (correlation coefficient: 0.49) with station observations than APHRODITE (correlation coefficient: 0.34) and MSWEP (correlation coefficient: 0.13) for the north area, but JRA55 was still had the best correlation (correlation coefficient: 0.90) shown in Figure 5.14.

Furthermore, we have examined a hydrological response in Bhutan using our precipitation product. River discharges were calculated by a hydrological model H08 using APHRODITE precipitation and our precipitation product as a forcing. The river discharges with our precipitation product in basin 11 and especially basin 13 in Bhutan (Figure 5.15) were well simulated than the river discharge with APHRODITE precipitation (Table 5.1).

Finally, we examined calibration errors using the developed precipitation data with the glacier model (detailed described in Chapter 3). We compared the calibration error of glacier mass balance with our precipitation product, APHRODITE, Sakai, and MSWEP (Figure 5.16). The calibration errors with our precipitation product were almost zero in grid numbers 3 and 8 while the calibration errors with other precipitation products haven't reached zero (Figure 5.18 and Figure 5.17). Although the validation is quite limited, we were able to show the possibility which our precipitation product can be utilized to simulate glacio-hydrology better than other precipitation products in specific areas.

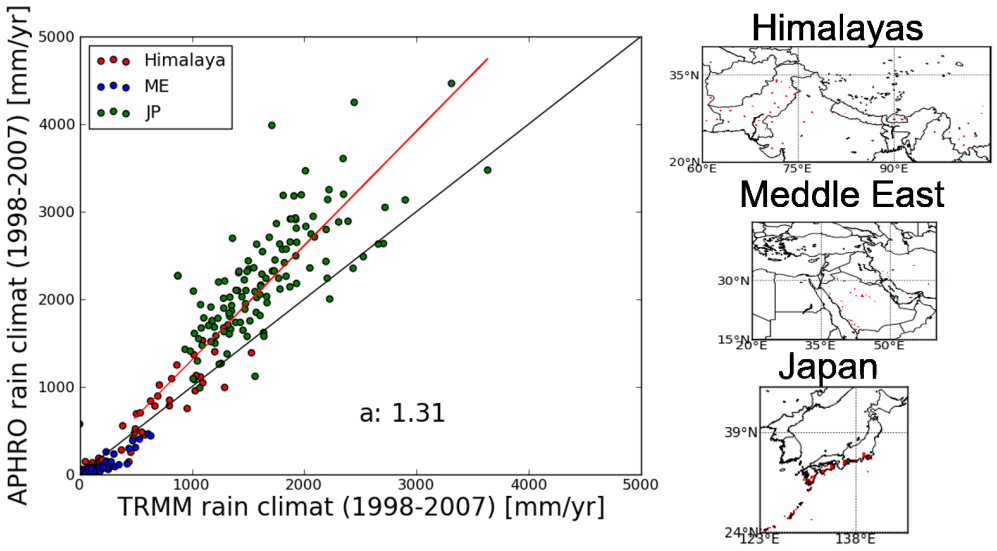

Figure 5.1: Mean annual precipitation for rain areas. Red line is regression line (y=1.31*x, r^2=0.94), red dots: Himalayas, blue dot: Meddle east and green dots: Japan

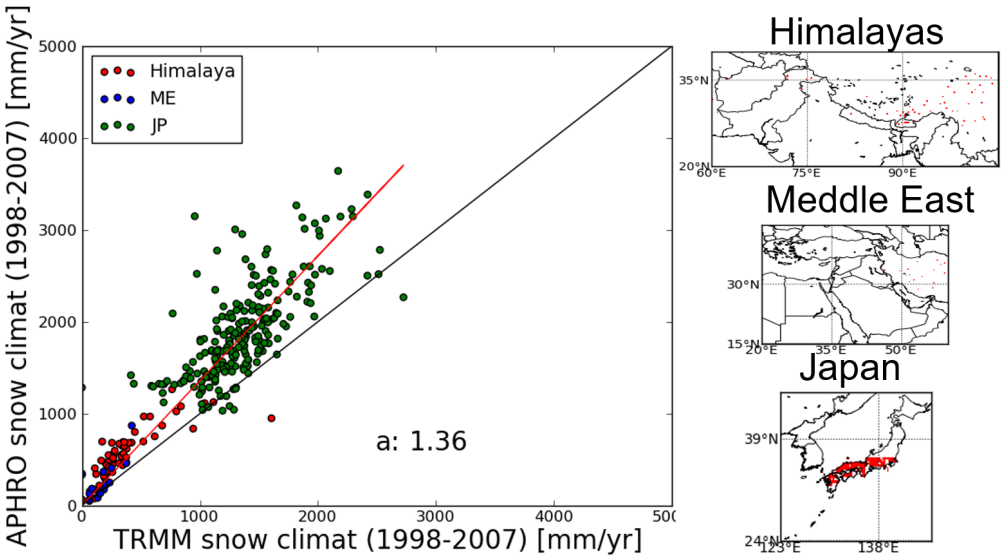

Figure 5.2: Mean annual precipitation for snow areas. Red line is regression line (y=1.36*x, r^2=0.90), red dots: Himalayas, blue dot: Meddle east and green dots: Japan

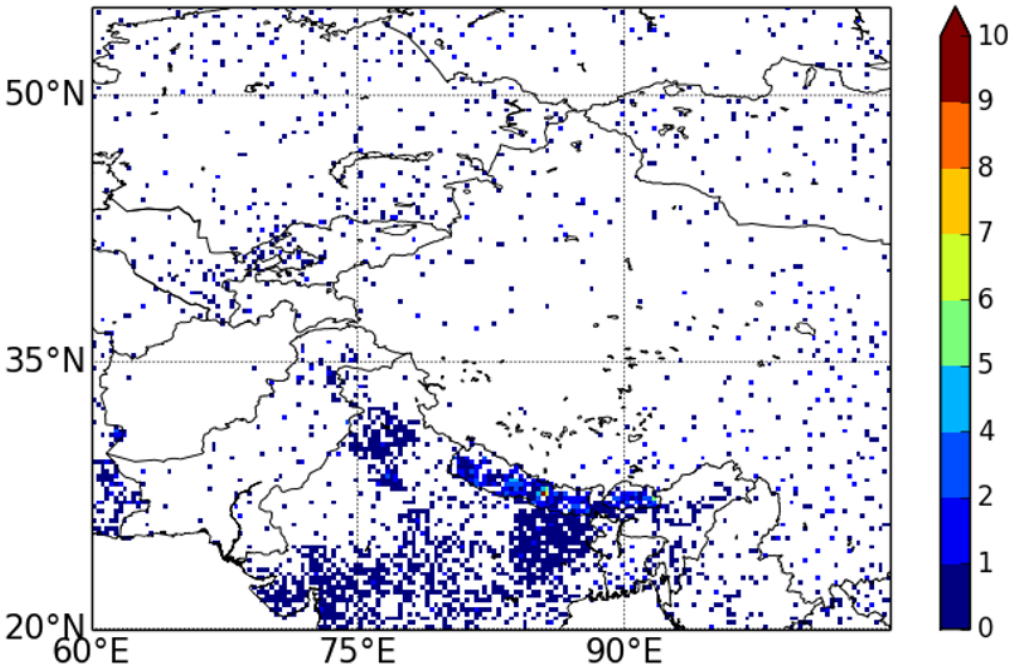

Figure 5.3: The location of rain gauge stations of APHRODITE

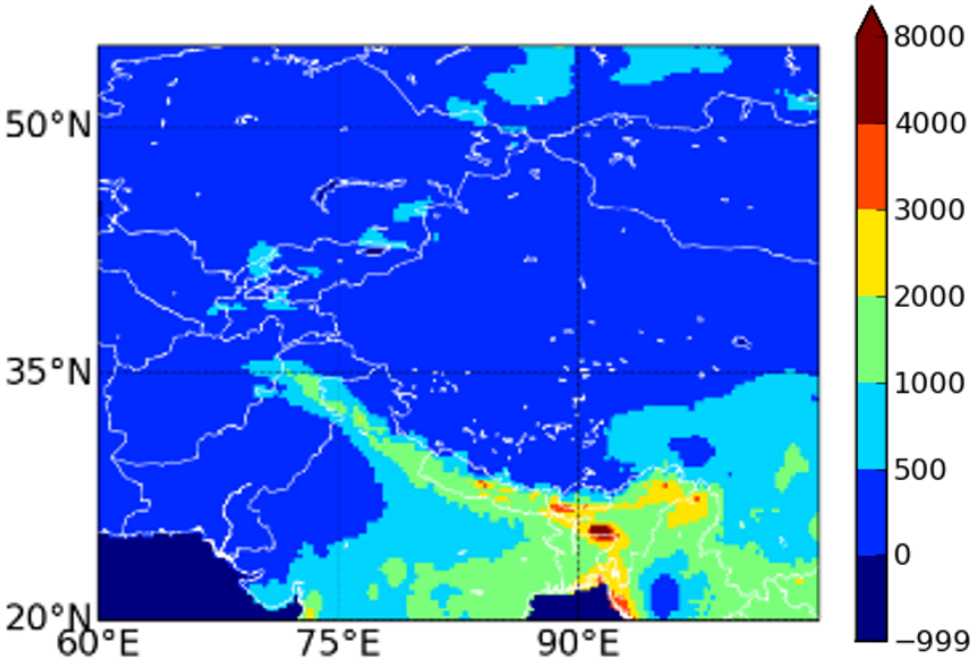

Figure 5.4: Annual precipitation in APHRODITE ($mm \quad year^{-1}$)

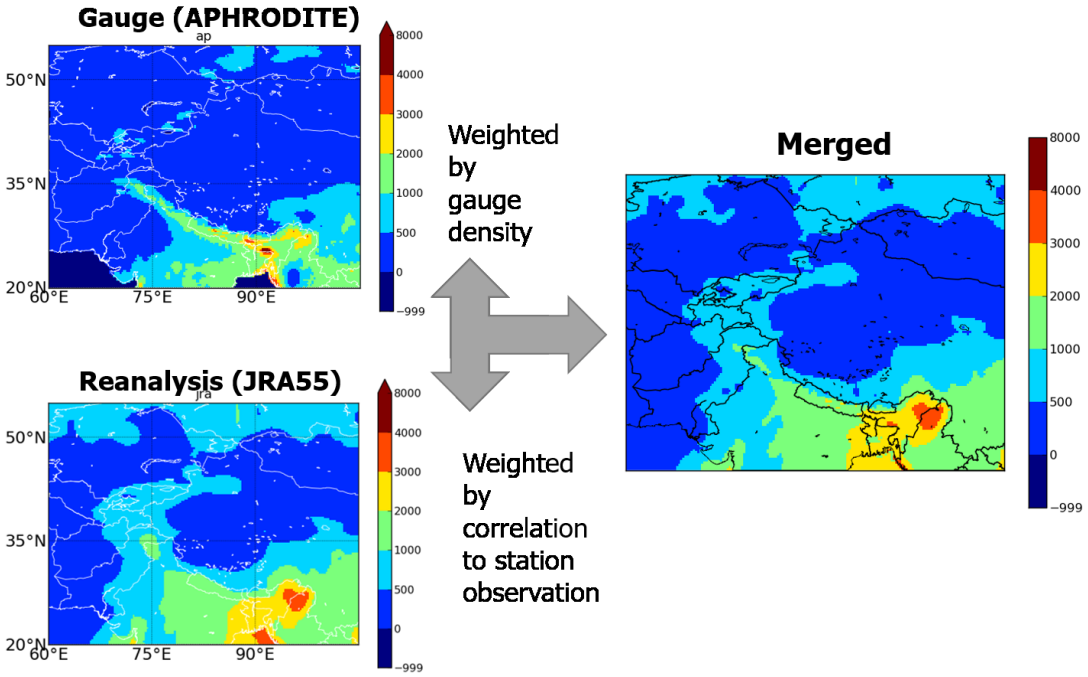

Figure 5.5: Merging the reanalysis data and the gauged data (mean annual precipitation ($mm \quad year^{-1}$))

Table 5.1: Application to a hydrological model in Bhutan. The Nash – Sutcliffe model efficiency coefficient (NSE) for monthly discharge in each basin descrived in Figure 5.15.

	9	10	11	12	13
APHRODITE	0.26	0.02	-0.17	0.29	0.49
This study	-0.15	-0.45	-0.04	0.19	0.74

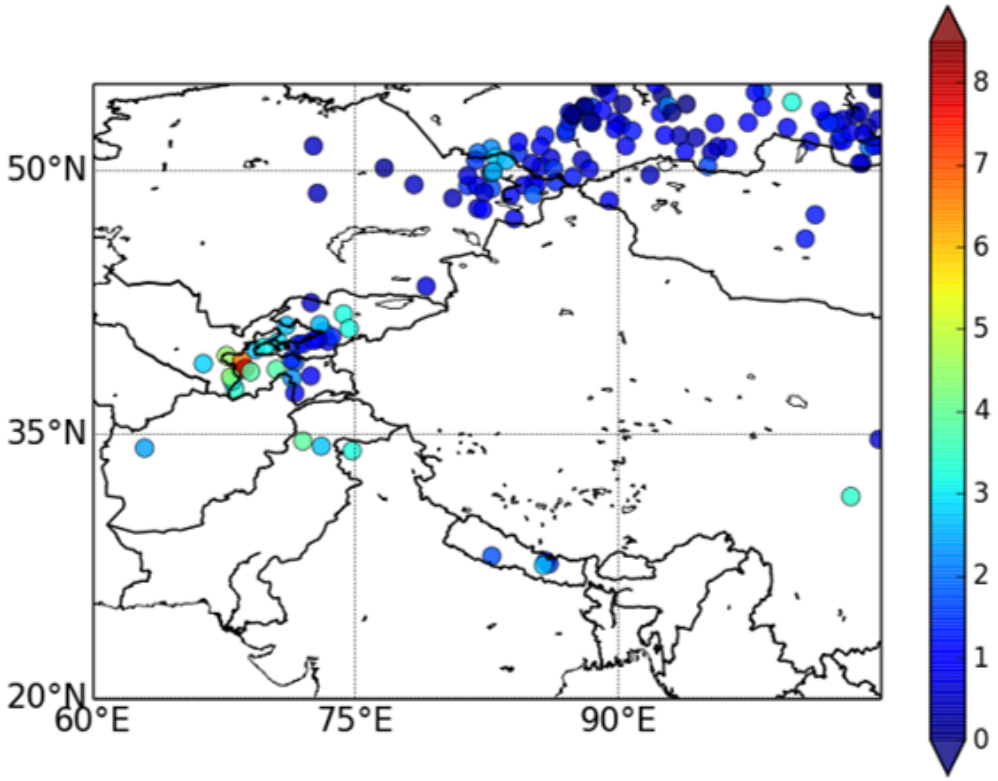

Figure 5.6: Correction ratios using the gauged discharges

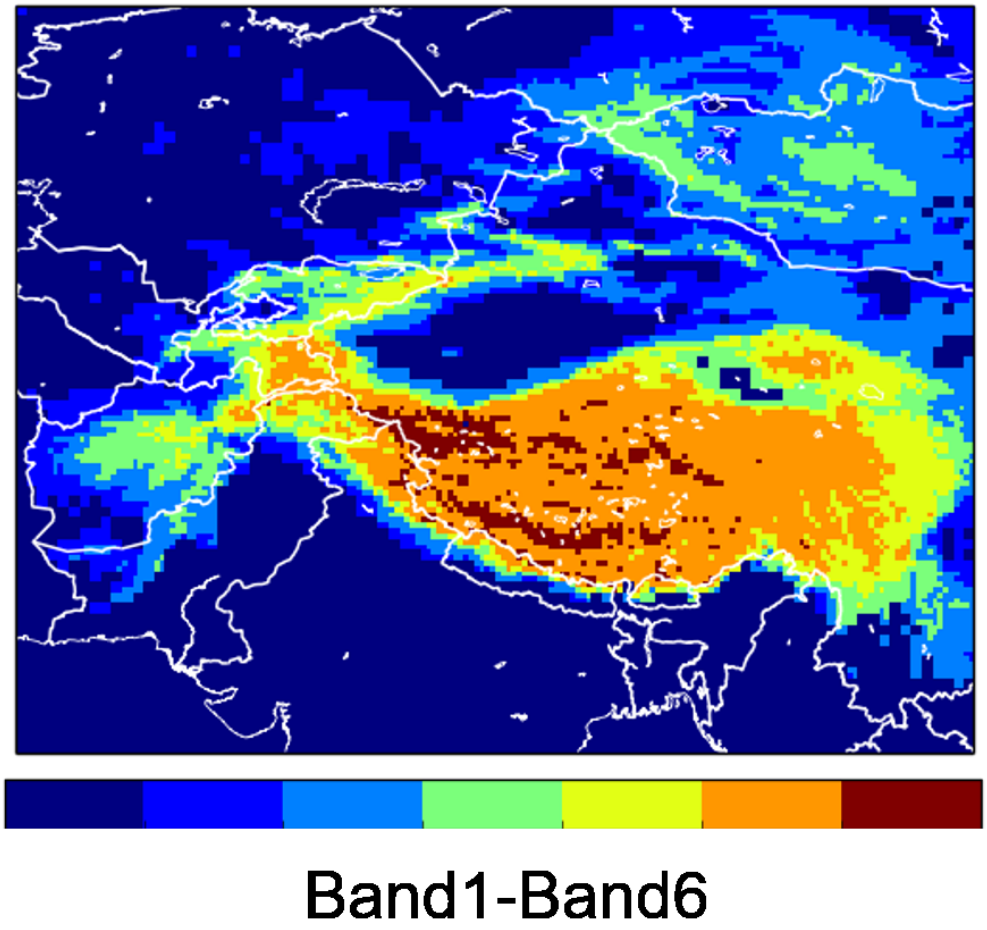

Figure 5.7: Elevation bands used to the interpolation

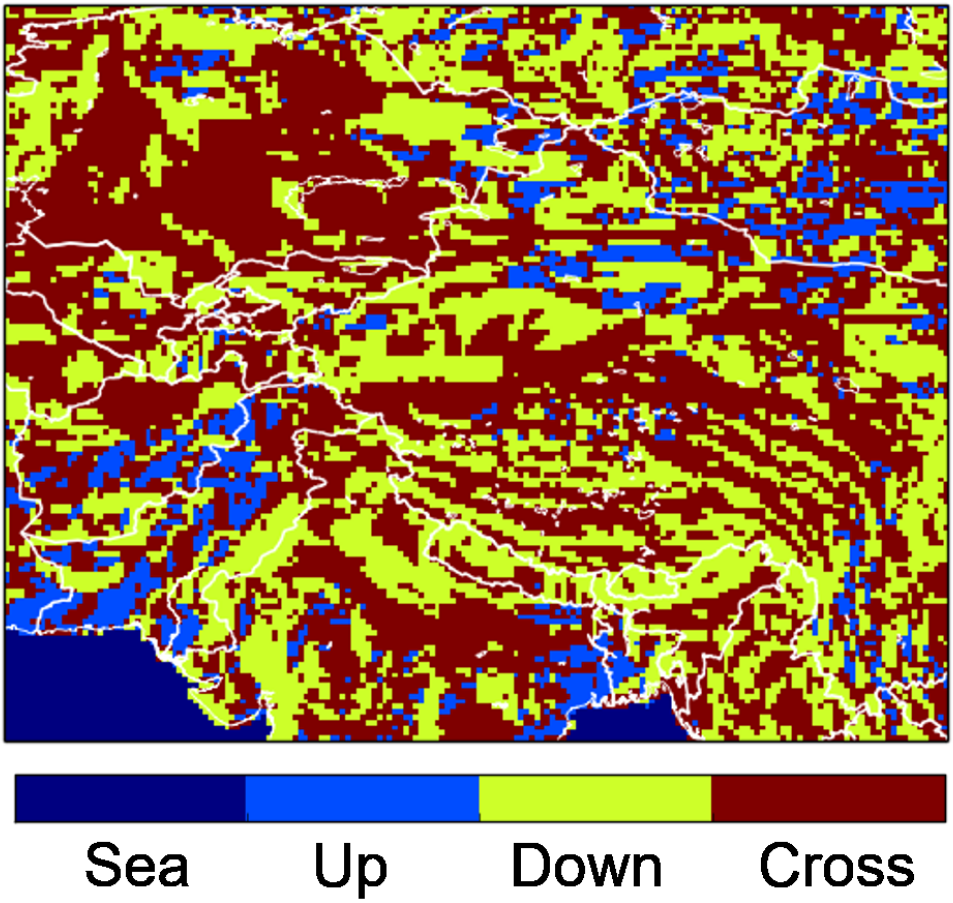

Figure 5.8: Wind direction used in the interpolation

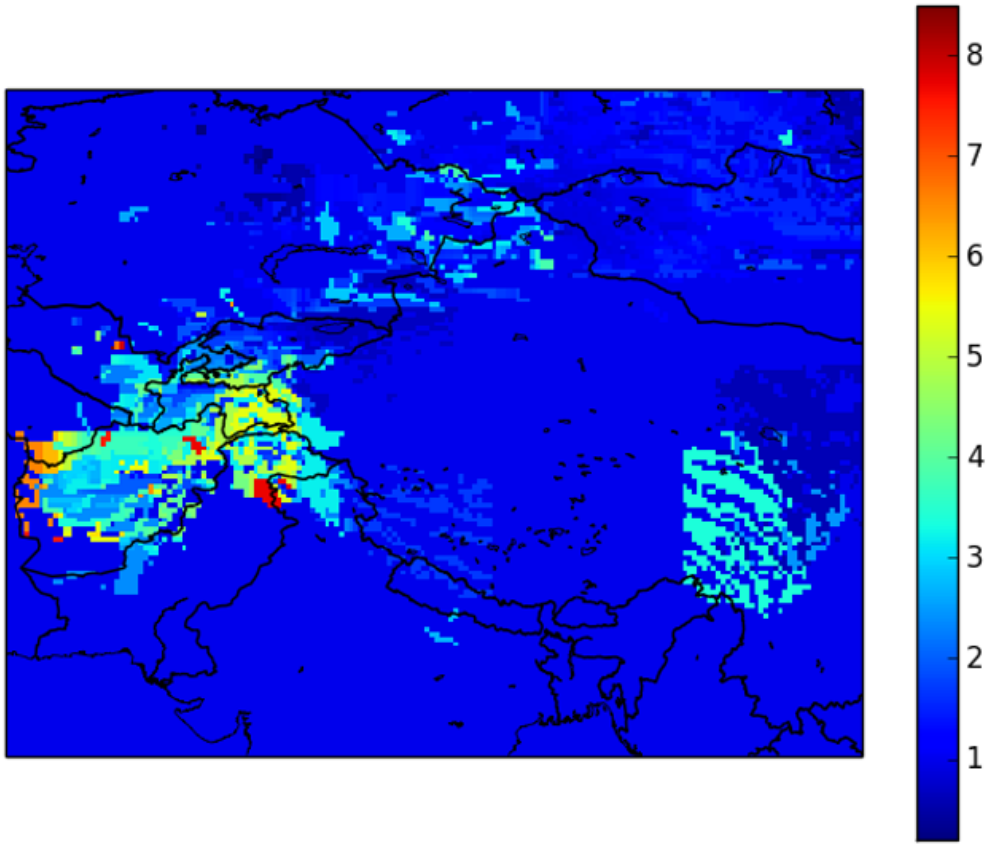

Figure 5.9: Interpolated correction ratios using the gauged discharges

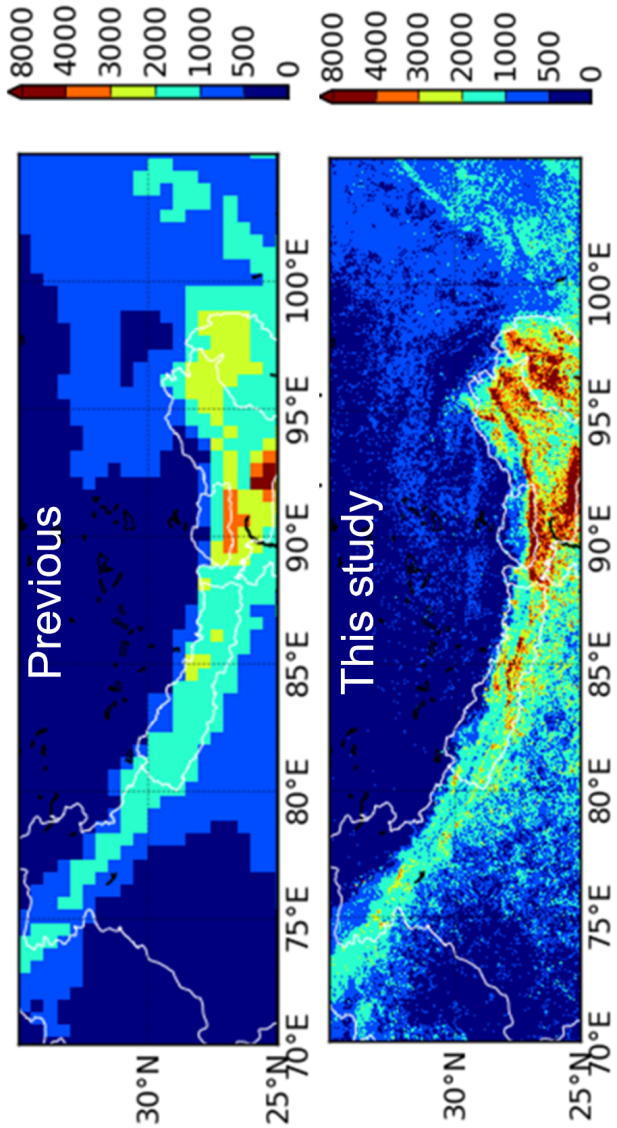

Figure 5.10: Comparison of mean annual precipitation ($mm \quad year^{-1}$)) (previous: input precipitation for a glacier model (Hirabayashiet al., 2008)

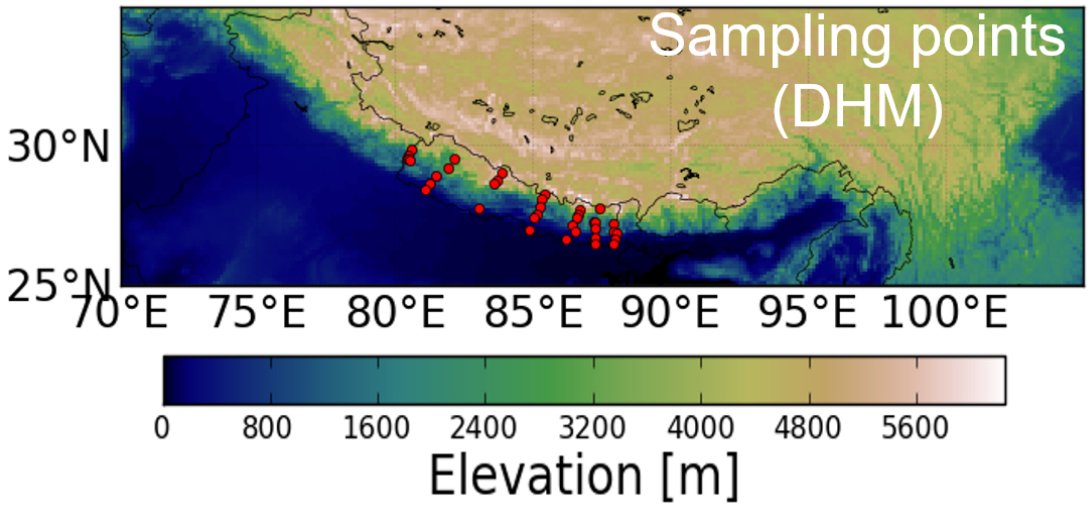

Figure 5.11: The location of rain gauge stations in Nepal

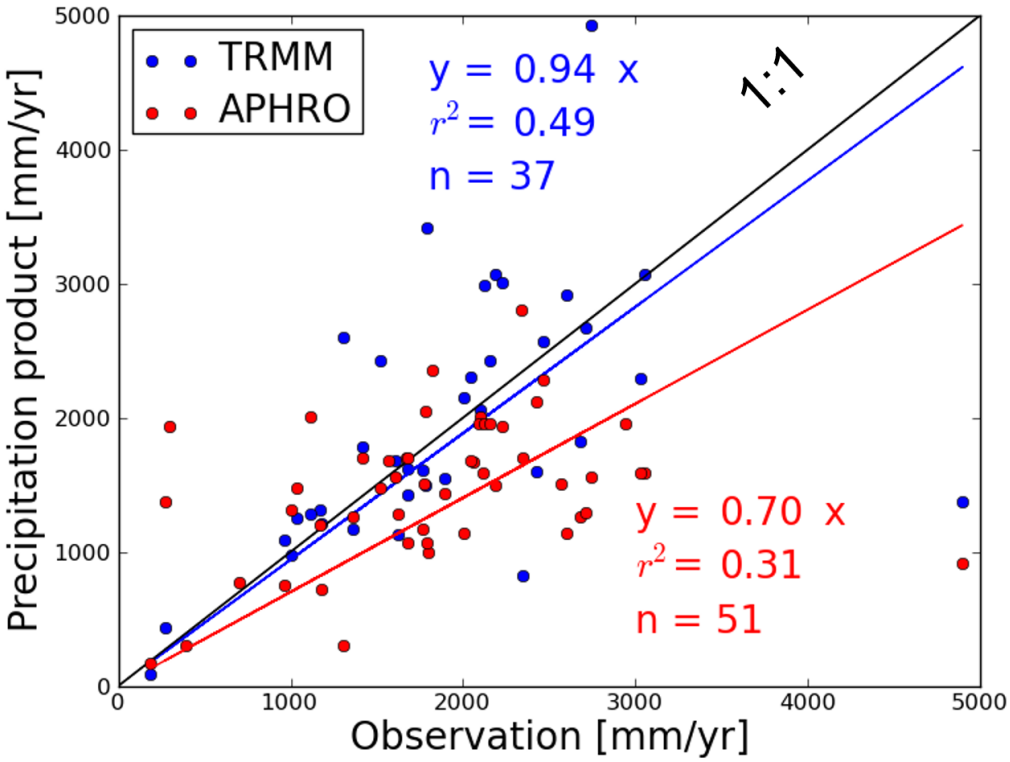

Figure 5.12: Validation of the developed precipitation datasets in Nepal

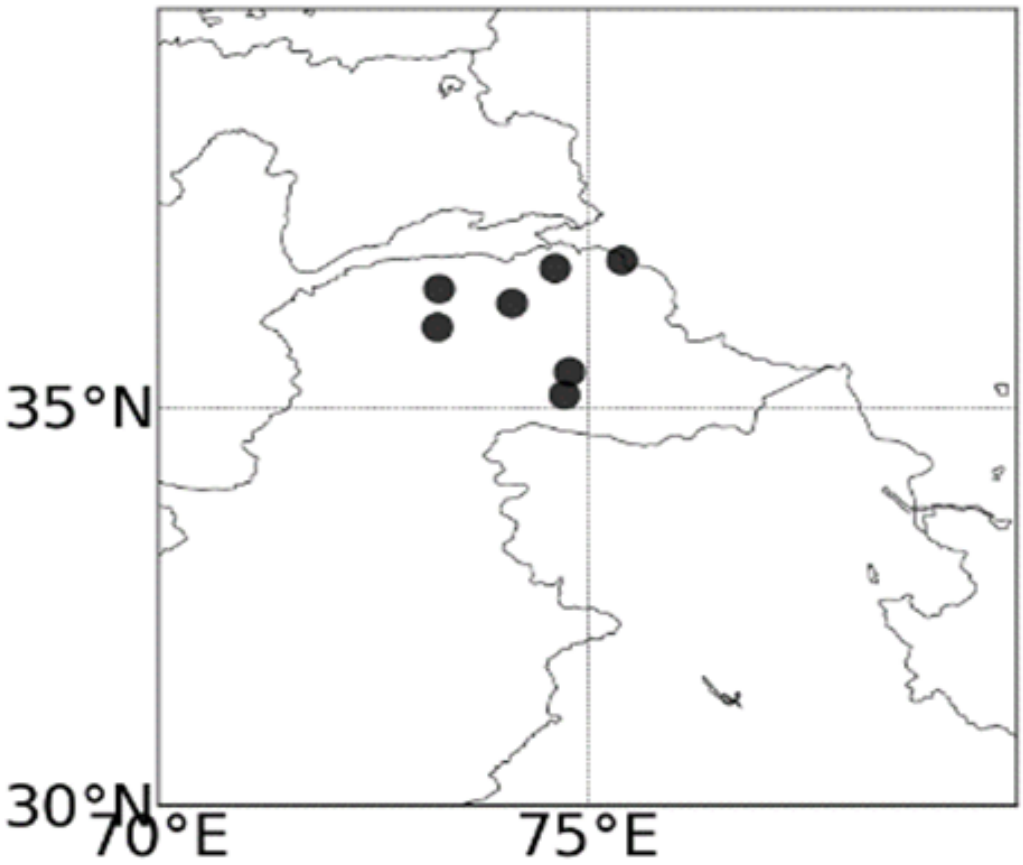

Figure 5.13: The location of rain gauge stations at Hunza in Indus basin

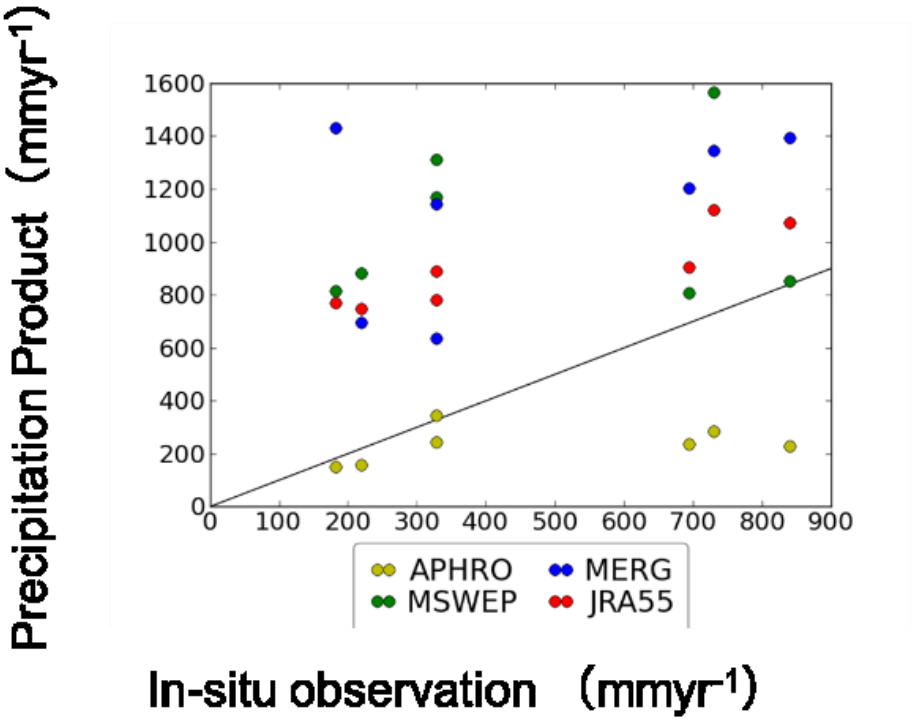

Figure 5.14: Validation of the developed precipitation datasets for northern area at Hunza in Indus basin. Comparison of annual mean precipitation between the precipitation datasets and in-situ observation by WAPDA; blue: this study; yellow: APHRODITE; green: MSWEP; red: JRA55 (b) The location of in-situ observations by WAPDA

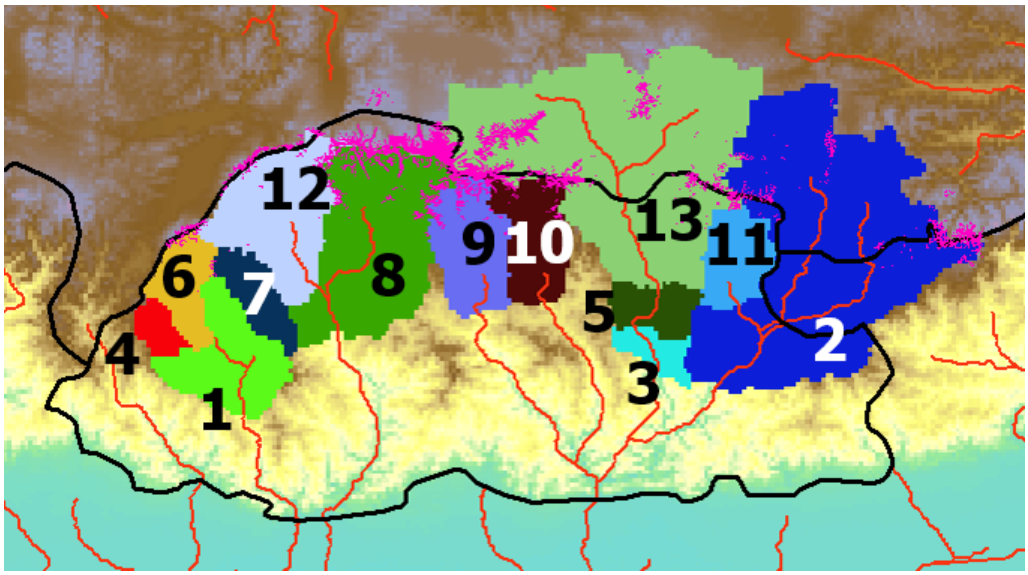

Figure 5.15: Basin map in Bhutan

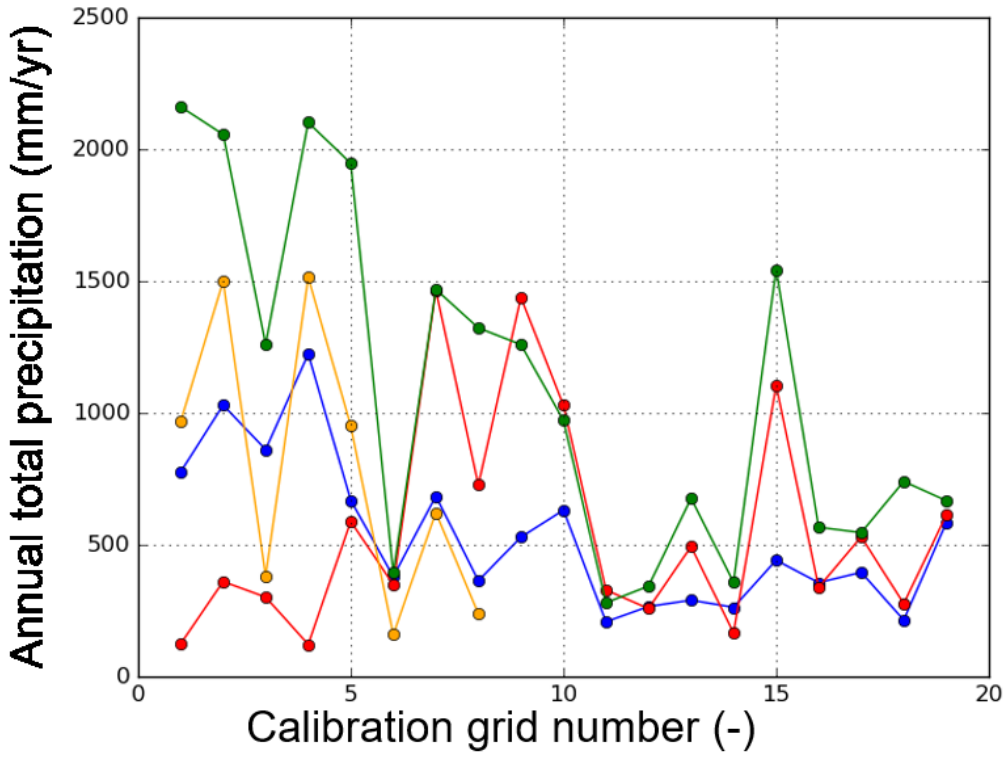

Figure 5.16: Precipitation as forcing of the calibration. Yellow: This study (PR); blue: APHRODITE; red: Sakai; green: MSWEP.

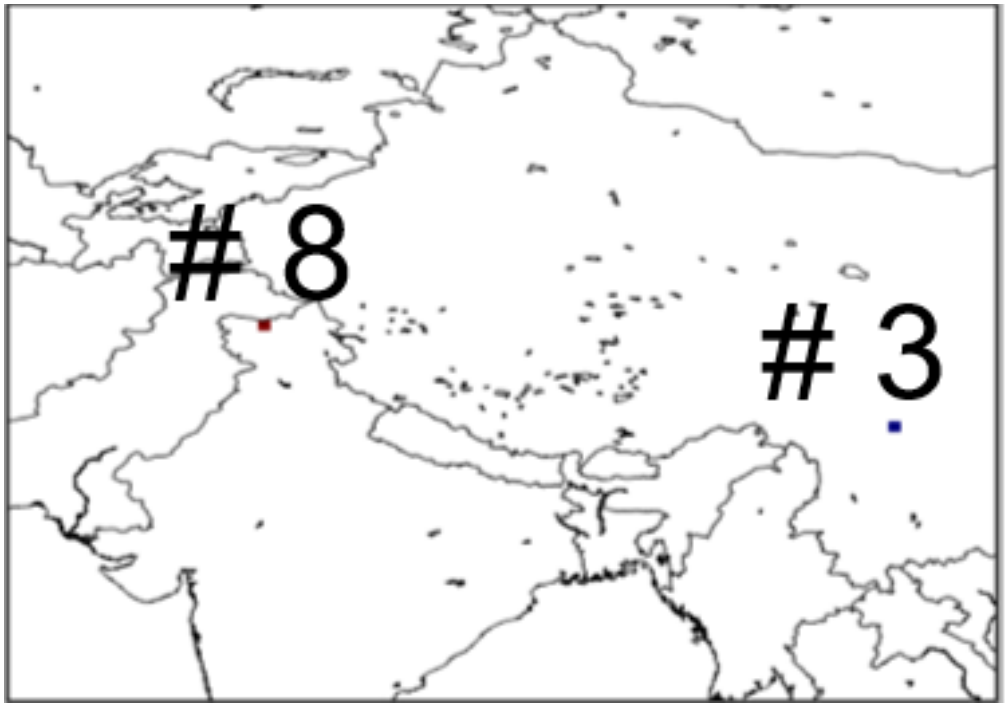

Figure 5.17: The location of calibration grids

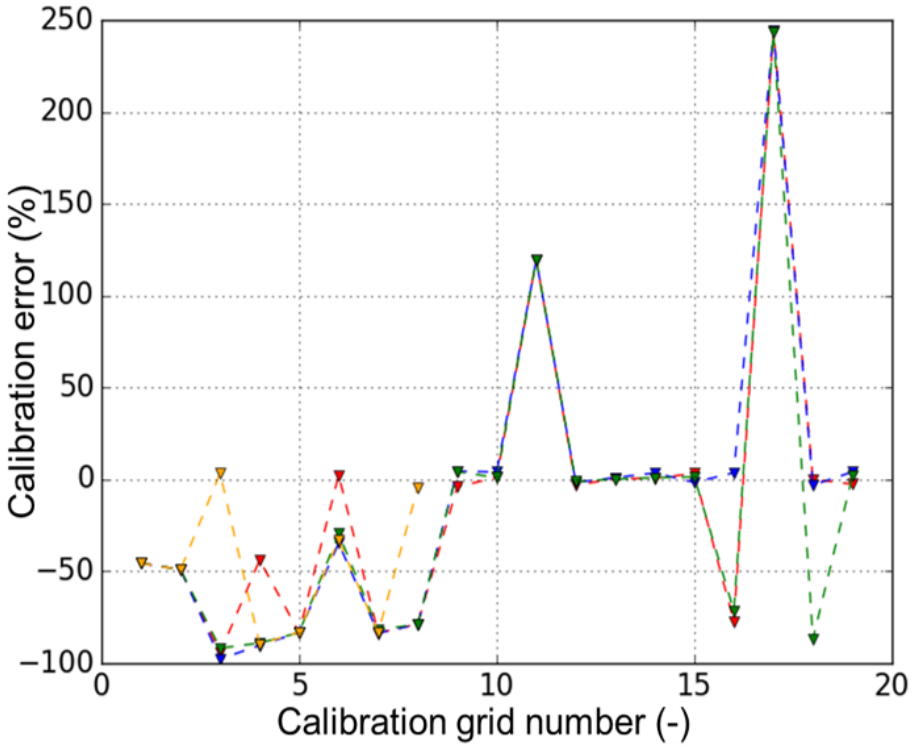

Figure 5.18: Calibration errors for glacier mass balance. Using ERA-Interim air temperature. Yellow: This study (PR); blue: APHRODITE; red: Sakai; green: MSWEP.

Chapter 6

Conclusions

This study assessed climate change impacts on sparsely observed High Mountain Asian glaciers and their uncertainty.

Chapter 2 showed that the future response of glaciers to climate change using the future changes of glacier melts projected by the glacier model. This study also quantified the future hydrological impact of glacier melts for the 11 downstream basins using the glacier melts projected by the glacier model and the runoff projected by the GCMs. The responses of glaciers to climate change differed depending on geographical features where glaciers are located at. The responses of glaciers to climate change differed depending on the annual mean air temperature where the glacier was located at. The 11 basins were classified into three types ("EARLY", "UNKNOWN", "ADVANCED") depending on the response of glaciers to climate changes except for the Ganges basin. The peak of glacier meltwater was projected to be before the early 21st century in the case of "ADVANCED Type". The peak of "EARLY Type" was projected to be after the 22nd century. Annual runoff was projected to increase in all 11 basins in the future. The main reason for these increases was not the increase in glacier melt. Future changes in glacier melt were not the most dominant factor to change annual runoff quantity at the major river basin scale. However, at Indus and Brahmaputra, dependency on glacier melt was projected to decrease dramatically. It implied that these basins could have a problem with water resources in dry seasons. The impact of seasonal runoff should be assessed as further work. In this study, the period for the assessment and the choice of glacier model and climate scenario could be an uncertainty of the result. Therefore, extending the assessment into the 22nd century or using a multi-glacier model and multi-climate scenario need to be achieved in future work.

In Chapter 3, in sparsely observed High Mountain Asian, to assess the propagation of uncertainty in projection of future glacier mass balance arising from the difference among observed past climate datasets I updated the calibration method of the glacier model. I updated the calibration method to exclude initial errors of the glacier mass balance simulation; otherwise, the initial error could affect the assessment of uncertainty arising from the difference among observed past climate datasets. After I additionally calibrated the adjustment factors for precipitation and air temperature, the modeled glacier mass had good agreement with the observed mass balance and the initial errors of modeled glacier mass balance were excluded.

In Chapter 4, I projected mass changes in Asian glaciers through 2100 using a glacier model. I used a set of 18 combinations of two observed past air temperature datasets, three observed past precipitation datasets, and projected air temperatures and precipitations from three GCMs as inputs to assess the uncertainties arising from each component. The uncertainty was partitioned into three distinct sources: GCM uncertainty observed past air temperature uncertainty, and observed past precipitation uncertainty. I found that the fractional uncertainties arising from the choice of observed past air temperature and precipitation datasets were about 15% by the end of the 21st century because of bias correction and parameter choice, although that due to climate projections by the various GCMs was dominant. The fractional uncertainties of observed past climatic datasets must be reduced. Differences in observed past climatic data affected estimates of future temperature and precipitation data input into the glacier model. However, these did not propagate equally into the major uncertainty in the projection of glacier mass based on the mass budget. Differences among observed past precipitations were more significant than those among observed past air temperatures, but the fractional precipitation uncertainty was about 33 – 50% that of temperature when glacier ablation was dominant. This study suggests that glacier models should use multiple observed past climate datasets for bias correction and glacier model calibration for projection of future changes in glacier mass.

Chapter 5 described the development of a highly resolved precipitation dataset at high elevations by combining gauge, satellite, reanalysis precipitation datasets. It was developed to decrease uncertainties in projecting future changes in glacier mass balance arising from the spread among observed datasets. The satellite radar-derived precipitation improved the spatial distribution at high elevations. The developed precipitation dataset was validated using the local rain gauge observation and the gauged discharge data. Our

result showed improvements at specific points and basins. Although future improvement is necessary, the developed precipitation data has the potential to precisely simulate glacio-hydrology.

References

Adam, J. C., E. A. Clark, D. P. Lettenmaier, and E. F. Wood, Correction of global precipitation products for orographic effects, *Journal of Climate*, *19*(1), 15–38, doi: 10.1175/JCLI3604.1, 2006.

Andermann, C., S. Bonnet, and R. Gloaguen, Evaluation of precipitation data sets along the Himalayan front, *Geochemistry, Geophysics, Geosystems*, *12*(7), doi:10.1029/ 2011GC003513, 2011.

Bahr, D. B., M. F. Meier, and S. D. Peckham, The physical basis of glacier volume-area scaling, *Journal of Geophysical Research: Solid Earth*, *102*(B9), 20,355–20,362, 1997.

Beck, C., J. Grieser, and B. Rudolf, A new monthly precipitation climatology for the global land areas for the period 1951 to 2000, *Tech. rep.*, 2005.

Beck, H. E., A. I. Van Dijk, V. Levizzani, J. Schellekens, D. G. Miralles, B. Martens, and A. De Roo, MSWEP: 3-hourly 0.25° global gridded precipitation (1979-2015) by merging gauge, satellite, and reanalysis data, *Hydrology and Earth System Sciences*, *21*(1), 589–615, doi:10.5194/hess-21-589-2017, 2017.

Biemans, H., R. W. A. Hutjes, P. Kabat, B. J. Strengers, D. Gerten, and S. Rost, Effects of Precipitation Uncertainty on Discharge Calculations for Main River Basins, *Journal of Hydrometeorology*, *10*(4), 1011–1025, doi:10.1175/2008JHM1067.1, 2009.

Bliss, A., R. Hock, and V. Radić, Global response of glacier runoff to twenty-first century climate change, *Journal of Geophysical Research (Earth Surface)*, *119*, 717–730, doi: 10.1002/2013JF002931, 2014.

Bolch, T., et al., The State and Fate of Himalayan Glaciers, *Science*, *336*(6079), 310–314, doi:10.1126/science.1215828, 2012.

Bookhagen, B., and M. R. Strecker, Orographic barriers, high-resolution TRMM rainfall, and relief variations along the eastern Andes, *Geophysical Research Letters*, *35*(6), 1–6, doi:10.1029/2007GL032011, 2008.

Brun, F., E. Berthier, P. Wagnon, A. Kääb, and D. Treichler, A spatially resolved estimate of High Mountain Asia glacier mass balances from 2000 to 2016, doi:10.1038/NGEO2999, 2017.

Chen, J., and A. Ohmura, Estimation of alpine glacier water resources and their change since the 1870s, 1990.

Cogley, J. G., A more complete version of the World Glacier Inventory, *Annals of Glaciology*, *50*, 32–38, doi:10.3189/172756410790595859, 2009.

Cuffey, K. M., and W. S. B. Paterson, *The Physics of Glaciers*, Elsevier Science & Technology Books.

Dahri, Z. H., F. Ludwig, E. Moors, B. Ahmad, A. Khan, and P. Kabat, An appraisal of precipitation distribution in the high-altitude catchments of the Indus basin, *Science of the Total Environment*, *548-549*, 289–306, doi:10.1016/j.scitotenv.2016.01.001, 2016.

Dee, D. P., et al., The era-interim reanalysis: configuration and performance of the data assimilation system, *Quarterly Journal of the Royal Meteorological Society*, *137*(656), 553–597, doi:10.1002/qj.828, 2011.

Dirmeyer, P. A., et al., GSWP-2: Multimodel Analysis and Implications for Our Perception of the Land Surface, *Bulletin of the American Meteorological Society*, *87*(10), 1381–1398, doi:10.1175/BAMS-87-10-1381, 2006.

Dyurgerov, M. B., Reanalysis of Glacier Changes: From the IGY to the IPY, 1960-2008, *Data of Glaciol. Studies*, *108*, 1–116, 2010.

Dyurgerov, M. B., and M. F. Meier, Mass Balance of Mountain and Subpolar Glaciers: A New Global Assessment for 1961-1990, *Arctic and Alpine Research*, *29*(4), 379–391, doi:10.2307/1551986, 1997.

Dyurgerov, M. B., and M. F. Meier, GLACIERS AND THE CHANGING EARTH SYSTEM: A 2004 SNAPSHOT, *Occasional Paper 58, Institute of Arctic and Alpine Research*, *15*(58), 2005.

Energy, G., and W. Exchanges, GEWEX Plans for 2013 and Beyond Global Energy and Water Exchanges GEWEX, (November 2012), 1–23, 2013.

Fujita, K., and T. Nuimura, Spatially heterogeneous wastage of himalayan glaciers, *Proceedings of the National Academy of Sciences*, *108*(34), 14,011–14,014, doi:10.1073/pnas.1106242108, 2011.

Fujita, K., A. Sakai, S. Takenaka, T. Nuimura, A. B. Surazakov, T. Sawagaki, and T. Yamanokuchi, Potential flood volume of himalayan glacial lakes, *Natural Hazards and Earth System Sciences*, *13*(7), 1827–1839, doi:10.5194/nhess-13-1827-2013, 2013.

Gardner, A. S., et al., A Reconciled Estimate of Glacier Contributions to Sea Level Rise: 2003 to 2009, *Science*, *340*, 852–857, doi:10.1126/science.1234532, 2013.

Giesen, R. H., and J. Oerlemans, Climate-model induced differences in the 21st century global and regional glacier contributions to sea-level rise, *Climate Dynamics*, *41*, 3283–3300, doi:10.1007/s00382-013-1743-7, 2013.

Gilbert, R. O., *Statistical methods for environmental pollution monitoring*, John Wiley & Sons, 1987.

Harada, Y., et al., The jra-55 reanalysis: Representation of atmospheric circulation and climate variability, *Journal of the Meteorological Society of Japan. Ser. II*, *94*(3), 269–302, 2016.

Hawkins, E., and R. Sutton, The potential to narrow uncertainty in projections of regional precipitation change, *Climate Dynamics*, *37*(1), 407–418, doi:10.1007/s00382-010-0810-6, 2011.

Hirabayashi, Y., S. Kanae, K. Motoya, K. Masuda, and P. Döll, A 59-year (1948-2006) global near-surface meteorological data set for land surface models. Part I: Development of daily forcing and assessment of precipitation intensity, *Hydrological Research Letters*, *2*(April), 36–40, doi:10.3178/hrl.2.36, 2008.

Hirabayashi, Y., Y. Zang, S. Watanabe, S. Koirala, and S. Kanae, Projection of glacier mass changes under a high-emission climate scenario using the global glacier model HYOGA2, *Hydrological Research Letters*, *7*, 6–11, doi:10.3178/hrl.7.6, 2013.

Hirose, M., S. Shimizu, R. Oki, T. Iguchi, D. A. Short, and K. Nakamura, Incidence-angle dependency of trmm pr rain estimates, *Journal of Atmospheric and Oceanic Technology*, *29*(2), 192–206, 2012.

Huss, M., and R. Hock, A new model for global glacier change and sea-level rise, *Frontiers in Earth Science*, *3*, 54, doi:10.3389/feart.2015.00054, 2015.

Huss, M., and R. Hock, Global-scale hydrological response to future glacier mass loss, *Nature Climate Change*, *8*, 135–140, doi:10.1038/s41558-017-0049-x, 2018.

Immerzeel, W. W., and M. F. P. Bierkens, Asia's water balance, *Nature Geoscience*, *5*, 841–842, doi:10.1038/ngeo1643, 2012.

Immerzeel, W. W., L. P. H. van Beek, and M. F. P. Bierkens, Climate Change Will Affect the Asian Water Towers, *Science*, *328*, 1382, doi:10.1126/science.1183188, 2010.

Immerzeel, W. W., F. Pellicciotti, and M. F. P. Bierkens, Rising river flows throughout the twenty-first century in two Himalayan glacierized watersheds, *Nature Geoscience*, *6*, 742–745, doi:10.1038/ngeo1896, 2013.

Jansson, P., R. Hock, and T. Schneider, The concept of glacier storage: a review, *Journal of Hydrology*, *282*, 116–129, doi:10.1016/S0022-1694(03)00258-0, 2003.

Kääb, A., E. Berthier, C. Nuth, J. Gardelle, and Y. Arnaud, Contrasting patterns of early twenty-first-century glacier mass change in the Himalayas, *Nature*, *488*, 495–498, doi:10.1038/nature11324, 2012.

Kääb, A., D. Treichler, C. Nuth, and E. Berthier, Brief Communication: Contending estimates of 2003-2008 glacier mass balance over the Pamir-Karakoram-Himalaya, *Cryosphere*, *9*(2), 557–564, doi:10.5194/tc-9-557-2015, 2015.

Kaser, G., M. Großhauser, and B. Marzeion, Contribution potential of glaciers to water availability in different climate regimes, *Proceedings of the National Academy of Science*, *107*, 20,223–20,227, doi:10.1073/pnas.1008162107, 2010.

Kobayashi, S., et al., The jra-55 reanalysis: General specifications and basic characteristics, *Journal of the Meteorological Society of Japan. Ser. II*, *93*(1), 5–48, 2015.

Koppes, M., S. Rupper, M. Asay, and A. Winter-Billington, Sensitivity of glacier runoff projections to baseline climate data in the Indus River basin, *Frontiers in Earth Science*, *3*(October), 1–14, doi:10.3389/feart.2015.00059, 2015.

Lutz, A. F., W. W. Immerzeel, A. B. Shrestha, and M. F. P. Bierkens, Consistent increase in high asia's runoff due to increasing glacier melt and precipitation, *Nature Climate Change*, *4*(7), 587–592, doi:10.1038/nclimate2237, 2014.

Marzeion, B., A. H. Jarosch, and M. Hofer, Past and future sea-level change from the surface mass balance of glaciers, *The Cryosphere*, *6*, 1295–1322, doi:10.5194/tc-6-1295-2012, 2012.

Marzeion, B., G. Kaser, F. Maussion, and N. Champollion, Limited influence of climate change mitigation on short-term glacier mass loss, *Nature Climate Change*, *8*, 305–308, doi:10.1038/s41558-018-0093-1, 2018.

Massonnet, F., O. Bellprat, V. Guemas, and F. J. Doblas-Reyes, Using climate models to estimate the quality of global observational data sets, *Science*, doi:10.1126/science.aaf6369, 2016.

Palazzi, E., J. V. Hardenberg, and A. Provenzale, Precipitation in the Karakorum and Himalaya from observations and global climate model simulations Circulation patterns in the Hindu-Kush Karakoram Himalaya (HKKH) and the Indian Subcontinent, (March), 13–15, 2012.

Parker, W. S., Reanalyses and observations: What's the Difference?, doi:10.1175/BAMS-D-14-00226.1, 2016.

Pfeffer, W. T., et al., The randolph glacier inventory: a globally complete inventory of glaciers, *Journal of glaciology*, *60*(221), 537–552, 2014.

Radić, V., A. Bliss, A. C. Beedlow, R. Hock, E. Miles, and J. G. Cogley, Regional and global projections of twenty-first century glacier mass changes in response to climate scenarios from global climate models, *Climate Dynamics*, *42*, 37–58, doi:10.1007/s00382-013-1719-7, 2014.

Rees, H. G., and D. N. Collins, Regional differences in response of flow in glacier-fed Himalayan rivers to climatic warming, *Hydrological Processes*, *20*(10), 2157–2169, doi:10.1002/hyp.6209, 2006.

Sakai, A., and K. Fujita, Contrasting glacier responses to recent climate change in high-mountain Asia, *Scientific Reports*, *7*, 13717, doi:10.1038/s41598-017-14256-5, 2017.

Sakai, A., T. Nuimura, K. Fujita, S. Takenaka, H. Nagai, and D. Lamsal, Climate regime of asian glaciers revealed by gamdam glacier inventory, *The Cryosphere*, *9*(3), 865–880, doi:10.5194/tc-9-865-2015, 2015.

Serreze, M. C., et al., Observational evidence of recent change in the northern high- latitude environment, *Climatic Change*, *46*(1-2), 159–207, doi:10.1023/A:1005504031923, 2000.

Slangen, A. B. A., F. Adloff, S. Jevrejeva, P. W. Leclercq, B. Marzeion, Y. Wada, and R. Winkelmann, A Review of Recent Updates of Sea-Level Projections at Global and Regional Scales, *Surveys in Geophysics*, *38*, 385–406, doi:10.1007/s10712-016-9374-2, 2017.

Stocker, T. F., *Climate change 2013*, 2014.

Wada, Y., et al., Multimodel projections and uncertainties of irrigation water demand under climate change, *Geophysical Research Letters*, *40*(17), 4626–4632, doi:10.1002/grl.50686, 2013.

Watanabe, M., A. Yanagawa, Y. Hirabayashi, S. Watanabe, A. Sakai, and S. Kanae, Uncertainty from climate forcing of projections in glacier melt for high mountain asia, *Annual journal of Hydraulic Engineering, JSCE*, *62*, I_211–216, 2018.

Watanabe, S., S. Kanae, S. Seto, P. J. F. Yeh, Y. Hirabayashi, and T. Oki, Intercomparison of bias-correction methods for monthly temperature and precipitation simulated by multiple climate models, *Journal of Geophysical Research Atmospheres*, *117*(23), 1–13, doi:10.1029/2012JD018192, 2012.

Yamazaki, D., S. Kanae, H. Kim, and T. Oki, A physically based description of floodplain inundation dynamics in a global river routing model, *Water Resources Research*, *47*(4), doi:10.1029/2010WR009726, 2011.

Yatagai, A., K. Kamiguchi, O. Arakawa, A. Hamada, N. Yasutomi, and A. Kitoh, Aphrodite constructing a long-term daily gridded precipitation dataset for Asia based on a dense network of rain gauges, *Bulletin of the American Meteorological Society*, *93*(9), 1401–1415, doi:10.1175/BAMS-D-11-00122.1, 2012.

Zemp, M., I. Gärtner-Roer, S. U. Nussbaumer, F. Hüsler, H. Machguth, N. Mölg, F. Paul, and M. Hoelzle, Global glacier change bulletin no. 1 (2012–2013), *Global Glacier Change Bulletin*, *1*, 2015.

Appendix A

Supplement for Chapter 4

A.1 GCM selection

The three GCMs were selected based on a preliminary experiment using nine GCMs and two RCPs to evaluate HMA glaciers. We examined changes in glacier mass and area. Below, we show some results of the preliminary experiment.

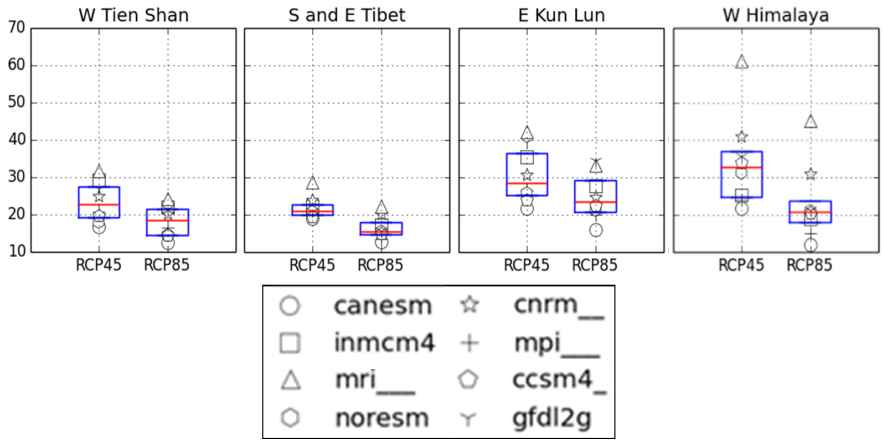

Figure A.1: A preliminary experiment. We used the HYOGA2 model with several ensembles of GCM simulations to select typical GCMs. Examples of projected changes in glacier areas (%) within West Tien Shan, South and East Tibet, East Kun Lun, and the West Himalaya are shown. We used eight GCMs and two RCPs.

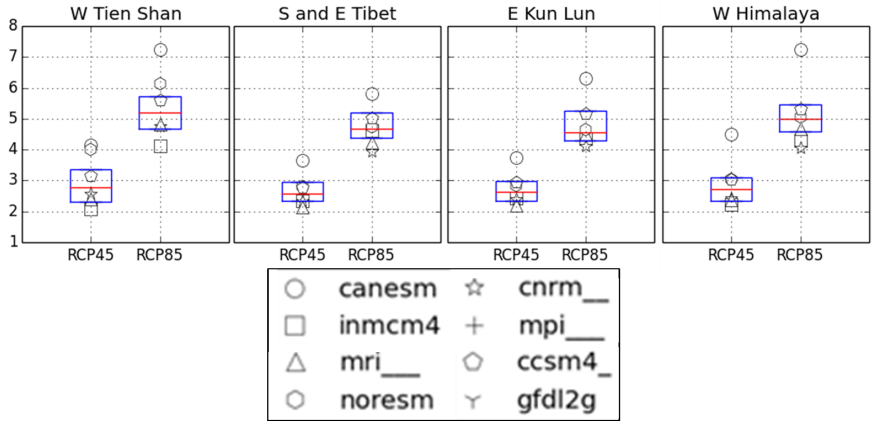

Figure A.2: A preliminary experiment. We used the HYOGA2 model with several ensembles of GCM simulations to select typical GCMs. Examples of projected changes in air temperature (℃) within West Tien Shan, South and East Tibet, East Kun Lun, and the West Himalaya are shown. We used eight GCMs and two RCPs.

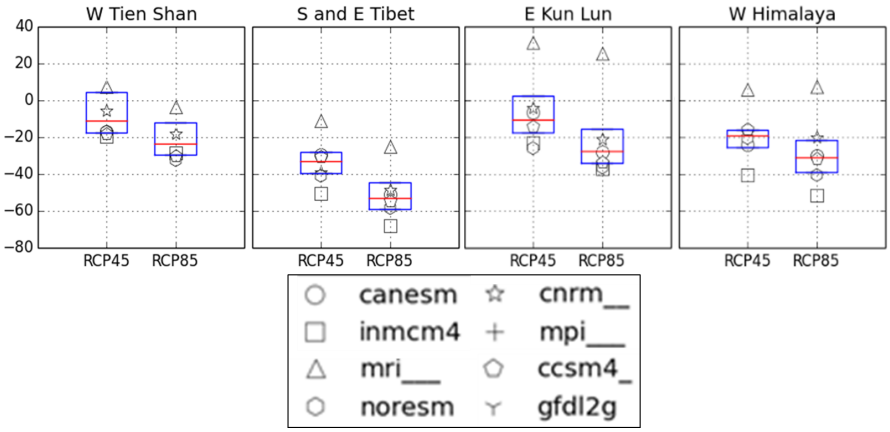

Figure A.3: A preliminary experiment. We used the HYOGA2 model with several ensembles of GCM simulations to select typical GCMs. Examples of projected changes in snowfall (%) within West Tien Shan, South and East Tibet, East Kun Lun, and the West Himalaya are shown. We used eight GCMs and two RCPs.

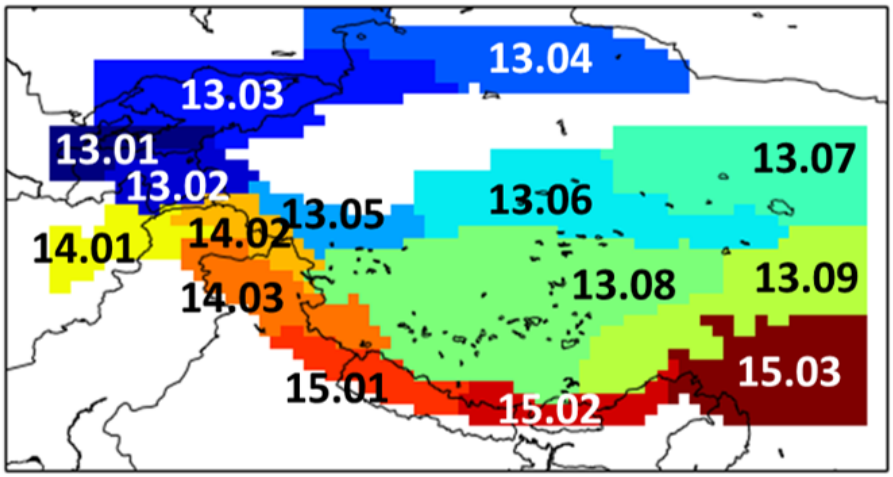

Figure A.4: The location of sub-regions

Table A.1: Sub-regions ID

Sub-region	Name
1301	HissarAlay
1302	Pamir
1303	W Tien Shan
1304	E Tien Shan
1305	W Kun Lun
1306	E Kun Lun
1307	Qilian Shan
1308	Inner Tibet
1309	S and E Tibet
1401	Hindu Kush
1402	Karakoram
1403	W Himalaya
1501	C Himalaya
1502	E Himalaya
1503	HengduanShan

Table A.2: Comparisons of averaged calibration errors. The calibration errors were calculated as the relative errors of modeled annual glacier mass balances compared to the observed mass balances for 1980 – 2004. The relative errors (%) were averaged for glacierized grids for which observed glacier mass balances were available. The DDFs were calibrated using Method 1 and the Cp, DDFs, and dT calibrated employing Method 2.

Climate forcing	Method1 (%) T	Method2 (%)
APHRODITE P - CRU T	260	52
Sakai P – CRU T	163	37
MSWEP P – CRU T	132	47
APHRODITE P – ERA-Interim T	54	50
Sakai P – ERA-Interim T	65	49
MSWEP P – ERA-Interim T	67	39

A.2 Calibration errors among simulations using various observed past climate datasets

We compared calibration errors using six combinations of observational datasets for air temperature and precipitation. Employing the HYOGA2 glacier model, forcing using the Sakai precipitation-CRU temperature data and MSWEP precipitation-ERA-Interim temperature data was associated with relatively small calibration errors (Sakai precipitation-CRU temperature: 37%; MSWEP precipitation-ERA-Interim temperature: 39%; see the following Table and Figure). Use of these two combinations was thus relatively appropriate when simulating past glacier mass balance. However, the appropriate combination may differ by the glacier model chosen. Currently, we are unsure whether the calibration results described above can be generalized.

A.3 Sensitivity testing of the time period used to derive moving averages

To assess uncertainties when projecting future changes in glacier mass, we used 30-year moving averages of the fractions of total variance (Fig. 4). When the time periods used to calculate moving averages were changed (10, 20, 30 or 40 years), the fractional uncertainty from observed past climate (air temperature and precipitation) datasets were projected

to be about 15% at the end of the 21st century. We confirmed that this did not change when any of 10-, 20-, 30-, and 40-year moving averages were employed (please see the three Figures below).

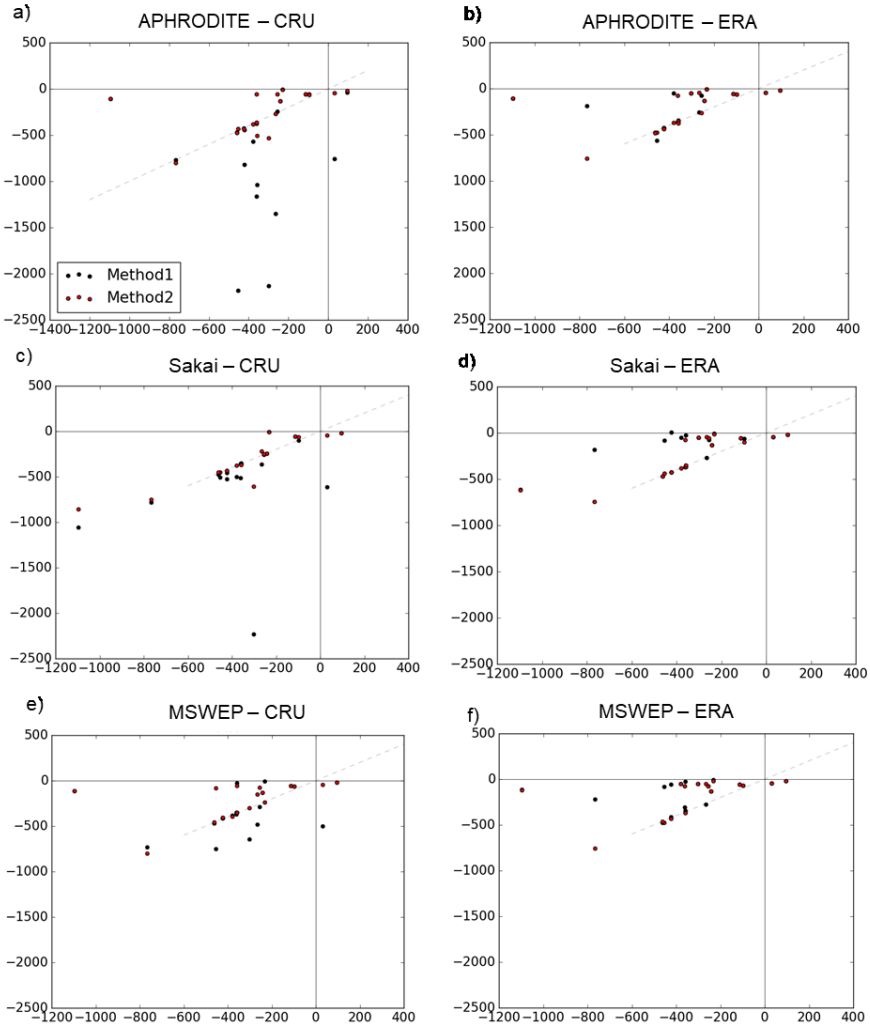

Figure A.5: Comparisons of modeled (y-axis) and observed (x-axis) average annual glacier mass changes (mm w.e. $year^{-1}$) from 1980 to 2004, using (a) APHRODITE precipitation and CRU temperature data; (b) APHRODITE precipitation and ERA-Interim temperature data; (c) Sakai precipitation and CRU temperature data; (d) Sakai precipitation and ERA-Interim temperature data; (e) MSWEP precipitation and CRU temperature data; and (f) MSWEP precipitation and ERA-Interim temperature data. The DDFs (the Cp, the DDFs, and the dT) were calibrated using Method 1 (Method 2).

A.4 Assessment of uncertainty of future air temperature and precipitation by GCM

Differences between "default experiments" (using future air temperature and precipitation from the same GCMs) and "shuffle experiments" (using combinations of future air temperature and precipitation from different GCMs) were calculated to estimate un-

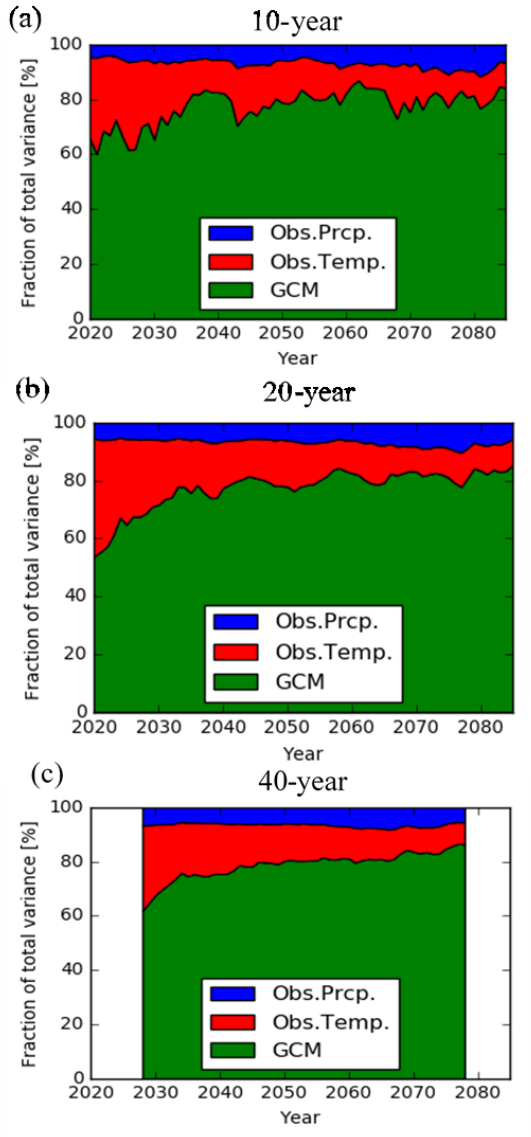

Figure A.6: Fraction of total variance in projections of changes in glacier mass explained by GCM, observed air temperature, and observed precipitation. (a) 10-year; (b) 20-year (c) 40-year moving average.

Table A.3: Setting of "default experiments" and "shuffle experiments" of GCM air temperature and precipitation

Past Obs.T	Past Obs.P T	GCM T	GCM P
		CCCma-CanESM2	CCCma-CanESM2
		NCAR-CCSM4	NCAR-CCSM4
		MRI-CGCM3	MRI-CGCM3
H08	APHRODITE	MRI-CGCM3	CCCma-CanESM2
		CCCma-CanESM2	MRI-CGCM3
		MRI-CGCM3	NCAR-CCSM4
		NCAR-CCSM4	MRI-CGCM3

certainties of GCM air temperature and GCM precipitation separately. The setting of shuffle experiments were described in (Table A.3). In most of the combination of future air temperature and precipitation from the different GCMs, when we shuffled GCM air temperature the differences from the default experiments were larger (the difference of glacier melt, 0.0348 km^3 for 2020-2040 in case of using CCCma-CanESM2) than that of GCM precipitation shuffle experiments (the difference of glacier melt, 0.0094 km^3 for 2020-2040 in case of using CCCma-CanESM2) for both of the projection periods 2020-2040 and 2060-2080 (Figure A.7, Table A.4). The shuffle experiments indicates that the uncertainty in projecting glacier melts arising from the spreads among GCM air temperature tend to be larger than that from the spreads among GCM precipitation in most cases of combinations of GCM outputs and periods. It is known that the spreads among GCM air temperature are smaller than the spreads among GCM precipitation. However, this study indicates that the impact of the spreads among GCM air temperature on projections of glacier melts could be larger than that of the spreads among GCM precipitation.

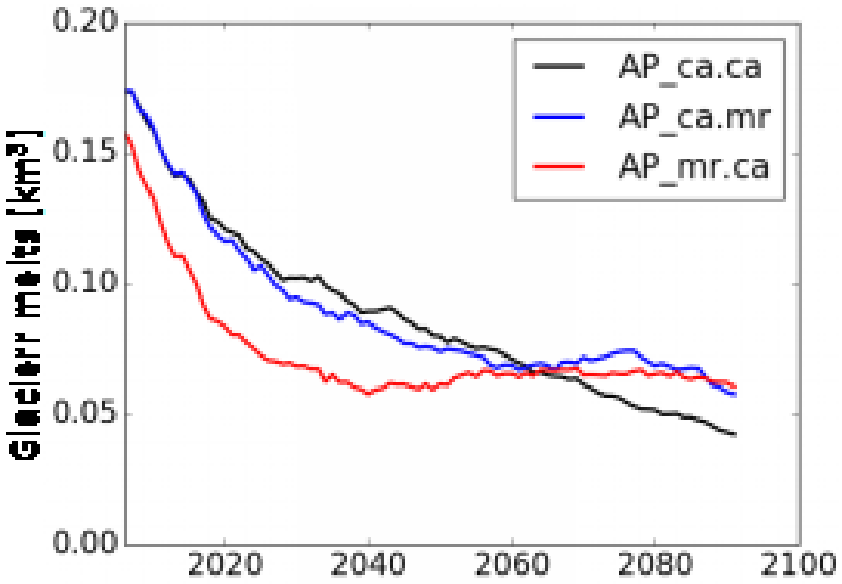

Figure A.7: Differences of "default experiments" and "shuffle experimets" of GCM air temperature and precipitation. Toal glacier melt (km^3) for selected 304 glaciers. CCCma-CanESM2 air temeprature and precipitation were used as the default experiment. CRU and APHRODITE were used as obserbed past air temperature and precipitation. Red: shuffle GCM air temperauture; Blue: shuffle GCM precipitation; ca: CCCma-CanESM2; cc: NCAR-CCSM4; mr: MRI-CGCM3.

Table A.4: Differences of "default experiments" and "shuffle experimets" of GCM air temperature and precipitation

Temp. × Prec.	Differences of glacier melt 2020-2040av (km^3)	Differences of glacier melt 2060-2080av (km^3)
(ca × ca) – (mr × ca)	0.0338	-0.0052
(ca × ca) – (ca × mr)	0.0094	-0.0105
(cc × cc) – (mr × cc)	0.0246	-0.0171
(cc × cc) – (cc × mr)	0.0059	0.0069
(mr × mr) – (cc × mr)	-0.0227	0.0186
(mr × mr) – (mr × cc)	-0.0041	-0.0055

A.5 Responses to the comments of reviewer

Hereafter, selected responses to the comment of reviewers of Climate Dynamics (Springer) to publish the manuscript will be introduced.

[1] L. 57-, L. 328-, Supplement 3 The definition of GCM uncertainty in this study mixes climate internal variability and model uncertainty. The authors should detail this assumption, following for example the works of Hingray et al. (2014) or Lafaysse et al. (2014). In addition, the uncertainty is estimated here for averages of temperature and precipitation over 30 years. The author should discuss whereas the uncertainty computed at other frequencies could be different.

1) Thank you. As you point out, "GCM uncertainty" includes both "model uncertainty" and "internal variability." We have now defined "GCM uncertainty" as follows: L. 57 "Uncertainty in terms of climate prediction has several distinct sources. Model uncertainty reflects limitations in model structure and the parameterization used to represent geophysical processes. The internal variability of a climate system reflects the natural fluctuations that arise in the absence of any radiative forcing of the planet. These model uncertainties and internal variabilities will here be termed "GCM uncertainties." We used a single climate scenario (RCP8.5); we did not explore scenario uncertainty."

2) To assess uncertainties when projecting future changes in glacier mass, we used 30-year moving averages of the fractions of total variance (Fig. 4). When the time periods used to calculate moving averages were changed (10, 20, 30 or 40 years), the fractional uncertainties caused by observed past climatic (air temperature and precipitation) datasets were projected to be about 15% at the end of the 21st century. We confirmed that this did not change when any of 10-, 20-, 30-, or 40-year moving averages were employed (please see the three Figures below).

[2] L. 174-, L. 371- What is defined as observations for temperature and precipitation in this study are not direct observations, but gridded products based on interpolation of local observations. A question is: Are you underestimating the observational uncertainty in the sense that only three gridded products are considered? Using also local observations with potential large differences compared to such gridded products, could we get stronger uncertainties related to bias correction and model calibration?

1) We used three combinations of gridded air temperatures and precipitation data when assessing uncertainty. As you mention, had we used more gridded products, we might have been able to evaluate uncertainties more rigorously. Unfortunately, suitable products are rare (temporal resolution: daily; spatial resolution: $\leq 0.5^{\circ}$, period: from 1980). We used gridded products that have often been employed for global glacier modeling (Marzeion et al. 2012a, 2018; Giesen and Oerlemans 2013; Hirabayashi et al. 2013b; Slangen et al. 2017) and also the latest such product (Beck et al. 2017). Therefore, we assessed the uncertainties associated with products used in previous glacier model studies although the number of gridded products used in this study was still limited. We now mention this in the manuscript (L. 174-).

2) As you point out, if local observations were available, the uncertainties associated with bias correction and model calibration would become clearer. This is a very interesting idea. However, very few local observations on or near HMA glaciers are available; the glaciers are in remote areas at high elevations. We now mention this in the manuscript (L. 371-).

[3] L. 350-, L. 352, Supplement 2 The approach that consists in detecting deficiencies in observational datasets using model outputs has been suggested for example by Massonnet et al. (2016). According to your investigations, would it be possible to provide an evaluation of temperature and precipitation observational datasets when using them to compute the model glacier mass balance?

1) We appreciate the suggestion. That method is quite interesting. Unfortunately, after careful consideration, we considered that the method was not the best for this case; we would explain why. Massonnet et al. (2016) use sea surface temperature (SST) to estimate the quality of observational data sets. Here, we use surface air temperature and precipitation as climatic variables. Climate models perform better when SSTs rather than surface air temperatures or precipitation are used, particularly when precipitation varies seasonally or annually. The surface air temperatures and precipitation were predicted using CMIP5 models, which reflect global warming. Thus, CMIP5 climate projections can be used to assess long-term trends, but CMIP5 seasonal or annual variation in climate projections cannot be compared to observations. Moreover, some new and improved SST observational datasets are available. The quality of observational surface air temperature and precipitation datasets require improvement; the data may be unreliable given the

sparse observational network particularly at high elevations. Therefore, we thought that the method of Massonnet et al. (2016), although valuable, was not appropriate for our work. We now mention this in the manuscript (L. 352-).

2) Instead, we compared calibration errors using six combinations of observational datasets on air temperature and precipitation. Using the HYOGA2 glacier model, forcing employing Sakai precipitation-CRU temperature data and MSWEP precipitation-ERA-Interim temperature data was associated with relatively smaller calibration errors (37 and 39% respectively; see the following Table and Figure). Use of these two combinations was thus relatively appropriate when simulating past glacier mass balance. However, the appropriate combination may differ by the glacier model chosen. Currently, we are unsure whether the calibration results described above can be generalized. We now mention this in the manuscript (L. 350-, Supplement 2).

[11] L. 99- Since your study focuses on the Asian glaciers, you could include some references to previous works describing the evolution of the glaciers in this area (e.g. Fujita et al., 2011; Bolch et al., 2012; Hewitt, 2005; Kääb et al., 2012; Brun et al., 2017; Mölg et al., 2012).

We have added a paragraph on glacier evolution in the study area and we now cite previous works (Fujita and Nuimura 2011; Bolch et al. 2012; Kääb et al. 2012; Brun et al. 2017); the new text reads:

"The HMA contains the largest mass of land glacier ice with the exception of the poles. The HMA glaciers are retreating and losing mass at rates comparable to glaciers in other regions of the world (Fujita and Nuimura 2011; Bolch et al. 2012; Kääb et al. 2012; Brun et al. 2017). Meltwaters from HMA glaciers flow into downstream rivers; large human populations depend on glacier-fed water supplies. The impact of climate change on the extent of glacier melt is of major interest. The HMA includes the Tibetan Plateau, for which observed climatic datasets and GCM climate projections are among the sparsest worldwide (Stocker 2014). This region is characterized by high-level orography and a large proportion of solid precipitation, both of which would be expected to greatly bias observations."

[12] Fig. 1 Could you include more details in the caption of Figure 1, and in particular the exact meaning of the "X", as well as a short description of each phase.

We have revised the text:

“Fig. 1. Overview of projection of changes in glacier mass. “Future Air Temperature and Precipitation” data from the climate projections of GCMs (CCCma-CanESM2, NCAR-CCSM4, and MRI-CGCM3) served as climate forcing factors when making predictions. The “Future Air Temperature and Precipitation” data were corrected by the “Bias Correction” procedure using “Observed Past Air Temperature” (CRU, ERA-Interim) and “Observed Past Precipitation” (APHRODITE, Sakai, MSWEP) as references. The “Observed Past Air Temperature” and the “Observed Past Precipitation” also served as forcing factors in the “Glacier model HYOGA2” during calibration of “Determining Parameters.” Finally, using “Bias Corrected Future Air Temperature and Precipitation” as a future climate forcing parameter, the “Glacier model HYOGA2” calculated “Future Glacier Mass Changes” for each combination of input data (18 combinations of three “Future Air Temperature and Precipitation” datasets of the GCMs, two “Observed Past Air Temperature” datasets, and three “Observed Past Precipitation” datasets). Here, “X” indicates combinations.”

[14] L. 127- L. 112: ”Eight of these data points were well calibrated (i.e., calibration errors were lower than $\pm$ 50%)”: Does it mean that others data points are badly calibrated ? In that case could you give examples of bad calibrations and explain why they are badly calibrated ?

The calibration errors lay outside the $\pm$ 50% window when we used the positive glacier mass balances for model calibration. We employed long-term (1981 – 2004) averaged observations. The original observations were not continuous over the whole period (1981 – 2004); some annual observations were missing. Positive glacier mass balances were observed in only a few years; no long-term trend was apparent. Quality issues with the observations caused large calibration errors because we set upper and lower limits for the calibration parameters. Another reason for poor calibration is the enormous bias evident in observed climatic datasets. A warm bias is evident in the observed air temperature dataset and a large spread among precipitation datasets.

[16] L. 156- L. 137: ”This was smaller than the error estimation for Central Asia reported by other glacier models”: Could you give numbers to support this statement, please ?

The root-mean-square error between the HYOGA2-modeled and observed mass balances (Gardner et al. 2013) was 0.14 m w.e. $year^{-1}$, thus less than the error ranges of other global glacier models reported by Marzeion et al. (2012) and Radić et al. (2014). Marzeion et al. (2012) reported a root mean-square error between the modeled and observed HMA (North) mass balance of 0.33 ± 0.11 m w.e. $year^{-1}$; for HMA (West), the figure was 0.42 ± 0.20 m w.e. $year^{-1}$; and for HMA (South) 0.37 ± 0.16 m w.e. $year^{-1}$. Radić et al. (2014) reported a root mean-square error between the modeled and observed HMA mass balance of 1.05 m w.e. $year^{-1}$.

[17] L. 144- L. 154: CRU temperature observation is used, applying a lapse rate to get the temperature at high altitude. Could you detail from which altitude is applied this lapse rate? In other words, what is the altitude associated to the CRU gridcells? Is the APHRODITE precipitation used homogeneously for each grid cell, or is there any correction used with the altitude, the wind direction/intensity, $\cdots$?

We used CRU altitude data and median glacier inventory altitudes (RGI) to derive the temperature lapse rate. We calculated the differences between the altitudes of CRU grid cells and median glacier altitudes; these yielded a temperature lapse rate for each glacier.

The APHRODITE precipitation was homogeneous at all elevation bands of each grid cell in the HYOGA2 glacier model. We did not apply a precipitation lapse rate to the precipitation datasets; we sought to avoid incorporation of an additional uncertain parameter. The original HYOGA2 model showed that that the modeled mass balance was insensitive to the precipitation lapse rate (Supplement of Hirabayashi et al. 2013a). We also did not correct for wind direction/intensity because APHRODITE precipitation used interpolation to consider orography. In addition, potential orographic effects on precipitation are indirectly adjusted via calibration.

[19] L. 227- L. 187: Bias correction: Even if the method relies on a previous publication, could you mention here if both the mean and the standard deviation are bias-corrected, and at which frequency?

Thank you. We briefly describe our bias corrections for temperature and precipitation below. We compared GCM simulation data to observation-based data when estimating biases over 30 years from 1981 to 2010 (1981 to 2007 for APHRODITE and Sakai precipitations) at a spatial resolution of 0.5° . Monthly and daily variances were simul-

taneously corrected. Monthly bias was corrected using the method of Watanabe et al. (2012). During bias correction, we adjusted means, temperature standard deviations, and precipitation coefficients of variance, on a monthly basis. Then monthly corrected data were obtained using an inverse cumulative distribution function. Daily time series were obtained from the bias-corrected monthly time series. The daily temperature time series was corrected using the method of Hirabayashi et al. (2013). The difference between the GCM-simulated and observed daily precipitation was used to compute a bias-corrected daily precipitation time series.

[25] Table 3-8, L. 216, L. 260: There is a lack of information in the captions of Table 3 and 4: what are the spatial domain and the temporal integrations considered to compute the numbers shown in Tables 3 and 4? Could you also show the corresponding values computed for the GCM, to get an idea of their error?

We have updated Table 3, 4 and 5 and added the following information in Table 3, 4, and 5 (the original versions of Table 3 and 4 were in error).

The spatial domain in Table 3 and 4 (Table 3, 4 and 5): It is spatially averaged values in the targeted glacier areas shown in Figure 2.

The period in Table 3 and 4 (Table 3, 4 and 5): 1980-2004

We have also calculated future climate forcing from the GCMs (annual average air temperatures and total precipitation for 2060-2080 in the targeted glacier areas). We have added Table 6, 7 and 8 following this comment (L. 216).

[28] L. 153- Some observations about the glacier mass balance for the period 1980-2000 should be included, to validate the model over 1980-present. Maybe by including some references to previous study showing such observations? For example, Brun et al. (2017) observe a negative mass balance of -0.18m w.e. $year^{-1}$ on average for the High Mountain Asia glaciers over the period 2000-2016. What is the corresponding value get with the model over the same period?

In lines 134 – 138 of the original manuscript, we validated our past period model using the satellite- derived observations of Gardner et al. (2013). The area averaged annual mass balance of the 28 HMA glaciers (Section 2.2 and Fig. 2) was simulated as – 0.21 ± 0.14 m w.e. $year^{-1}$ (the – 298 ± 181 m w.e. $year^{-1}$ of the original manuscript was an error) from 2003 – 2009 as shown by the glacier model. The observed annual mass balance of

all HMA glaciers was – 0.22 ± 0.10 m w.e. $year^{-1}$ in the work of Gardner et al. (2013) for the interval 2003 – 2009. The modeled value is quite close to the observed value. We have discussed this in [Answer 16]. The root mean-square error between the modeled and observed mass balances (Gardner et al. 2013) was 0.14 m w.e. $year^{-1}$, thus less than the error estimation ranges of other global glacier models reported by Marzeion et al. (2012) and Radić et al. (2014). Marzeion et al. (2012) reported root mean-square errors between modeled and observed HMA mass balances as: HMA (North): 0.33 ± 0.11 m w.e. $year^{-1}$; HMA (West): 0.42 ± 0.20 m w.e. $year^{-1}$; and HMA (South): 0.37 ± 0.16 m w.e. $year^{-1}$. Radić et al. (2014) reported a root mean-square error between the modeled and observed HMA mass balances of 1.05 m w.e. $year^{-1}$.

Following your comment, we examined the value obtained using the data of Brun et al. (2017) for the same period. The cited authors reported an average HMA glacier negative mass balance of – 0.18 m w.e. $year^{-1}$ over the period 2000 – 2016. In the present study, the area-averaged annual mass balance of 28 HMA glaciers was simulated as – 0.44 ± 0.16 m w.e. $year^{-1}$ from 2000 to 2016.

However, we calculated values for 28 HMA glaciers; Gardner et al. 2013 and Brun et al. 2017) evaluated all HMA glaciers. The data are not directly comparable. We present the other values just for reference.

The reason for the discrepancy between the observation in Brun et al. 2017) and our modeled value remains unclear. The latter value is based on simulations including years after 2005, global warming was thus considered. This may explain why the model overestimates glacier mass loss compared to the observations of the cited authors.

In a previous study (Huss and Hock 2015), the estimates were – 0.05 m w.e. $year^{-1}$ for 2001 – 2005 and – 0.3 m w.e. $year^{-1}$ for 2006 – 2010 (HMA; Figure 5). Our data were similar (– 0.02 m w.e. $year^{-1}$ for 2001 – 2005 and -0.36 m w.e. $year^{-1}$ for 2006 – 2010).

[31] L. 355- L. 319: Radar measurement are efficient to measure precipitation amounts spatially, but they have strong biases over mountainous areas, because of the complex topography, clouds and the difficulty to catch solid precipitation. I would mention also the possibility to measure the rates of total precipitation (including snowfall) with modern rain gauge networks (Geonor system for example, e.g. Morin et al., 2012; Rasmussen et al., 2012).

Thank you. Modern rain gauges reliably measure solid precipitation. We now mention that such observations could be combined with satellite observations to complement the particular weaknesses of both systems (for example, it is not possible to place large numbers of gauges). Modern rain gauges could be used to correct satellite-derived observations.

We have revised the text: L 355- "State-of-the-art remote sensing satellites such as the Global Precipitation Measurement (GPM) Dual-Frequency Precipitation Radar (DPR) will reduce the differences among observed past climate datasets in regions with glaciers region. The GPM GPR seeks to measure both light and solid precipitation accurately and comprehensively. Modern rain gauges with windshields (e.g., the Geonor system) will be used to correct satellite observations, which may be unreliable if the topography is complex."